

NASA CR-170,406

Rec Room  
MS 2559

NASA Contractor Report 170406

NASA-CR-170406  
19840006090

---

# Space Shuttle Flying Qualities and Flight Control System Assessment Study – Phase II

---

T. T. Myers, D. E. Johnston, and D. T. McRuer

---

Contract NAS4-2940  
December 1983

LIBRARY COPY

JAN 11 1984

LANGLEY RESEARCH CENTER  
LIBRARY NASA  
HAMPTON, VIRGINIA



NF02559

**NASA**  
National Aeronautics and  
Space Administration

---

# Space Shuttle Flying Qualities and Flight Control System Assessment Study – Phase II

---

T. T. Myers, D. E. Johnston, and D. T. McRuer  
Systems Technology, Inc., Hawthorne, California 90250

Prepared for  
Ames Research Center  
Dryden Flight Research Facility  
Edwards, California  
under Contract NAS4-2940

1983



National Aeronautics and  
Space Administration

**Ames Research Center**

Dryden Flight Research Facility  
Edwards, California 93523

N84-14158<sup>#</sup>

**This Page Intentionally Left Blank**

## TABLE OF CONTENTS

	<u>Page</u>
I. INTRODUCTION.....	1
II. CONTINUED REVIEW OF KEY FLYING QUALITY ISSUES.....	3
A. Flying Quality Consequences of Superaugmentation.....	4
B. Recent Experimental Results Relevant to Superaugmentation.....	26
C. Path Dynamics.....	37
D. Shuttle Flight Mechanics for Manual Approach and Landing.....	44
E. Summary of Shuttle Flying Qualities and Flight Control System Issues.....	54
III. REVIEW OF FLYING QUALITIES INFORMATION FROM SPACE SHUTTLE FLIGHT 1-4.....	58
A. Individual Flights.....	59
B. Summary.....	64
IV. OVERVIEW OF THE SHUTTLE OEX PLAN.....	66
A. Elements of an Ideal Flying Qualities Flight Test.....	67
B. Limitations and Expectations for OEX Flight Experiments.....	69
C. The Proposed OEX Procedure.....	72
V. PROPOSED INDIRECT OEX APPROACH.....	81
A. Prototype Pilot Models for Shuttle Approach and Landing.....	81
B. Non-Intrusive Pilot/Vehicle/Workload Measurement Methods.....	98
C. Instrumentation and Software Requirements for Data Processing.....	107
VI. POSSIBLE OEX SIMULATION EXPERIMENTS.....	122
A. Simulation Possibilities for Specific Flying Qualities Issues.....	123
B. Experimental Design.....	125

REFERENCES.....	R-1
APPENDIX A. SPACE SHUTTLE FLIGHT MECHANICS IN APPROACH AND LANDING.....	A-1
APPENDIX B. PRELIMINARY QUESTIONS REGARDING STS-4 MANUAL FLYING QUALITIES.....	B-1
APPENDIX C. SPACE SHUTTLE FLYING QUALITIES QUESTIONNAIRE.....	C-1

## LIST OF FIGURES

	<u>Page</u>
1. Closed-Loop Precision Path Control with Attitude Control Inner Loop.....	5
2. Effective Aircraft Dynamics (Aircraft + Augmentation System) for Conventional and Superaugmented Aircraft.....	7
3. General Pitch Rate Response to Step Pilot Input.....	9
4. Maximum Pitch Rate Overshoot Variation for Superaugmented Aircraft.....	13
5. Pitch Overshoot Variation with Static Margin for Conventional Aircraft (Generic Aircraft in Cruise).....	14
6. Pitch SAS for Shuttle.....	17
7. Basic Structure of the FCS Used in the Ref. 3 Study.....	27
8. Bode Root Locus Plot Indicating the Effect of Closure of the $q \rightarrow \delta_e$ Loop ( $K_q = -0.333$ rad/sec) Configuration F-4 of Ref. 3.....	29
9. Normalized Indicinal Pitch Rate Response of Ref. 3 "F" Configurations Compared to Exemplary Criteria ( $T_{\theta_2} = 1.4$ sec).....	31
10. System Survey for the Ref. 5 Short-Aft Tail, Extra High $K_q$ , $T_q = 0.5$ sec Configuration.....	33
11. Normalized Indicinal Pitch Rate Response to Stick Force, Ref. 5 Short Aft Tail, Extra High $K_q$ , $T_q = 0.5$ Configuration.....	34
12. System Survey for Ref. 5 Short Aft Tail, High $K_q$ , $T_q = 1.0$ sec Configuration.....	35
13. Normalized Indicinal Pitch Rate Response to Stick Force, Ref. 5 Short Aft Tail, High $K_q$ , $T_q = 1$ sec Configuration.....	36
14. Variation of Pilot Rating with Relative Pilot/ICR Location, Ref. 5 Data.....	39
15. Migration of High Frequency Altitude Zeros at Pilot Station as Pilot is Moved Forward from c.g., Short Aft Tail Configuration.....	41

	<u>Page</u>
16. Path-to-Attitude Frequency Response for 3 Pilot Positions, Short Aft Tail Configurations.....	42
17. Normal Acceleration and Altitude at Various Pilot Stations in Short Aft Tail Configuration, High Augmentation, $T_1 = A$ (From Ref. 5).....	43
18. Nominal Trajectory and Airspeed Variation for Shuttle Approach and Landing.....	45
19. Equilibrium Glideslope-Airspeed Curves for the Shuttle on Steep Glideslope.....	47
20. Idealized Shallow Glide and Final Flare Under Manual Control.....	48
21. Variation of Touchdown Variables in the Pilot's $T_f - \gamma_0$ Control Plane.....	50
22. Variation of Speed at Flare Initiation with Glideslope.....	52
23. Block Diagram of Pilot-Vehicle-Task System.....	75
24. Development of the Structural Isomorphic Pilot-Vehicle-Task Model.....	76
25. Steep Glideslope Tracking.....	82
26. Preflare Pullup.....	83
27. Shallow Glideslope.....	84
28. Final Flare.....	85
29. Determination of $Y_{p\theta}$ .....	88
30. Sampled Data Model for Pitch Control.....	89
31. Visual Approach Geometry for Homing on an Aimpoint on the Earth's Surface (from Ref. 38).....	91
32. Determination of Form of $Y_{p\gamma}$ .....	94
33. Determination of Form of $Y_{p\beta}$ .....	97
34. An Example of a Pilot-Vehicle System.....	100
35. Single Loop Pilot/Vehicle System for Application of Cross-Spectral Methods.....	101

	<u>Page</u>
36. Altitude-Sinkrate Variation from Preflare through Touchdown.....	105
37. Radar Altitude and Sinkrate Time Responses from Ref. 25.....	107
38. Instrumentation System Block Diagram (from Ref. 41).....	108
39. OEX Data Flow Diagram from Ref. 42.....	110
40. Simplified Block Diagram of Shuttle Attitude Processor (from Ref. 46).....	118
A-1. Tangent Normal Coordinate System.....	A-2
A-2. Low Speed $C_L$ vs. $\alpha$ , $\delta_e = 0$ .....	A-4
A-3. Extraction of Drag Polar Constants, $\delta_{SB} = 0$ , Gear Up.....	A-6
A-4. Speed Brake Effectiveness.....	A-7
A-5. Relative Contribution of Parasite and Induced Drag Terms to Deceleration.....	A-16
A-6. Variation of Touchdown Sinkrate with Shallow Glideslope.....	A-22
A-7. Variation of Touchdown Speed with Shallow Sinkrate.....	A-23
A-8. Variation of Touchdown Point with Shallow Glideslope.....	A-24

## LIST OF TABLES

	<u>Page</u>
1. Comparison of Pitch Attitude Response Governing Parameters for Conventional and Superaugmented Aircraft.....	10
2. System Architectural Possibilities and Mechanizational Side Effects for Superaugmented Aircraft (Systems Based on Attitude, Pitch Rate, or Normal Acceleration).....	21
3. System Architectural Possibilities and Mechanizational Side Effects for Superaugmented Aircraft (Systems Based on Angle of Attack or Speed).....	22
4. $q/q_c(s)$ Transfer Functions, F Configurations of Ref. 3.....	30
5. Summary of Manual Pitch and Speed Brake Control, STS-1-4.....	60
6. Summary of Data Available from the NASA DFRF MMLE File.....	112
7. Minimum Sample Rates Based on NIPIP Criterion.....	114
8. Manual Trim Inputs Desired for the OEX.....	115
9. Switches and FCS Discrettes Desired for the OEX.....	116

## NOMENCLATURE

$A_x, A_y, A_z$	Acceleration components along the body x, y, z axes
$c$	Reference chord length
$C_D$	Drag coefficient; $\frac{2D}{\rho U^2 S}$
$C_{D_0}$	Zero lift drag coefficient
$C_{D_u}$	$\frac{U}{2} \frac{\partial C_D}{\partial U}$
$C_{D_\alpha}$	$\frac{\partial C_D}{\partial \alpha}$
$C_L$	Lift coefficient; $\frac{2L}{\rho U^2 S}$
$C_{L_0}$	Lift coefficient, $\alpha = \delta_e = 0$
$C_{L_u}$	$\frac{U}{2} \frac{\partial C_L}{\partial U}$
$C_{L_\alpha}$	$\frac{\partial C_L}{\partial \alpha}$
$C_{L_{\dot{\alpha}}}$	$\frac{\partial C_L}{\partial (\dot{\alpha} c / 2U)}$
$C_{L_q}$	$\frac{\partial C_L}{\partial (q c / 2U)}$
$C_{L_\delta}$	$\frac{\partial C_L}{\partial \delta}$

$C_M$	Pitching moment coefficient; $\frac{2M}{\rho U^2 S c}$
$C_{M_u}$	$\frac{U}{2} \frac{\partial C_M}{\partial U}$
$C_{M_\alpha}$	$\frac{\partial C_M}{\partial \alpha}$
$C_{M_{\dot{\alpha}}}$	$\frac{\partial C_M}{\partial (\dot{\alpha} c / 2U)}$
$C_{M_q}$	$\frac{\partial C_M}{\partial (q c / 2U)}$
$C_{M_\delta}$	$\frac{\partial C_M}{\partial \delta}$
d	Beam deviation
D	Aerodynamic drag
$E_k$	Specific kinetic energy
$f_N$	Nyquist frequency, hz
FD	Flight director signal
g	Acceleration due to gravity (32.2 ft/sec <sup>2</sup> )
$G_{wo}$	Washout equalization
h	Path deviation; altitude
$h_c$	Desired path
$h_e$	Path error
$h_f$	Flare initiation altitude
$h_o$	Altitude at start of shallow glide
$I_y$	Moment of inertia in pitch
K	Gain
$K_q$	Controller gain

L	Aerodynamic lift
$l_p$	Distance between pilot and c.g., positive for pilot forward
m	Aircraft mass
M	Aerodynamic pitching moment; Mach number
$M_q$	(Single degree of freedom) pitch damping; Pitching acceleration per unit pitching velocity;
	$M_q = \frac{\rho S U c^2}{4 I_y} C_{M_q}$
$M_u$	Pitching acceleration per unit forward velocity;
	$M_u = \frac{\rho S U c}{I_y} (C_M + C_{M_u})$
$M_w, (M_\alpha)$	Weathercock stability; Pitching acceleration per unit vertical velocity (angle of attack);
	$M_\alpha = U_o M_w \quad ; \quad M_w = \frac{\rho S U c}{2 I_y} C_{M_\alpha}$
$M_{\dot{\alpha}}$	Pitching acceleration per unit angle of attack rate
	$M_{\dot{\alpha}} = \frac{\rho S U c^2}{4 I_y} C_{M_{\dot{\alpha}}}$
$M_\delta$	Pitching acceleration per unit control surface deflection
	$M_\delta = \frac{\rho S U^2 c}{2 I_y} C_{M_\delta}$
n	Load factor
$n_z$	Load factor in z direction
$N_{\delta_e}^h$	Altitude-to-elevator numerator

$N_{\delta e}^{\theta}$	Pitch attitude-to-elevator numerator
P, Q, R	Angular velocity components about the x, y, z axes
q	Pitching velocity (perturbation)
$q_e$	Pitching velocity error
$q_{ss}$	Steady-state pitching velocity
$\bar{q}$	Dynamic pressure
R	Radius, (Fig. 18); Ratio of real roots, Gas constant
$R_0$	Equilibrium yaw rate
s	Laplace Operator
S	Reference planform area
T	Time constant; sampling period
$T_f$	Flare time constant
$T_{h1}, T_{h2}, T_{h3}$	Time constants, altitude numerator
$T_q$	Lead time constant in augmentation system
$T_r$	Rise time
$T_{SP1}, T_{SP2}$	Time constants, real short period roots
$T_{\theta 1}, T_{\theta 2}$	Time constants, pitch attitude numerator
$T_{\theta 2}$	Lead time constant in short-period $\theta/\delta$ transfer function for conventional airplane dynamics. Lag time constant between flight path angle, $\gamma$ , and pitch attitude, $\theta$ .

$$1/T_{\theta 2} = -Z_w + Z_{\delta} M_w / M_{\delta} \doteq -Z_w$$

U	Speed (x stability axis)
$U_0$	Speed in reference condition

V	Speed
V <sub>E</sub>	Equilibrium speed
w	Vertical velocity
w <sub>g</sub>	Vertical gust velocity
W	Gross weight; Aircraft weight
X <sub>f</sub>	Flare distance
X <sub>u</sub>	Forward acceleration per unit speed change $X_u = \frac{\rho S U}{m} (-C_D - C_{D_u})$
X <sub>w</sub> , X <sub>α</sub>	Forward acceleration per unit vertical velocity $X_\alpha = U_0 X_w \quad ; \quad X_w = \frac{\rho S U}{2m} (C_L - C_{D_\alpha})$
Y <sub>Ph</sub>	Pilot describing function for pilot control action on path deviation
Y <sub>Pθ</sub>	Pilot describing function for pilot control action on attitude
Z <sub>u</sub>	Vertical acceleration per unit forward velocity $Z_u = \frac{\rho S U}{m} (-C_L - C_{L_u})$
Z <sub>w</sub> , (Z <sub>α</sub> )	Heave damping; vertical acceleration per unit vertical velocity (angle of attack); $Z_\alpha = U_0 Z_w \quad ; \quad Z_w = \frac{\rho S U}{2m} (-C_{L_\alpha} - C_D)$
Z <sub>δ</sub>	Vertical acceleration per unit control surface deflection $Z_\delta = \frac{\rho S U^2}{2m} (-C_{L_\delta})$

$\alpha$	Angle of attack; Lapse rate
$\alpha_A$	Aerodynamic angle of attack, $(w - w_g)/U_0$
$\alpha_I$	Inertial angle of attack, $w/U_0$
$\beta$	Sideslip angle, $v/U_0$
$\gamma$	Flight path angle
$\gamma_0$	Selected flight path angle, Fig. 22
$\delta$	Generic control (elevator, horizontal tail, etc.) surface deflection
$\delta_a$	Aileron deflection
$\delta_{BF}$	Body flap deflection
$\delta_{BFC}$	Body flap controller
$\delta_e$	Elevator deflection
$\delta_{e_p}$	Pilot command input
$\delta_{PED}$	Rudder pedal deflection
$\delta_{RHC}$	Rotational hand controller deflection
$\delta_r$	Rudder deflection
$\delta_{SB}$	Speed brake
$\delta_{SBC}$	Speed brake controller
$\delta_T$	Throttle deflection
$\Delta l_p$	Distance between pilot and ICR, positive for pilot forward
$\epsilon_v$	Visual angle error
$\zeta$	Damping ratio
$\zeta_{sp}$	Short period damping ratio
$\theta$	Pitch attitude (perturbation)
$\dot{\theta}$	Pitch attitude rate

$\theta_c$	Attitude Command
$\theta_e$	Attitude Error
$\rho$	Atmospheric Density
$\sigma$	Real component of complex variable, s
$\tau$	Time delay; Density ratio
$\tau_M$	Delay margin, $\phi_M/\omega_c$
$\tau_p$	Pilot's time delay
$\Phi, \phi$	Bank Angle
$\phi_M$	Phase Margin
$\Psi, \theta, \phi$	Euler angles to aircraft body axes (heading, pitch, roll sequence)
$\omega$	Imaginary component of complex variable, s
$\omega_c$	Crossover Frequency
$\omega_{ca}$	Crossover frequency of amplitude ratio asymptote
$\omega_n$	Natural frequency
$\omega_{SP}$	Short period frequency

## ACRONYMS AND ABBREVIATIONS

ACIP	Aerodynamic Coefficient Identification Package
ADI	Attitude director instrument
ADS	Air data system
AGL	Above ground level
ALT	Approach and Landing Test
AMI	Shuttle display ( $\alpha$ , $A_x$ , $M$ , $V$ )
APU	Auxiliary power unit
AR	Aspect ratio
ARC	Ames Research Center
AVVI	Shuttle display ( $\ddot{h}$ , $\dot{h}$ , $h$ )
BET	Best estimated trajectory
BFCSS	Backup flight control system
CCIT	Cross coupled instability task
CHPR	Cooper Harper Pilot Rating
CSS	Control stick steering
CTT	Critical task tester
DAP	Digital autopilot
DFA	Describing function analysis
DFI	Developmental flight instrumentation
DFRF	Dryden Flight Research Facility
EPR	Eye-point-of-regard
FAR	Federal Air Regulations
FBW	Fly-by-wire
FCS	Flight control system

FD	Flight director
FSAA	Flight simulator for advanced aircraft
FSL	Flight Simulation Laboratory
FWD	Forward
GPC	General purpose computer
HAC	Heading alignment cylinder
HSI	Heading situation indicator
HUD	Head-up display
Hz	Hertz
ICR	Instantaneous center of rotation for elevator inputs
IMU	Inertial measurement unit
JSC	Johnson Space Center
KEAS	Knots equivalent airspeed
LAHOS	Landing and Approach Higher Order System
LOES	Lower order equivalent system
MMLE	Modified maximum likelihood estimator
NIPIP	Non-intrusive parameter identification program
NLR	National Aerospace Laboratory (the Netherlands)
OEX	Orbiter experiment
OFT	Orbiter Flight Test
OI	Operational instrumentation
PCM	Pulse code modulation
PIO	Pilot induced oscillation
PTI	Programmed test input
RGA	Rate gyro assembly
RHC	Rotational hand controller

RSS	Relaxed static stability
SMS	Shuttle Mission Simulator
STA	Shuttle training aircraft
STI	Systems Technology, Inc.
STS	Space Transportation System
TAEM	Terminal area energy management
TIFS	Total Inflight Simulator
TRFN	STI transfer function computer program
USAM	STI unified servo analysis method computer program
VMS	Vertical Motion Simulator

## SECTION I

### INTRODUCTION

Flying qualities criteria for advanced aircraft have been based on many years of experience with civil and military aircraft. For evolutionary designs this experience has provided an orderly and continuous base of data that could be applied to each new design with a modest extrapolation. However, the Space Shuttle combines the characteristics of a spacecraft and aircraft. It is radically different in configuration, operational envelope, and complexity than any vehicle flown before. It is a highly augmented, fly-by-wire vehicle whose control system design preceded by several years those of current military aircraft. Consequently, large extrapolations had to be made to establish handling qualities and flight control system design criteria for the atmospheric flight phases of the Shuttle mission. These criteria are based primarily on Shuttle-specific simulations and on experience with high performance aircraft; however, because the Space Shuttle is a large departure from past experience, much uncertainty has existed as to the validity and application of existing criteria.

As noted by STS-4 Commander Capt. T. K. Mattingly at a recent meeting of the Society of Experimental Test Pilots, "the importance of flying qualities is inversely proportional to your altitude." Experience gained from the five ALT and first four STS flights indicate that the Shuttle flying qualities in landing leave something to be desired.

The purpose of this study is to define an effective program of flying qualities and flight control system design criteria experiments as an Orbiter Experiment (OEX) Program. The first phase effort, documented in Ref. 1, was devoted to review of existing flying quality and flight control system specification and criteria; review of Shuttle experimental and flight data; identification of specification shortcomings; and preparation of a preliminary OEX approach to produce the optimum use of flight data to develop modified flying qualities criteria for Space Shuttle craft in general. This second phase effort has been devoted to continued review and analysis of applicable experimental and Shuttle

flight data and to further definition of the OEX plan. Accordingly, this report is a direct follow-on to Ref. 1.

The OEX technical approach given primary emphasis is an "indirect" approach which is somewhat unconventional and has been developed to produce maximum useful data under the special conditions of Shuttle flights. The indirect approach consists of inflight experiments combined with a correlated research simulation program. The simulation program will allow study of critical flight situations not likely to be permitted on Shuttle flights. An unconventional feature of the approach is the use of pilot strategy (model) identification procedures in flight and simulation to connect the two in a formal way.

Section II provides a review of new data and analyses relevant to Shuttle flying qualities and flight control system design. The implications of "superaugmented" pitch attitude dynamics, first noted in Ref. 1, are further considered. New data on path dynamics and pilot location effects are reviewed and an analysis of the implications of decelerating flight on Shuttle manual control is presented. Section II ends with a summary of flying qualities/flight control system issues to be addressed in the OEX.

Section III contains a review of the STS-1 through 4 flights regarding flying qualities and manual control as extracted from flight data and pilot commentary.

Section IV presents an overview of the technical approach for the OEX plan beginning with a review of requirements and limitations for Shuttle flight experiments. The "indirect" OEX approach involving a correlated program of flight and simulator experiments linked through formal pilot model identification is presented as the best approach to cope with Shuttle-specific flight test problems.

Section V provides further details of the indirect OEX approach including development of pilot models, non-intrusive pilot technique identification procedures and instrumentation and software requirements.

Section VI presents the possibilities for the research simulation program coordinated with flight experiments for the indirect OEX plan.

## SECTION II

### CONTINUED REVIEW OF KEY FLYING QUALITY ISSUES

Extensive review of the Shuttle Orbiter flying quality and control system requirements and comparison of these with other flying quality requirements and data in Ref. 1 revealed several areas of disagreement and possible deficiencies in the Orbiter requirements. The key longitudinal issues were the allowable dead time or effective time delay,  $\tau$ ; the normalized pitch rate time response upper (overshoot) boundary; the difference between the effective vehicle pitch numerator time constant,  $T_q$ , and path response time constant,  $T_{\theta_2}$ ; and possible motion cue conflicts due to the pilot's location behind the instantaneous center of rotation for elevator inputs. Apparent disagreements between Shuttle Orbiter requirements and those of other specifications or design guides could not be resolved because the available empirical data is largely based on conventional aircraft (configurations and control system) and may not be applicable to the unconventional Shuttle Orbiter.

Following the Ref. 1 study, results of an investigation of superaugmented transport aircraft dynamic characteristics and key parameters (Ref. 2), and two sources of more appropriate in-flight simulation data (Refs. 3-6) were obtained. These appear to shed some light on unresolved questions of Ref. 1 and are reviewed in Subsections A and B respectively. Following the discussion of attitude dynamics (i.e.,  $\theta/\delta_{RHC}$ ), path dynamics (i.e.,  $h/\theta$ ) are considered in Subsection C, including a review of the present specifications and newly available data on the effects of pilot location with respect to the instantaneous center of rotation. Since the Shuttle lands as a glider, it may also be distinguished from conventional transport aircraft by significant decelerating flight conditions in landing. The significance of this face with respect to manual control is analyzed in Subsection D. Subsection E summarizes, by priority, the flying qualities/flight control system issues to be addressed in the OEX.

## A. FLYING QUALITY CONSEQUENCES OF SUPERAUGMENTATION

### 1. Pitch Attitude Short-Term Characteristics

Those aircraft control functions which demand the greatest pilot attention and skill require primary consideration in flying qualities assessments. Probably the most demanding high workload pilot/aircraft closed-loop control operations involve precision path control in unfavorable environmental conditions. All flight phases require some form of path control, which incorporates both flight path changes and flight path maintenance or regulation. In most ordinary flight circumstances, path control, while an essential pilot skill, is nonetheless a relatively benign and low-stress function. On the other hand, when the path task is itself very demanding and the environment unfavorable (e.g., low visibility approach and landing in turbulence and shear), the precision path control task becomes exceedingly exacting. Thus precision path control is used here as the control task to explore the effects of heavy augmentation on closed-loop pilot/aircraft system flying qualities.

A block diagram that indicates the pilot's activities in precision path control is shown in Fig. 1. On the right the augmented aircraft has path deviation and pitch attitude as the output variables stemming from aircraft dynamics which are forced by external atmospheric disturbances and the pilot control output,  $\delta$ . The augmented aircraft itself is a closed-loop system comprising the airplane-alone and augmentation system. Thus, the sensors, computation, and actuation elements involved in the feedback control augmentation system, as well as the aircraft, are encompassed by the "Augmented Aircraft Pitch Dynamics" block in Fig. 1. (An underlying assumption in this diagram is that other aircraft control effectors such as speed brake or body flap are not being continuously modulated by pilot control action; trim management using these aircraft effectors, however, is not excluded.)

Even though trimmed precisely, the augmented aircraft will not by itself maintain exactly the prescribed path and attitude in the presence of disturbances. Consequently, the pilot must exert control not only to

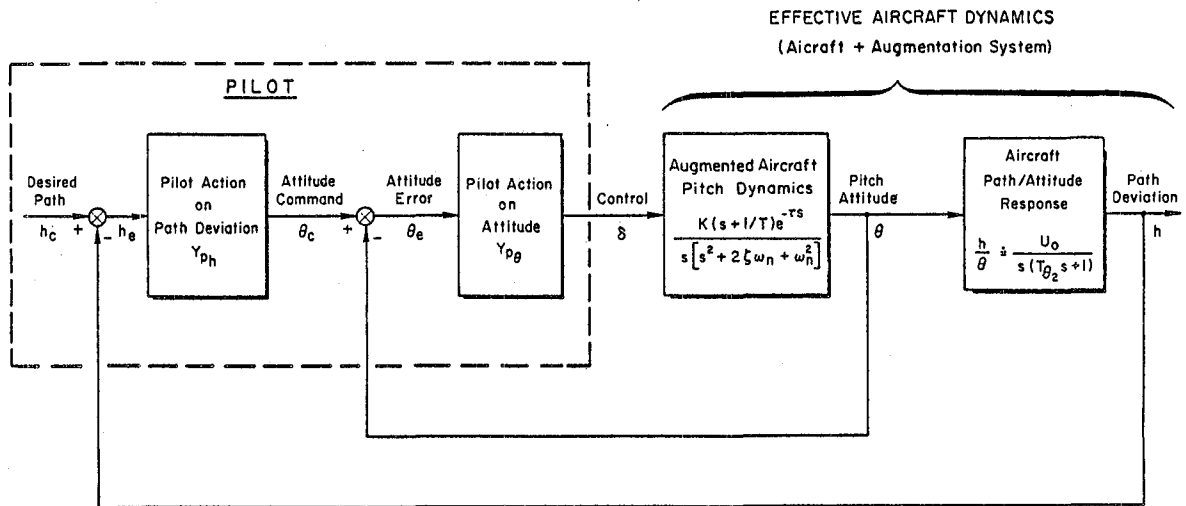


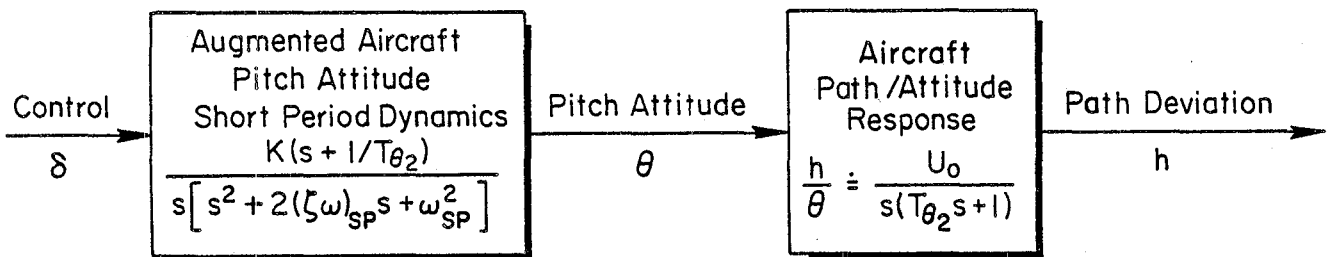
Figure 1. Closed-Loop Precision Path Control with  
Attitude Control Inner Loop

establish the desired path but also to correct any deviations from the desired attitude and path. This is accomplished by the pilot acting as a closed-loop controller, which means simply that the pilot's control output is dependent on (i.e., a function of) path deviation and attitude. Thus, a component of the pilot's control output is correlated with an attitude error, and another component is correlated with the difference between the desired and actual path. This relationship is depicted in the Fig. 1 block diagram as a "series" pilot closure, i.e., the pilot's action on path deviation acts in series with, and provides an internal "attitude command" for, the pilot's action on attitude error. These pilot activities are represented in Fig. 1 by the symbolic transfer characteristics  $Y_{ph}$  and  $Y_{p\theta}$ . Several research studies using elaborate and detailed measurements of just this situation (e.g., Refs. 7 and 8) indicate that this series structure and general pilot behavior control model is appropriate for path control situations. In essence, the pilot's higher-frequency control actions are devoted primarily to attitude so that the "inner" attitude loop is tightly closed, and the attitude is well regulated. This tight inner loop makes possible the effective closure of the "outer" path deviation loop without

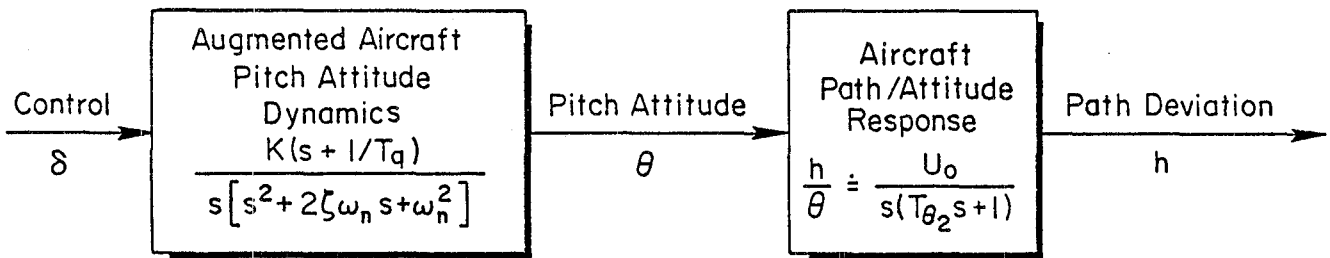
excessive pilot equalization or compensation. Without good control of attitude the pilot would have to be way ahead of any path changing trends, requiring very difficult anticipation and high workload. (Examples include altitude control using only airspeed and altimeter or control during approach using only airspeed and the raw ILS glidepath data.) If the attitude loop is difficult for the pilot to interact with and close (i.e., if the augmented aircraft pitch attitude dynamics are deficient in that they require excessive pilot compensation and attentional workload), attitude control will suffer directly and path control indirectly.

It will evolve below that a key issue in the differences between the flying qualities of conventionally augmented aircraft and superaugmented aircraft resides in the differences in the transfer characteristics for the augmented pitch attitude and the similarities for the path/attitude response. By focusing on these facets we can expose the major differences between heavy and conventional augmentation without an elaborate argument involving the pilot's detailed control actions. It is extremely important to recognize, however, that the closed-loop piloting aspects are a central issue in that the pilot's assessment of the suitability of the aircraft inherently depends upon his actions required to accomplish control. (As an adaptive controller the pilot adjusts his control actions as needed to compensate for the aircraft dynamics; so different aircraft dynamics mean different pilot actions and different pilot assessments.) Thus, the feedback loop structure and what the pilot actions are in responding to path deviation and attitude are of central concern to set the context of the control task. Yet, within this context, one can focus primarily on the augmented aircraft pitch dynamics and the aircraft path/attitude response to explore differences between conventional and highly-augmented aircraft.

Figure 2 shows a simplified comparison of conventional and heavily augmented aircraft dynamics. The latter represents the closed-loop dynamics of the aircraft plus augmentor when idealized at the superaugmented extreme. The term "superaugmentation," as used here, implies little or no dependence of the closed-loop attitude/pilot control



*a) Conventional Aircraft*



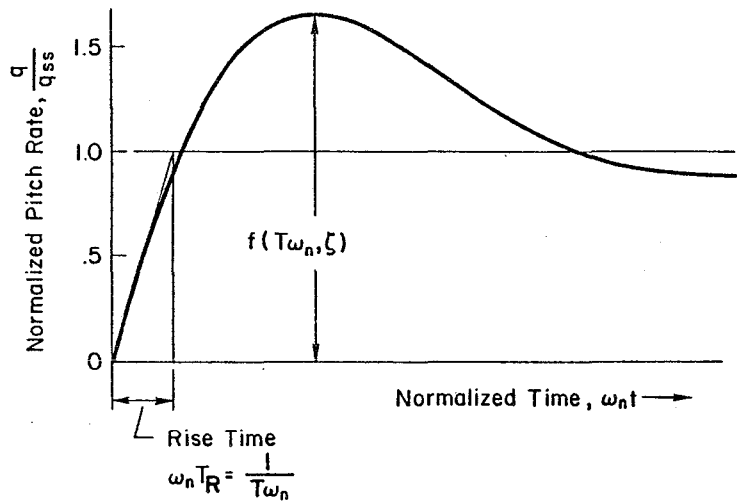
*b) Superaugmented Aircraft*

Figure 2. Effective Aircraft Dynamics (Aircraft + Augmentation System) for Conventional and Superaugmented Aircraft

responses on the airframe-alone lead ( $T_{\theta_2}$ ) and short period divergence and subsidence ( $T_{sp_1}$  and  $T_{sp_2}$ ) modes. The two blocks for each case constitute the effective aircraft dynamics portion of the total precision path control system of Fig. 1. The distinction between conventional and superaugmented closed loop aircraft/augmentation system dynamics is present in the pitch attitude characteristics block. Although the forms are the same, the parameters are different in both the numerator lead and the denominator quadratic which describes the aircraft's high frequency (short-time) attitude response characteristics. As shown in Refs. 2 and 9, the key distinctions are:

- The aircraft path/attitude response,  $h/\theta$ , is the same for both conventional and superaugmented aircraft;
- The augmented aircraft pitch attitude short-term characteristics differ in that:
  - 1) The lead,  $T_{\theta_2}$ , for the conventional aircraft is the same as the path/attitude lag whereas the lead for the superaugmented aircraft,  $T_q$ , may be quite different from  $T_{\theta_2}$ .
  - 2) The undamped natural frequency and damping of the effective short-period mode for the conventional aircraft depends primarily on aircraft flight condition, weathercock stability, and pitch damping (sometimes augmented).
  - 3) The undamped natural frequency and damping for the superaugmented aircraft depends predominantly on the augmentation system (lead and gain) and aircraft control effectiveness ( $M_\delta$ ) parameters.
- The low frequency and trim characteristics for the conventional aircraft are not reflected by the short-period attitude dynamics approximation, whereas the superaugmented aircraft pitch attitude dynamics are appropriate for low frequency and trim.

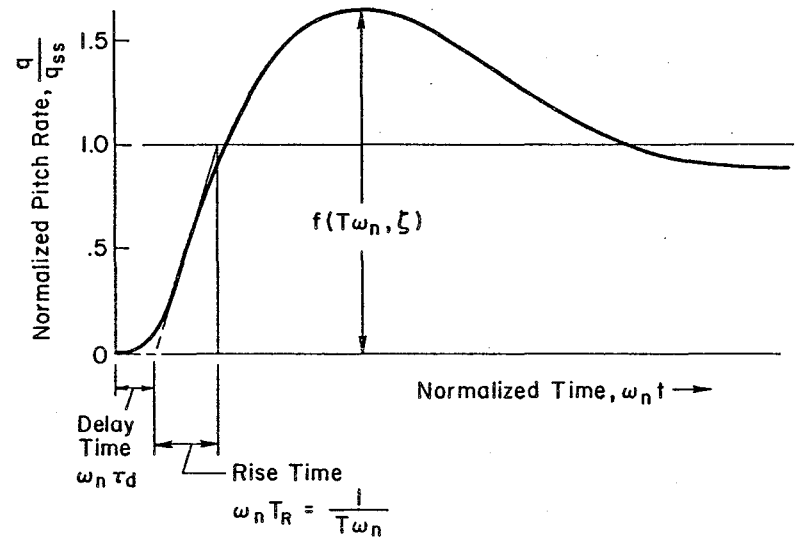
A comparison of the key pitch attitude response parameters for conventional aircraft and for superaugmented aircraft is accomplished in Table 1 and Fig. 3. Figure 3a is idealized with no control system or other lags between the pilot step function input and the control effects. Figure 3b includes such delays and approximates their net effect as a dead time  $\tau_d$ . For the conventional airplane, covered at the left, the table reiterates that the attitude lead and short-period



General Form:

$$\frac{q}{q_{ss}} = \frac{(Ts+1)}{s \left[ \left( \frac{s}{\omega_n} \right)^2 + \frac{2\zeta_n}{\omega_n} s + 1 \right]}$$

a) *Idealized Dynamics for a Superaugmented Aircraft or for Short-Period Attitude Dynamics for a Conventional Aircraft With Large Static Stability*



General Form:

$$\frac{q}{q_{ss}} = \frac{(Ts+1)e^{\tau_d s}}{s \left[ \left( \frac{s}{\omega_n} \right)^2 + \frac{2\zeta}{\omega_n} s + 1 \right]}$$

b) *Attitude Dynamics With Effective Time Delay*

Figure 3. General Pitch Rate Response to Step Pilot Input

TABLE 1. COMPARISON OF PITCH ATTITUDE RESPONSE GOVERNING PARAMETERS FOR CONVENTIONAL AND SUPERAUGMENTED AIRCRAFT

DYNAMIC PROPERTY	CONVENTIONAL		SUPERAUGMENTED	
	PARAMETERS	PRIMARY DESIGN FACTORS	PARAMETERS	PRIMARY DESIGN FACTORS
Lead Time Constant T	$\frac{1}{T_{\theta 2}} = -Z_W + \frac{Z_{\delta}}{M_{\delta}} M_W$	Set Predominantly by Airframe $C_{L\alpha}$ ; wing Maneuver Margin; $C_{MCL}$ ; Tail	$T_q$	Closed-loop control system Stability Response, and Margins  <b>Control System Parameters</b> $T_q$ - Lead time constant $K_q$ - Gain  <b>Airframe Parameter</b> $M_{\delta}$ - Surface effectiveness ( $C_{m\delta}$ )
Undamped Natural Frequency $\omega_n$	$\omega_{sp}^2 = Z_W M_q - M_{\alpha}$		$\omega_n^2 = \frac{\omega_{ca}}{T_q} = \frac{K_q}{T_q} [M_{\delta}]$	
Normalized Rise Time $\omega_n T_r$ Rise Time $T_r$	$\frac{1}{T_{\theta 2} \omega_{sp}}$		$\frac{1}{T_q \omega_n} = \frac{1}{\sqrt{T_q \omega_{ca}}}$  $\frac{1}{\omega_{ca}}$	
Damping Ratio $\zeta$	$(\zeta \omega)_{sp} = -(Z_W + M_q + M_{\alpha})$	$C_{L\alpha}$ ; Wing $C_{mq}$ ; Tail Pitch Damper	$\zeta = \frac{\sqrt{T_q \omega_{ca}}}{2} = \frac{1}{2} \sqrt{K_q T_q} [M_{\delta}]$	
Delay Time $\tau_d$		Actuator and Manual Control lags	Actuator lag + Stick filters + Bending Mode filters + Computational delays	

undamped natural frequency, and hence the rise time in Fig. 3a, depend primarily on aircraft configuration characteristics and the way the aircraft is balanced. The damping ratio also is predominantly a function of configuration, although a pitch damper can provide a good deal of design latitude.

For the superaugmented aircraft, there is a relative lack of sensitivity to aircraft configuration characteristics and dominance of the controller properties as they affect the closed-loop aircraft/augmenter system. As can be seen from Table 1 the factors underlying the dynamics of the superaugmented vehicle are the closed loop crossover frequency (of the asymptote),  $\omega_{c_a}$  and the controller lead  $T_q$ . The crossover frequency is given by

$$\begin{aligned}\omega_{c_a} &= K_q M_\delta \left( 1 + \frac{Z_\delta}{M_\delta} M_w^* \right) \\ &\doteq K_q M_\delta\end{aligned}\tag{1}$$

It is of overwhelming importance because it defines:

- The total system gain comprising both controller ( $K_q$ ) and aircraft control effectiveness ( $M_\delta$ ) parameters.
- The system bandwidth, which indicates the frequency range of good command following and disturbance suppression.
- The rapidity of system response, i.e., rise time  $T_r = 1/\omega_{c_a}$ .
- The system damping ratio, in that  $\omega_{c_a}$  is a key factor (together with the controller lead time constant,  $T_q$ ) in setting the damping ratio,  $\zeta$ .

The first three properties of the crossover frequency listed above are qualitatively applicable to all feedback control systems which have a low-pass closed-loop character. (Low pass here means that at frequencies up to the bandwidth the output follows the input quite well, whereas at higher frequencies the output will drop off in amplitude relative to the input -- thus the low frequencies are "passed" through the system while frequencies higher than the bandwidth are attenuated or "not passed.") The fourth property is a special one for superaugmented

systems which share the specific characteristics of the example case. It is one reflection of the idealized superaugmented situation wherein only two parameters, the attitude lead ( $T_q$ ) and crossover frequency ( $\omega_{c_a}$ ), define all the system input/output characteristics except the overall response scaling between output and input.

Another manifestation of the two-parameter character of the idealized superaugmented aircraft can be seen in connection with the maximum pitch rate overshoot versus  $1/T_q \omega_n$ . This is shown in Fig. 4. The possible variation in damping ratio, overshoot, and normalized rise time for a superaugmented transport aircraft is encompassed by the straight line. Notice that for a normalized rise time of 1, the damping ratio is 0.5 and the undamped natural frequency is  $1/T_q$ . At the other end is a normalized rise time of 0.5, accompanied by a  $\zeta = 1$  and an  $\omega_n = 2/T_q$ . Any system between these two extremes has excellent closed-loop control, system stability, and margins. Again the parameters which set the actual location on the attainable line are the crossover frequency,  $\omega_{c_a}$ , and the control system lead time constant,  $T_q$ .

It is instructive to compare the pitch overshoot variation with static margin of conventional aircraft Fig. 5, with the Fig. 4 law of overshoot for superaugmented airplanes (Ref. 2). As noted above, for the conventional case the usual variable is the way the aircraft is balanced, i.e., the static margin, whereas in the superaugmented case the  $\omega_{c_a} T_q$  product provides the variation. The first thing to notice is that the trends are in somewhat different directions relative to the background constant damping ratio ( $\zeta$ ) coordinates. For the conventional aircraft (Fig. 5), increased static margin has a concomitant increase in the undamped natural frequency and decrease in the normalized rise time. This aspect is similar to that for  $\omega_n$  and normalized rise time,  $1/T_q \omega_n$ , for the superaugmented aircraft. On the other hand, the damping ratio of the short period decreases and the overshoot increases for the conventional aircraft, while the opposite trend is present for the superaugmented airplane.

A major distinction can also be made between the superaugmented and conventional aircraft with reference to the aerodynamic characteristics

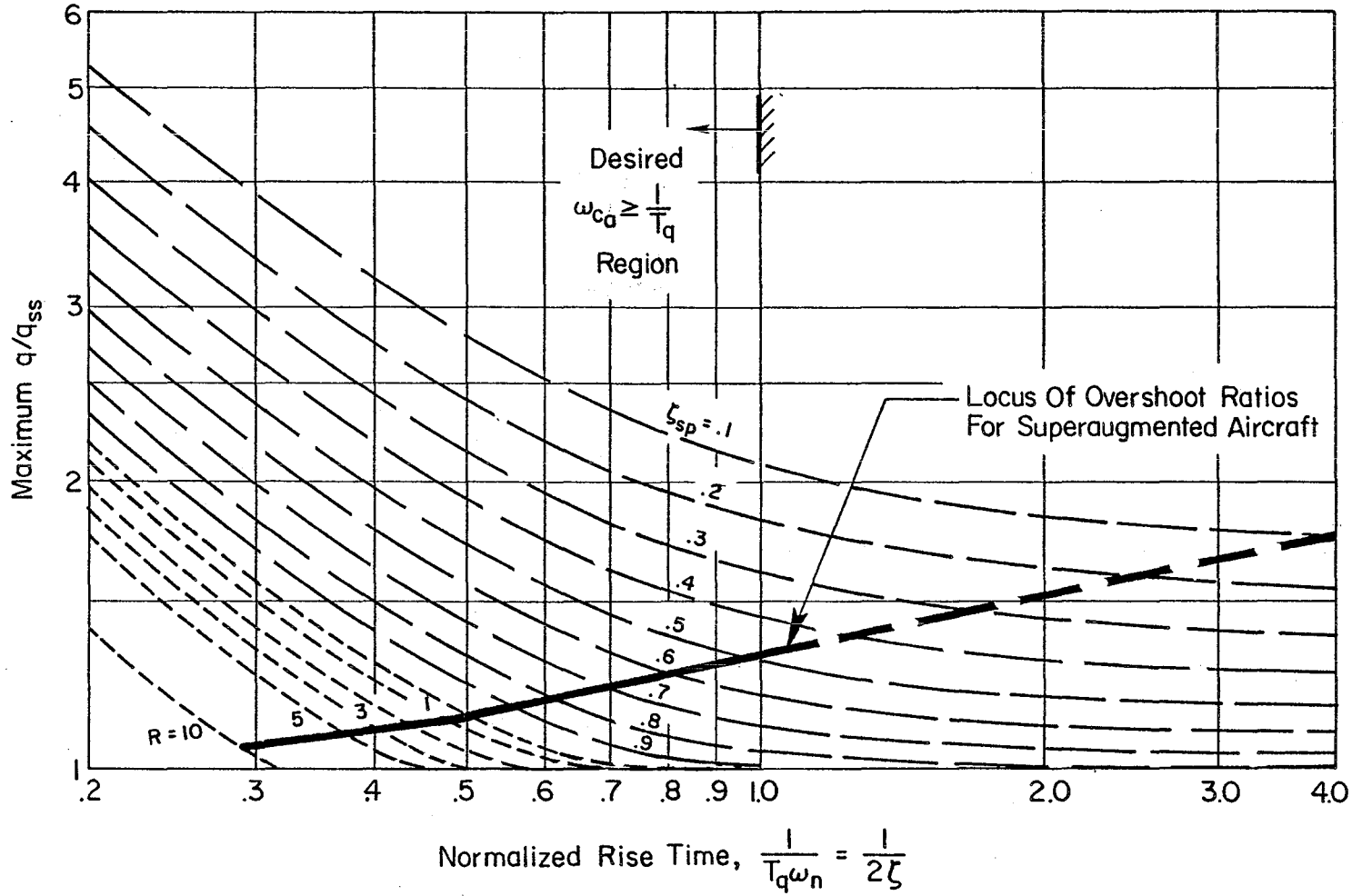


Figure 4. Maximum Pitch Rate Overshoot Variation for Superaugmented Aircraft

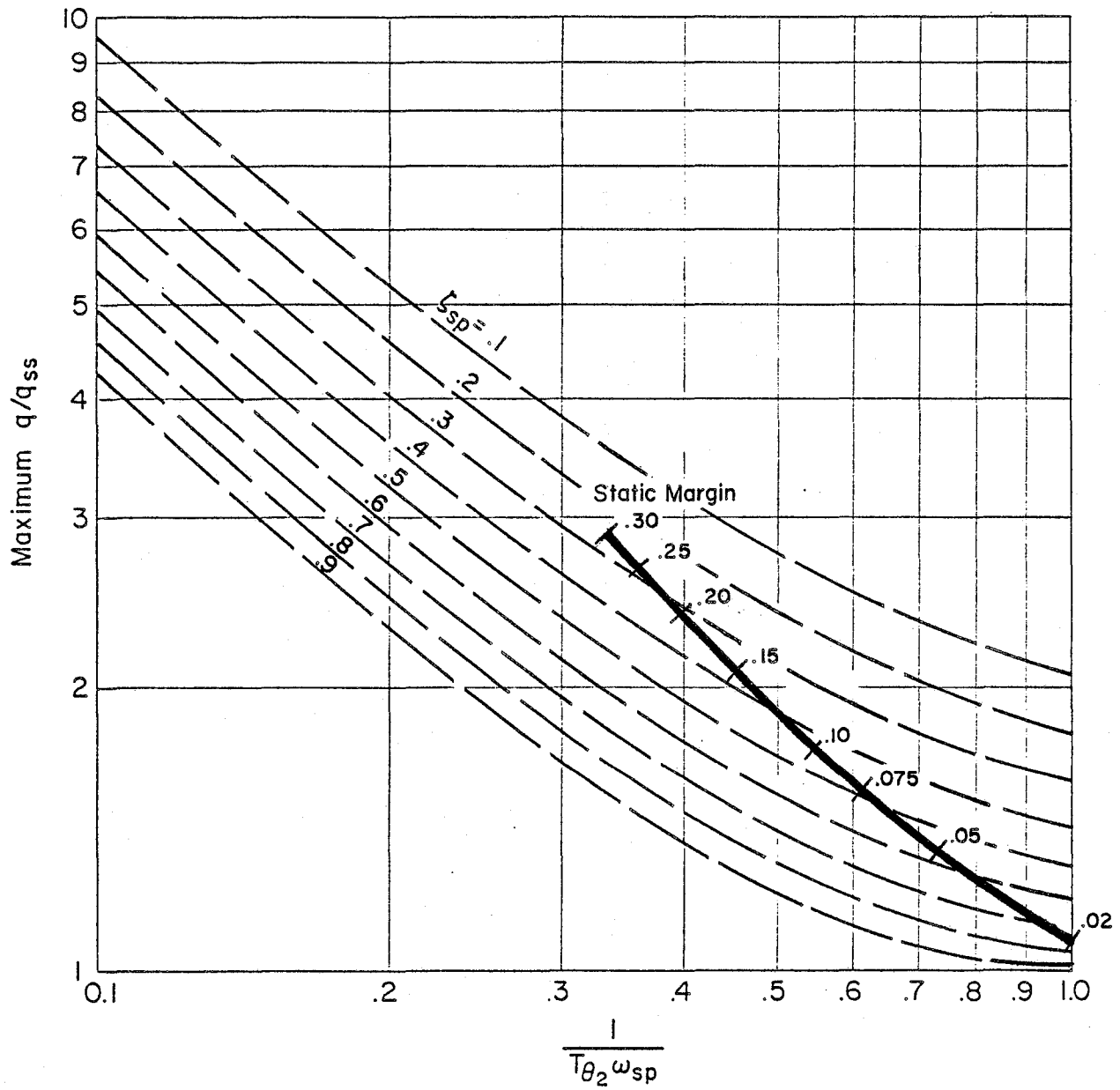


Figure 5. Pitch Overshoot Variation with Static Margin for Conventional Aircraft (Generic Aircraft in Cruise)

which underlie their responses. For the conventional aircraft, even in the short period, the stability derivatives  $Z_w$ ,  $M_q$ , and  $M_\alpha$  together with their variations with flight condition, are major governing parameters. When the complete three-degree-of-freedom airplane characteristics are also taken into account, several more derivatives become important (e.g.,  $Z_u$ ,  $M_u$ ,  $X_w$ , etc.). On the other hand, to the extent that the augmentation system can be made to approach the superaugmented characteristics, the aerodynamic parameters of importance reduce to the surface effectiveness,  $M_\delta$ . Potential variations in other derivatives must, of course, be assessed in the design process to assure that no possible variation could upset this appellation, but in actual system operation the primary sensitivity and variations of interest are those of  $M_\delta$ . In some ways, this sparsity of airplane-characteristic-dependence for aircraft which approach the superaugmented state offers a major advantage when one is faced with identifying the effective airframe from flight data or in validating various simulations.

Finally, the ultimate comparison of the conventional and superaugmented vehicles is connected with the closed-loop precision path control flying quality aspects. As shown in Fig. 2, the attitude leads are either  $T_{\theta_2}$  (conventional) or  $T_q$  (superaugmented), while the undamped natural frequency and damping ratio of the superaugmented vehicle are unrelated to those of the conventional short period. Thus, as already noted, the augmented aircraft pitch attitude dynamics are potentially fundamentally different than those of a conventionally augmented aircraft. Not the least important of these differences is the replacement of the  $T_{\theta_2}$  lead by  $T_q$ , for now the attitude lead is not the same as the path/attitude response lag (which is  $T_{\theta_2}$  for both the conventional and superaugmented situations). On the Shuttle, there is a substantial difference between these two properties. In a typical approach flight condition the value of  $1/T_{\theta_2}$  is about  $0.54 \text{ sec}^{-1}$  whereas  $1/T_q$  is  $1.5 \text{ sec}^{-1}$  (Ref. 1). This difference between the attitude/path lag and the effective lead in pitch attitude, as well as the potential differences in the basic high-frequency response mode, may be of fundamental importance in flying qualities and flying qualities research.

## 2. RHC Force Variation With Speed

For conventional, statically stable aircraft it is expected that there will be no tendency for airspeed to diverge aperiodically when the vehicle is disturbed from trim with the cockpit controls fixed or with them free. Further, stable control gradients are generally specified which result in increasing pull forces and aft motion of the longitudinal pitch control to maintain nose-up attitudes at slower speed and the opposite to maintain nose down attitudes at faster airspeeds. This positive stick force gradient with speed change fundamentally assures the absence of an aperiodic divergence, permits trimability in both a short and long term framework, and provides tactile feedback cues to the pilot to indicate desirable or undesirable airspeed deviation from trim. It thus tends to minimize pilot workload during combined attitude/path/airspeed control.

This conventional airplane situation has long been codified in requirements and specifications. For example, the U.S. Federal Air Regulations (FAR), Part 25 (Ref. 10), paragraph 25.173a states:

"A pull must be required to obtain and maintain speeds below the specified trim speed and a push must be required to obtain and maintain speeds above the specified trim speed."

Similar requirements have been included in the U.S. military flying qualities specifications (e.g., paragraph 3.2.1.1 of MIL-F-8785B and C, Refs. 11 and 12).

Let us turn now to the relaxed static stability Shuttle orbiter equipped with an augmentation system which, in its essentials, corresponds to that shown in Fig. 6. For this aircraft/augmentor combination, the closed-loop system will be stable and will exhibit no aperiodic divergences. The basic system, however, is one which is rate-command/attitude hold, so that the pilot command  $\delta_{e_p}$  gives rise to a pitch rate (even in the steady state) rather than to a (steady state) pitch attitude as in the conventional aircraft. The control system when not activated by the pilot thus fundamentally maintains the airplane trim in attitude, rather than in angle of attack (or its surrogate, speed). The stick force gradient with speed is, in fact, zero.

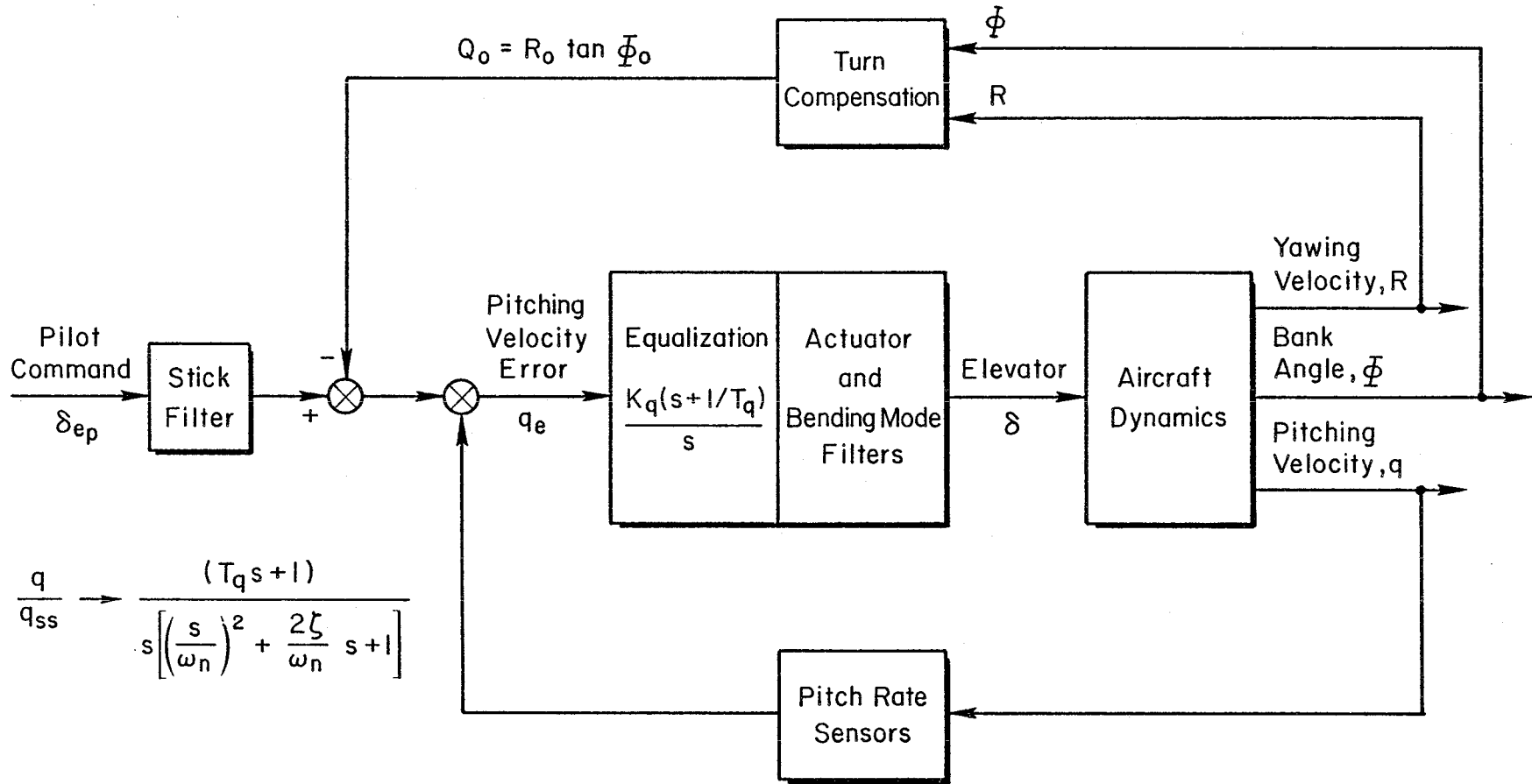


Figure 6. Pitch SAS for Shuttle

The original (1973) Shuttle flying qualities spec, Ref. 13, contained a single "Controller-Speed Characteristics" requirement, paragraph 3.4.3.6:

"With all other controls fixed, aft motion of the pitch control shall be required to initiate a change to a slower airspeed in forward motion to initiate a change to a faster airspeed."

The use of the word "initiate" is significant -- in relation to the phrase "obtain and maintain" in the FAR -- because it does not require a stick force to maintain a steady state change in airspeed. This fact, coupled with the explicit requirement for a pitch rate command system in Ref. 13 implies recognition and acceptance of neutral speed stability. However, the value of paragraph 3.4.3.6 is questionable because it is hard to imagine an aircraft which could not meet it.

The present MIL-Spec, Ref. 12, does explicitly allow for zero (and even negative) stick force/speed gradient, i.e., paragraph 3.2.1.1:

"...This requirement will be considered satisfied if stability with respect to speed is provided through the flight control system, even though the resulting pitch control force and deflection gradients may be zero."

This particular paragraph was, in fact, placed in MIL-8785C as a recognition of the generally favorable features of rate command, attitude hold systems. These are made manifest by many simulations and flight experiment results with augmentation systems akin to that of Fig. 6 wherein the neutral speed stability has not been an important issue when contrasted with the very favorable features provided by the rate command/attitude hold augmentation (e.g., Refs. 14-16). The need for positive stick force stability with pitch rate command/attitude hold systems was specifically addressed in the flight tests of Refs. 16, 17. The conclusion was that there were no clear advantages to positive over neutral speed stability, at least when the aircraft was operated at the bottom or front side of the thrust required versus speed curve. The fundamental attitude stability, as opposed to weathercock stability, is ordinarily very favorable in terminal operations and other conditions wherein atmospheric disturbances can seriously affect precision path control. On the other hand, the development of proper pilot technique

appears to require some initial familiarization, especially in landing. The initial tendency, which is rapidly corrected by one or two practice landings, is to land long.

The above discussion of speed stability is based on experience with conventional aircraft which have constant speed approaches. The Shuttle is in decelerating flight during its final landing phases and the desirability or even acceptability of speed stability is not clearly established. The influence of deceleration on the Shuttle landing task will be further considered in Subsection D.

There is another feature of rate command/attitude hold systems which has received some pilot comment. Consider, for instance, that at the outset of flare, the aircraft is in trim and the pilot begins to pull back to reduce the sinkrate. As the aircraft begins to enter ground effect the pilot in a conventional aircraft will tend to pull further. Thus, in landing a conventional aircraft without any trim adjustment, the pilot is holding back pressure on the column. If now, a corrective change is required in pitch attitude, the pilot accomplishes it either by further back pressure or a slight release of the back pressure. For the rate command/attitude hold type system, however, no back pressure is held. Consequently, if the attitude is to be reduced, the pilot must move the control forward from its neutral position. This feature of rate command/attitude hold systems has sometimes been remarked as undesirable and can be conducive to PIO due to the additional pilot latencies involved, controller thresholds about neutral, force break-outs, etc.

From the above comments, it can be appreciated that a distinct tradeoff exists between the good features of aircraft which approach superaugmented configurations and a conventional statically stable aircraft as far as the trimability features are concerned. Some have "solved" this type of problem by using a lag-lead for the augmentor equalization instead of the integrator lead combination of Fig. 6 (Refs. 18, 19, and 20) at the cost of retaining a long term divergence. Others have considered the augmentation of  $M_{\alpha}$  or  $M_u$  instead of creating a pitch attitude related stability. These can introduce unfavorable

effects of a different kind and are not as straightforward in mechanization, especially in multiple redundant flight critical situations.

### 3. Alternative Augmentation Considerations

The preceding has shown that the Shuttle relaxed static stability configuration and attendant  $(q + \int q) + \delta$  augmentation mechanization is responsible for its unconventional pitch dynamic characteristics and neutral speed stability. The obvious question becomes "what if the augmentation mechanization is changed?" It was indicated before that for the relaxed static stability airframe two general effects were important. The first was to increase static stability and the second was to improve the short period damping. Those quantities useful for increasing the static stability fall into two fundamental categories. The first involve creation of an effective pitching moment proportional to an attitude quantity, such as the pitch attitude,  $\theta$ , itself or an integral of pitching velocity,  $\int q dt$ . In this same class is the integral of normal acceleration because  $a_z$  is a linear function of the pitching velocity,  $q$ . With these systems, the effective aircraft dynamics include a new or created stability derivative, such as  $M_\theta$ , which is not present in the conventional aircraft dynamics. The aircraft tends to be attitude stable rather than stable relative to angle of attack or speed. It assumes a rigidity in pitch attitude rather than a stability relative to the air mass. These types of systems therefore provide an attitude hold feature in addition to stabilizing the divergence. At the same time, the speed stability for the primary pilot command is neutral as discussed in the last article.

In counterdistinction to the attitude type of system are those wherein an attempt is made to augment naturally occurring stability derivatives of the airplane alone for correction of a reduced static margin. This implies augmentation of  $M_\alpha$  or  $M_u$ . In either of these cases, the speed stability will not be neutral. The nature of the speed stability therefore serves as a fundamental distinction between systems. This is reflected in Tables 2 and 3 which are taken from Ref. 2. Those systems with neutral speed stability, that is systems based on attitude,

TABLE 2. SYSTEM ARCHITECTURAL POSSIBILITIES AND MECHANIZATIONAL SIDE EFFECTS FOR SUPERAUGMENTED AIRCRAFT  
Systems Based on Attitude, Pitch Rate, or Normal Acceleration

---



---

$q \rightarrow \delta_e$

Reduces divergences, but does not get all the way to stability.  
Requires some up-elevator relief in turns; e.g.,  $q_e = q - R_0 \tan \phi_0$

$\int q dt, q \rightarrow \delta_e$

Generally suitable for complete correction of instability.  
Requires up-elevator relief in turns; e.g.,  $q_e = q - R_0 \tan \phi_0$

$\int a_z dt, G_{wo}q \rightarrow \delta_e$  ( $G_{wo}$  = Washout equalization)

Corrects for instability when operating on the frontside of the speed/power curves. Can have backside instability and equivalent backside in climbs.  
Has bias ( $a_{z_0} \neq 1 g$ ) when accelerometer is not oriented along stability axis for level flight; further bias in climbs and dives; yet another bias with a roll limit cycle.  
Requires up-elevator relief in turns; e.g.,  $a_{z_e} = a_z - \cos \theta_0 \sec \phi_0$  plus increment for  $q$  feedback in turn entry/exit.  
Requires more airspeed compensation than attitude-based systems.

$1/(\hat{T}_{\theta_2}s + 1) \int Uq dt, G_{wo}q \rightarrow \delta_e$  [Pseudo  $a_z$ ]

Generally suitable for complete correction of instability (replaces  $dy/dV$ -based limitations with  $1/T_{\theta_1}$ ; removes accelerometer bias issues).  
Requires up-elevator relief in turns.  
Requires more airspeed compensation than attitude-based systems.

$\theta, \dot{\theta} \rightarrow \delta_e$

Generally suitable for complete correction of instability.  
Gain changes in turns, with associated  $F_s/g$  lightening, etc.  
Requires elevator signal relief (trim) for  $\theta \neq 0$ .

$\theta, q$  or  $\theta, G_{wo}q \rightarrow \delta_e$

Generally suitable for complete correction of instability.  
Gain changes in climbing/diving turns.  
Climb/dive steady-state signal relief.  
Requires up-elevator relief in turn entries/exits, depending on specifics of  $G_{wo}$ .

---



---

TABLE 3. SYSTEM ARCHITECTURAL POSSIBILITIES AND MECHANIZATIONAL  
SIDE EFFECTS FOR SUPERAUGMENTED AIRCRAFT  
Systems Based on Angle of Attack or Speed

---



---

$\alpha_A, q$  or  $\alpha_A, G_{wo}q \rightarrow \delta_e$  ( $\alpha_A$  = aerodynamic  $\alpha$ )

Generally suitable for correction of instability.  
Phugoid not much modified if  $G_{wo}$  focuses only on high frequencies.  
Gust sensitivity associated with  $\alpha_A$ .  
 $\alpha_{bias}$  position and scale factor errors ( $\alpha$  sensor installation).  
Requires trim set point.  
Requires up-elevator relief in turn entries/exits, depending on specifics of  $G_{wo}$ .

$\alpha_I, q$  or  $\alpha_I, G_{wo}q \rightarrow \delta_e$  ( $\alpha_I$  = inertial  $\alpha$ )

Generally suitable for correction of instability.  
Phugoid not much modified if  $G_{wo}$  focuses only on high frequencies.  
Requires trim set point.  
Requires up-elevator relief in turns, depending on specifics of  $G_{wo}$ .

Variants of  $\alpha$  Systems

$$\hat{\alpha} \doteq \frac{U_0}{[Z_w - M_w(Z_\delta/M_\delta)]} \frac{a_z}{U^2}$$

and other means of computing  $\alpha$ .

$u_I, G_{wo}q \rightarrow \delta_e$  ( $u_I$  = inertial  $u$ )

Generally suitable for correction of the instability.  
May be subject to excessive pitching with a  $u_g$  input.  
Must establish a set point or trim,  $U = U_0$ .  
Phugoid damping ratio is reduced if  $G_{wo}$  focuses only on high frequencies.  
Requires up-elevator relief in turns, depending on specifics of  $G_{wo}$ .

$u_A, G_{wo}q \rightarrow \delta_e$

As in item above.  
Gust Sensitivity associated with  $u_A$ .  
Scale and bias errors associated with  $u$  sensor installation.

---



---

pitch rate or normal acceleration, are assigned to Table 2, whereas those with non-neutral speed stability, based on angle of attack or speed, are listed in Table 3.

Other important distinctions between possible systems are very much architectural dependent. These are considered side effects and can be more or less corrected by increasing the degree of complexity in the system design. They amount to those incidental features of a particular system mechanization which are over and above its primary purpose of improving static stability and short period damping. In the Shuttle (Fig. 6) system, the primary side effect was the need to provide an up elevator compensation in turns proportional to  $R_0 \tan \Phi_0$  to offset the steady state pitching velocity that occurs in turning. In Table 2 the Shuttle system is the second one listed,  $\int q dt, q \rightarrow \delta_e$ .

When other sensors, such as normal accelerometers, pitch gyros, etc. are used, the side effects may become more involved. They derive, in general, from three sources.

- Biases associated with the particular instrumentation used in the system, e.g., normal accelerometers pick up the total acceleration whereas the augmentation system ideally needs only acceleration perturbed from steady state conditions.
- The degree of airspeed compensation for adjustment of the augmentor system total open loop gain. This differs with the nature of the sensor (e.g.,  $a_z$  has a component  $U_0 q$  so normal accelerometer based systems will typically require a greater range of airspeed compensation than will  $\theta$  or  $q$  based systems).
- The potential for correction of the aperiodic divergence is different for different feedback quantities (e.g., the  $a_z/\delta_e$  airplane transfer function has a low frequency zero,  $1/T_{h1}$ ,\* which can, itself, be negative. When this is the case, the divergence due to the negative static margin cannot be stabilized but simply approaches the value of  $1/T_{h1}$ ).

---

\* $1/T_{h1} = (1/3)(dy/dV)$  when expressed in degrees/knot.

Table 2 summarizes these side effects for the attitude type neutral stability systems. The effects on flying qualities depend inherently on the degree to which these characteristics are corrected. The issue for a given system then becomes how far one must go to correct the side effect created by the architectures selected. These are matters which have not been investigated on a comprehensive basis for the type of systems described in Table 2.

Relaxed static stability aircraft which are heavily augmented with systems based on angle of attack (e.g., F-16) or speed to correct any static divergences have effective aircraft dynamic characteristics which are essentially conventional in form. This is particularly true as far as piloted control is concerned because the derivatives  $M_\alpha$  or  $M_u$  for static stability correction are simply augmented to stabilizing levels. For aircraft responses to disturbances however, a distinction between conventional and heavily augmented aircraft may be pertinent depending upon the nature of the sensors used in the augmentation system. The disturbance sensitivities will specifically depend on whether an angle of attack system is based upon an inertial or aerodynamic angle of attack; similarly, for a speed system on whether inertial or air speed is used. The primary difference, however, between these types of systems and those based upon some form of attitude is in the nature of the stabilizing characteristic. The angle of attack system tends to stabilize the aircraft relative to the instantaneous (in the case of aerodynamic  $\alpha_A$ ) or steady state (for inertial  $\alpha_I = W/U_0$ ) velocity vector orientation. This is, in essence, a weathercock stability and may involve significant pitching. The speed based systems create pitching moments proportional to changes from a trim or set speed  $U_0$ . There can be significant sensitivity to shears and forward gusts with this type of system since the aircraft must pitch to accomplish a balance of fore and aft forces.

Neither the angle of attack nor incremental speed feedbacks are especially simple to instrument, particularly on a multiple redundant basis and over the extraordinarily wide flight regimes of the Shuttle. Systems of this type are more likely to involve sophisticated state

reconstruction filters or observers and computation to generate the appropriate feedback signals. Unlike the attitude variety feedbacks, which do an excellent job in stabilizing the phugoid characteristics, angle of attack and speed are by themselves not particularly valuable in improving the phugoid dynamics. Indeed, in a normal airplane, the phugoid oscillation has very small angle of attack changes. The stability derivative,  $M_{\dot{u}}$  tends to affect the phugoid frequency rather than its damping, which would require the creation of a new derivative,  $M_{\dot{u}}$ . This type of phugoid damping improvement, unfortunately, can create some exciting pitching motions when the aircraft is disturbed by forward gusts or shears. Consequently, in both types of systems, a certain amount of pitching velocity or its equivalent is desirable at phugoid frequencies to improve the phugoid damping. These are indicated by the  $G_{w\dot{o}q}$  terms in Table 3, which signify a washed-out pitching velocity feedback or its equivalent. This type of feedback is, of course, also very effective for short period damping augmentation. When it is used for this purpose, with gains that are suitable for relatively heavily augmented aircraft, then the effective short period characteristics are dominated by the pitching velocity feedback. They can then be very similar to those of the attitude based systems as far as the short term time response characteristics are concerned. For potential Shuttle application the list of side effects for the angle of attack or speed base systems does not compare favorably with those for the attitude systems.

Because pitching velocity feedbacks are likely to be present with relatively high gains in the Table 3 systems, the general issue of a distinction between an effective pitch attitude numerator lead,  $T_q$ , contrasting with the flight path lag,  $T_{\theta_2}$ , present in the idealized super-augmented configuration is potentially present with these systems as well. Thus the conclusions previously drawn on this issue and those of the distinctions between  $\omega_n$  and  $\zeta$  with the conventional aircraft short period dynamics will apply.

## B. RECENT EXPERIMENTAL RESULTS RELEVANT TO SUPERAUGMENTATION

### 1. Two Recent Simulation Studies

Two recent simulation studies provide the best available data relevant to the flying qualities of superaugmented aircraft. The program discussed in Refs. 3 and 4 involved simulation of a relaxed static stability (RSS) version of the Fokker F-28 medium transport on the NLR ground simulator and on the Calspan TIFS aircraft. A rate-command attitude hold FCS was employed which was somewhat different in concept from the Shuttle system, however, some of the configurations are of interest.

A second TIFS simulation of interest is the Calspan "million pound airplane" study of Refs. 5 and 6 which was, in part, devoted to study of Shuttle related issues. Three "airframes" were simulated -- "long aft tail," "short aft tail" and "canard" -- which essentially differed only in  $Z_{\delta_e}$  and therefore in instantaneous center of rotation location for elevator inputs. Other variables in the experiment were the two FCS designs (one of which was identical to the Shuttle concept), effective time delays and pilot location.

### 2. NLR Experiments

The NLR experiment, Refs. 3 and 4, employed an FCS (shown conceptually in Fig. 7) somewhat more general than the Shuttle system. In particular, the feedback time constant,  $T_q$ , and the feedforward time constant,  $\tau_m$ , were varied independently. The configurations of interest here are the four in the "F" series (see Fig. 7) in which  $1/T_q = K_\theta/K_q$  was fixed at  $1.40 \text{ sec}^{-1}$  while  $1/\tau_m$  was varied between  $0.186 \text{ sec}^{-1}$  and  $0.870 \text{ sec}^{-1}$ . The feedback around the airframe produced closed loop dynamics of the form

$$\frac{sN_\theta}{\Delta'} \Big|_{q \rightarrow \delta_e} = \frac{A_\theta K_q s (1/T_{\theta_1}) (1/T_{\theta_2})}{(1/T'_{sp1}) (1/T'_{sp2}) [\zeta', \omega_n']}$$

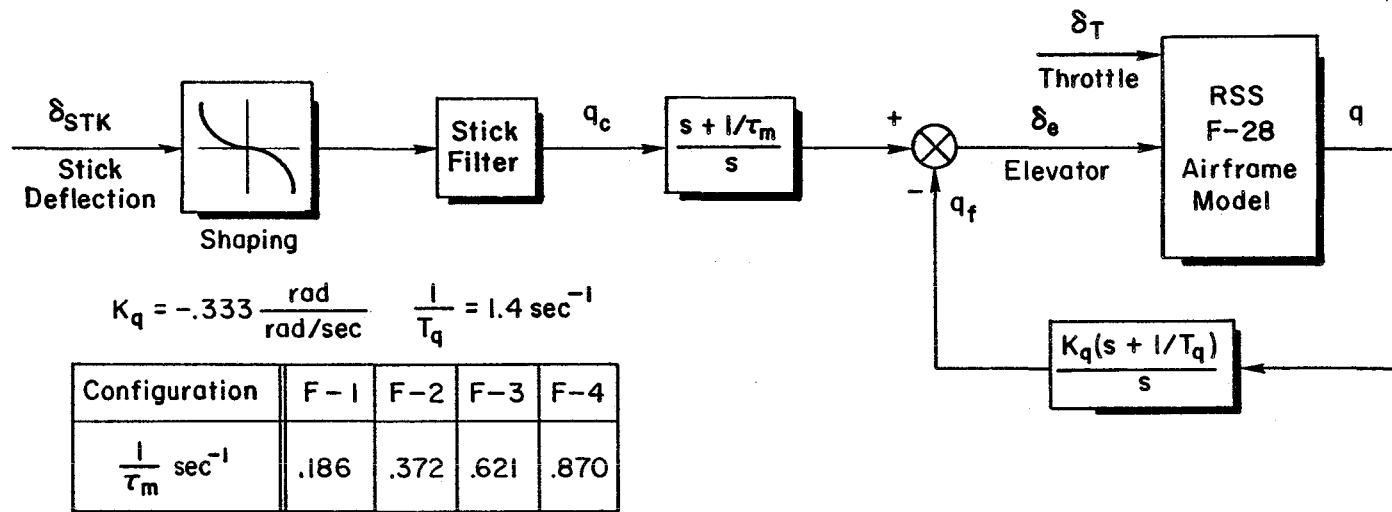


Figure 7. Basic Structure of the FCS Used in the Ref. 3 Study

e.g., see the Bode-Siggie plot of Fig. 8. The resulting pitch rate-to-pitch rate command transfer functions are tabulated in Table 4 in the form

$$\frac{q}{q_c}(s) = \frac{K(1/T_{\theta_1})(1/T_{\theta_2})(1/\tau_m)}{(1/T'_{sp2})(1/T'_{sp1})[\zeta', \omega'_n]} \quad (2)$$

This represents a superaugmented configuration to the extent that

$$\frac{1}{T'_{sp2}} \doteq \frac{1}{T_{\theta_1}} = 0.0835 \text{ sec}^{-1}$$

$$\frac{1}{T'_{sp1}} \doteq \frac{1}{T_{\theta_2}} = 0.715 \text{ sec}^{-1}$$

and thus

$$\frac{q}{q_c}(s) \doteq \frac{K(1/\tau_m)}{[\zeta', \omega'_n]}$$

The effective attitude zero is thus  $(1/\tau_m)$ . Unfortunately all values of  $1/\tau_m$  are less than or equal to  $1/T_{\theta_2}$  and thus these configurations do not provide data specifically relevant to the Shuttle path/attitude issue (i.e., the  $1/T_q \gg 1/T_{\theta_2}$  situation). However, some tentative conclusions may be reached. In particular, the normalized time responses to step commands, Fig. 9, show that increasing the frequency of the effective attitude zero (at least to  $1/\tau_m \doteq 1/T_{\theta_2}$ ) improves flying qualities. Figure 9 also shows that this variation increases rise time while decreasing overshoot. The Fig. 9 trend when compared to the LAHOS data correlation in Ref. 1 strengthens the argument that superaugmented aircraft have "unconventional" flying qualities. As an aside, it should be noted that the F-4 configuration is essentially a conventional aircraft in that the effective attitude lead is close to  $1/T_{\theta_2}$  (see Fig. 8). It is also of interest to note that the best-rated (Level 1) configuration F-4 (though not technically Shuttle-like as noted) satisfies the present Shuttle pitch rate specification.

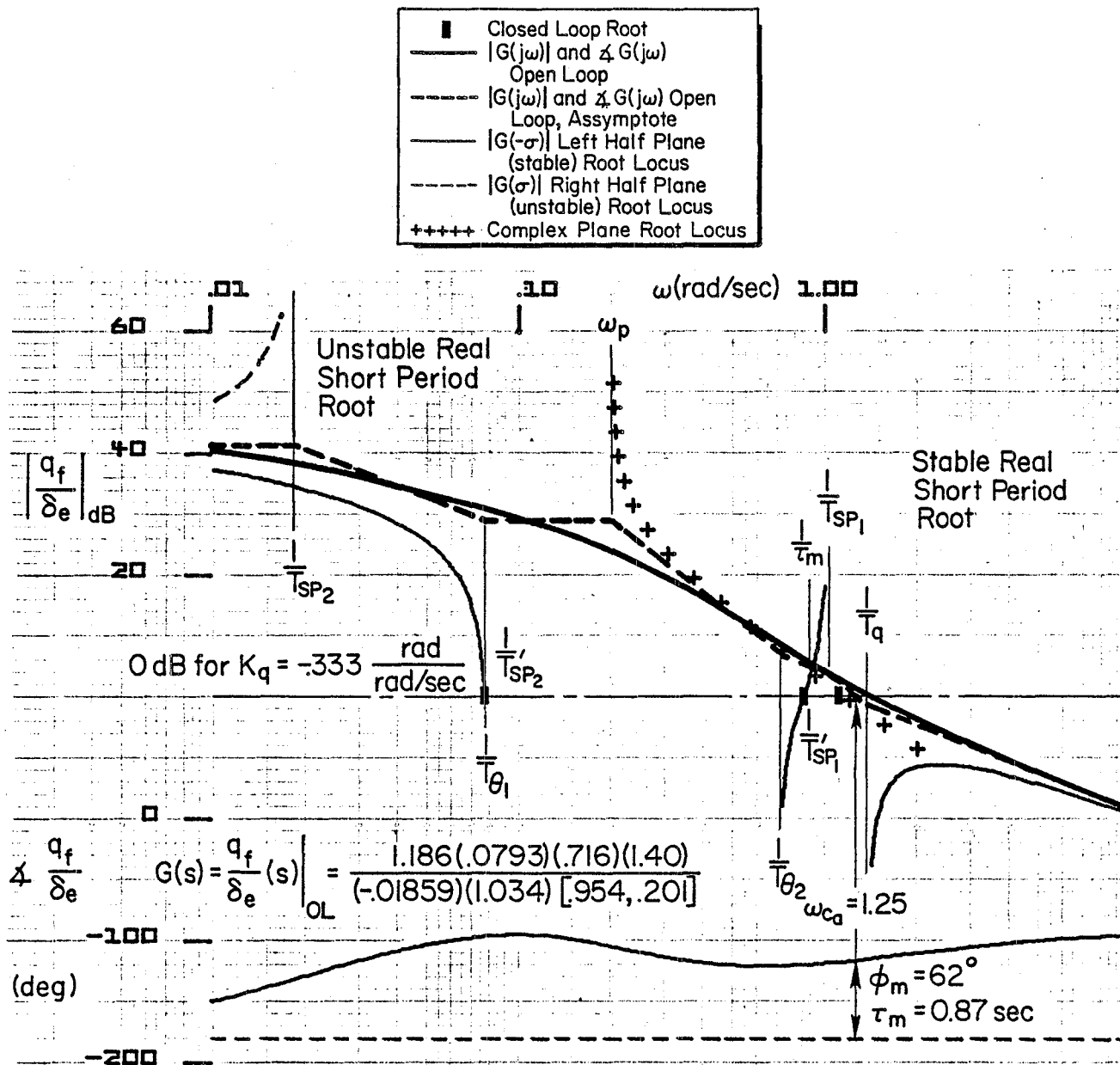


Figure 8. Bode Root Locus Plot Indicating the Effect of Closure of the  $q \rightarrow \delta_e$  Loop ( $K_q = -0.333 \text{ rad/sec}$ ) Configuration F-4 of Ref. 3

TABLE 4

$\frac{q}{q_c}(s)$  transfer functions, F Configurations of Ref. 3

CONF.	$\frac{q}{q_c}(s), \left[ \frac{\text{rad/s}}{\text{rad/s}} \right]$
F-1	$\frac{90.4(0.0835)(0.715)(0.186)}{\Delta'}$
F-2	$\frac{45.0(0.0835)(0.715)(0.372)}{\Delta'}$
F-3	$\frac{27.0(0.0835)(0.715)(0.621)}{\Delta'}$
F-4	$\frac{19.3(0.0835)(0.715)(0.868)}{\Delta'}$

$$\Delta' = (0.0780)(0.857)(10.)[0.703, 1.194]$$

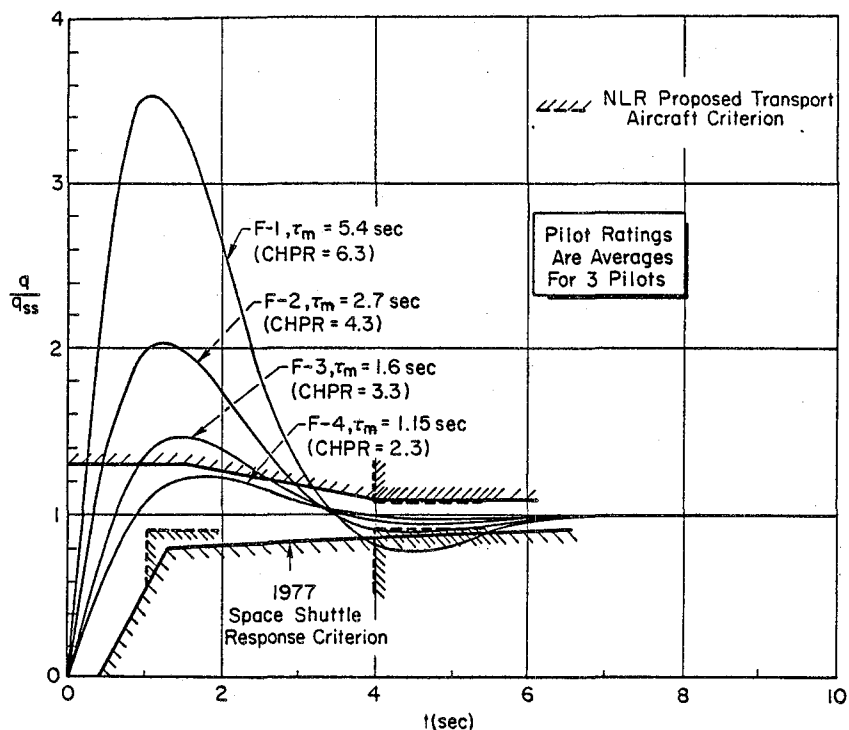


Figure 9. Normalized Indicial Pitch Rate Response of Ref. 3 "F" Configurations Compared to Exemplary Criteria ( $T_{\theta_2} = 1.4$  sec)

Time domain pitch response criteria for transport aircraft, similar in concept to the Shuttle criterion, were proposed in the NLR study. They consist of rise time and settling time boundaries as shown in Fig. 9. The settling time requirement is only slightly 'tighter' than the Shuttle spec but the rise time requirement is notably more stringent. Interestingly, there is no NLR requirement proposed for overshoot.

### 3. Calspan Experiments

The "million pound airplane" study (Refs. 5 and 6) provides an interesting comparison between what are perhaps the two fundamental approaches to augmentation of RSS aircraft -- the Shuttle-type  $q, \int q \rightarrow \delta_e$  system and the " $M_\alpha$  augmentor", a pure gain  $\alpha \rightarrow \delta_e$  system. As discussed in the last article, either system will provide a stable vehicle but with different side effects -- e.g., sensitivity to turbulence for the  $\alpha$  system and neutral speed stability for the  $q$  system. On the basis

of gross comparison between the two, the (higher gain)  $q$  systems were rated better by the evaluation pilots.

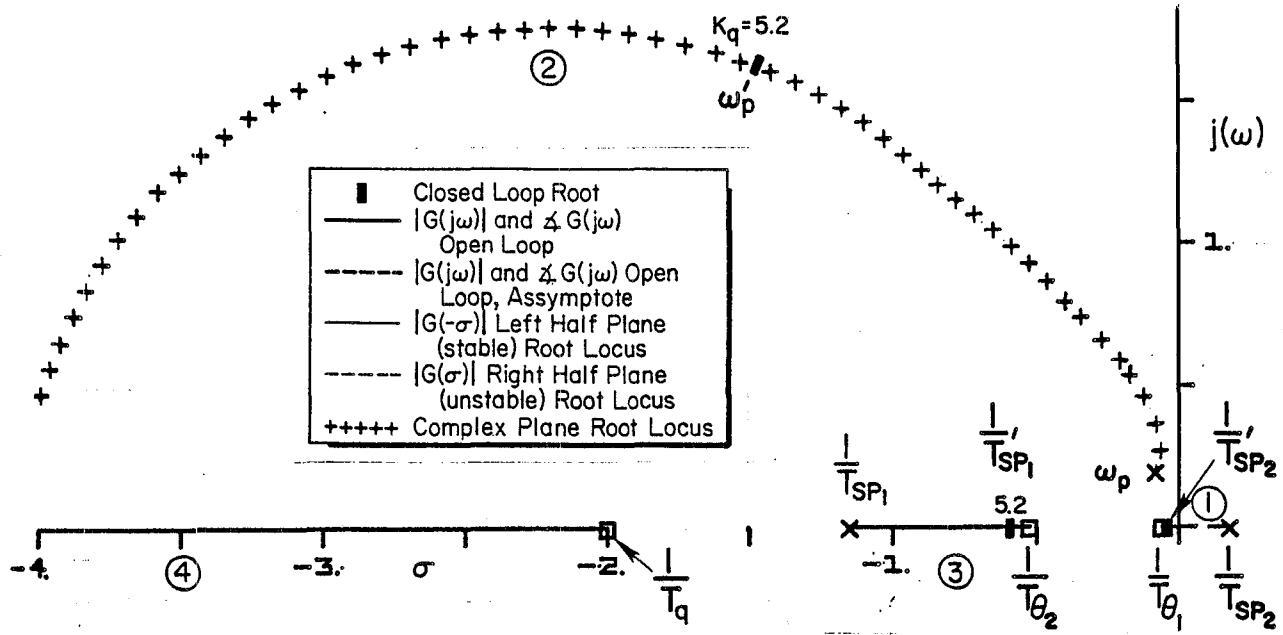
For the Shuttle-like  $q$ -systems several gain levels and two  $T_q$  values were used to vary the augmented aircraft response. Only the higher gain systems are relevant here. Of these, only one configuration was (technically) similar to the Shuttle (i.e.,  $1/T_q > 1/T_{sp1} > 1/T_{\theta 2}$ ). This was the short aft tail, extra high  $K_q$  configuration with  $1/T_q = 2.0 \text{ sec}^{-1}$ . A system survey for this is shown in Fig. 10 and a step response in Fig. 11. In terms of the Ref. 1 analytic LOES model:

$$\frac{q'}{q_c} = \frac{1.31(1.50)e^{-.174s}}{[.468, 1.40]} \quad \text{Shuttle OFT, Ref. 1} \quad (3)$$

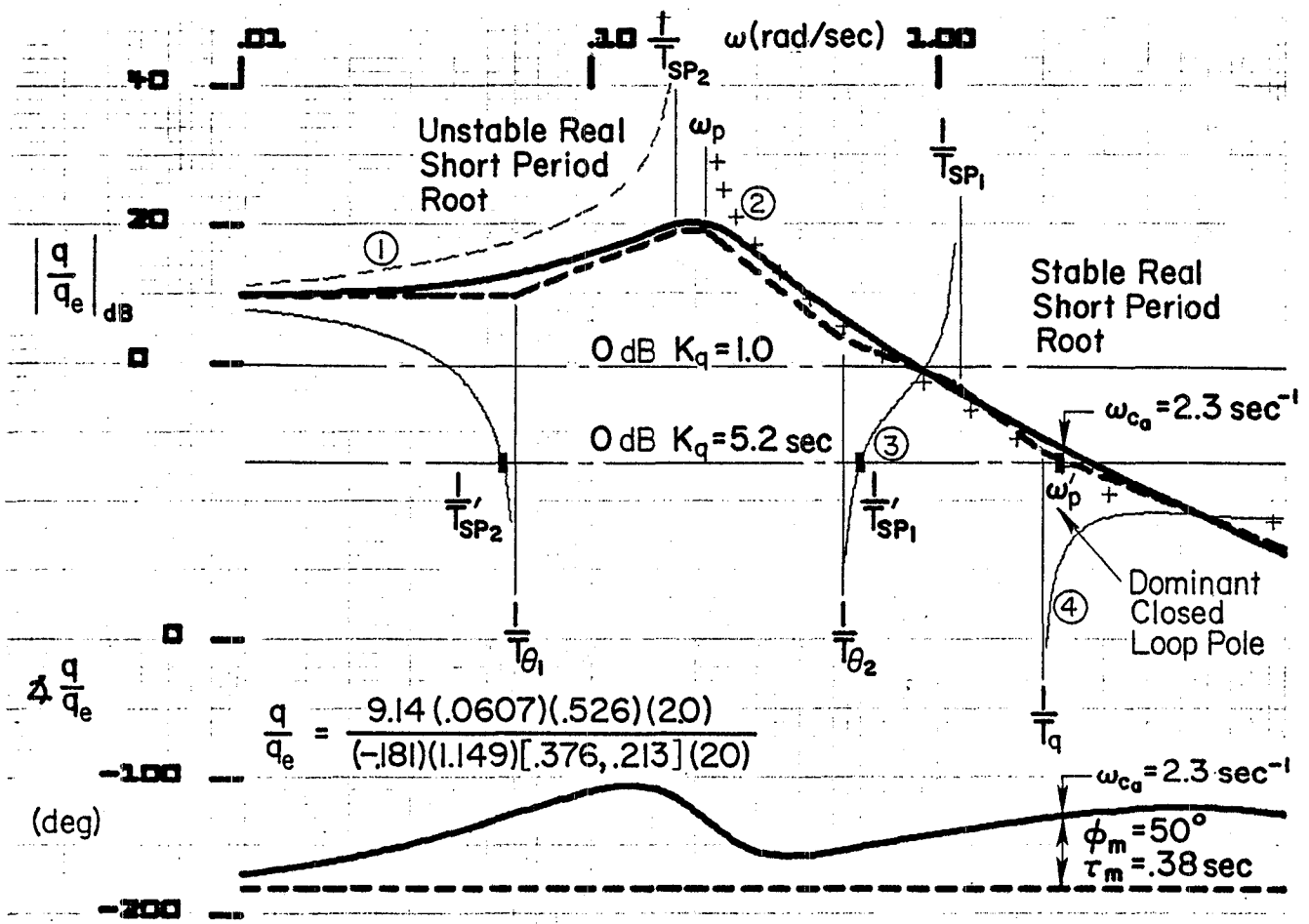
$$\frac{q'}{q_c} = \frac{2.29(2.0)e^{-.11s}}{[.54, 2.14]} \quad \begin{array}{l} \text{Short aft tail,} \\ \text{Extra-high } K_q, \text{ Ref. 5} \end{array} \quad (4)$$

Unfortunately only a single pilot rating is available for this configuration (CHPR = 4). Pilot comments do not indicate a specific problem and there is no reference to airspeed control problems related to neutral speed stability.

Three Ref. 5 "high  $K_q$ " pitch rate system configurations differ technically from the effective Shuttle dynamics in that  $1/T_{sp1} > 1/T_q > 1/T_{\theta 2}$ . However, these configurations are superaugmented in the sense that the effective dynamics are dominated by the FCS parameters. Figure 12 presents a system survey for the short aft tail case. Figure 13 shows the step response for the short aft tail, high  $K_q$  configuration. The overshoot, while less than the maximum in the present Shuttle boundary is extended somewhat further and the rise time is also fairly large. Nonetheless, this pitch rate response is not too far removed from the exemplary boundaries. This configuration was evaluated by both evaluation pilots used in the study and received generally good ratings. In



a) Conventional Root Locus



b) Bode Root Locus

Figure 10. System Survey for the Ref. 5 Short-Aft Tail, Extra High  $K_q$ ,  $T_q = 0.5 \text{ sec}$  Configuration

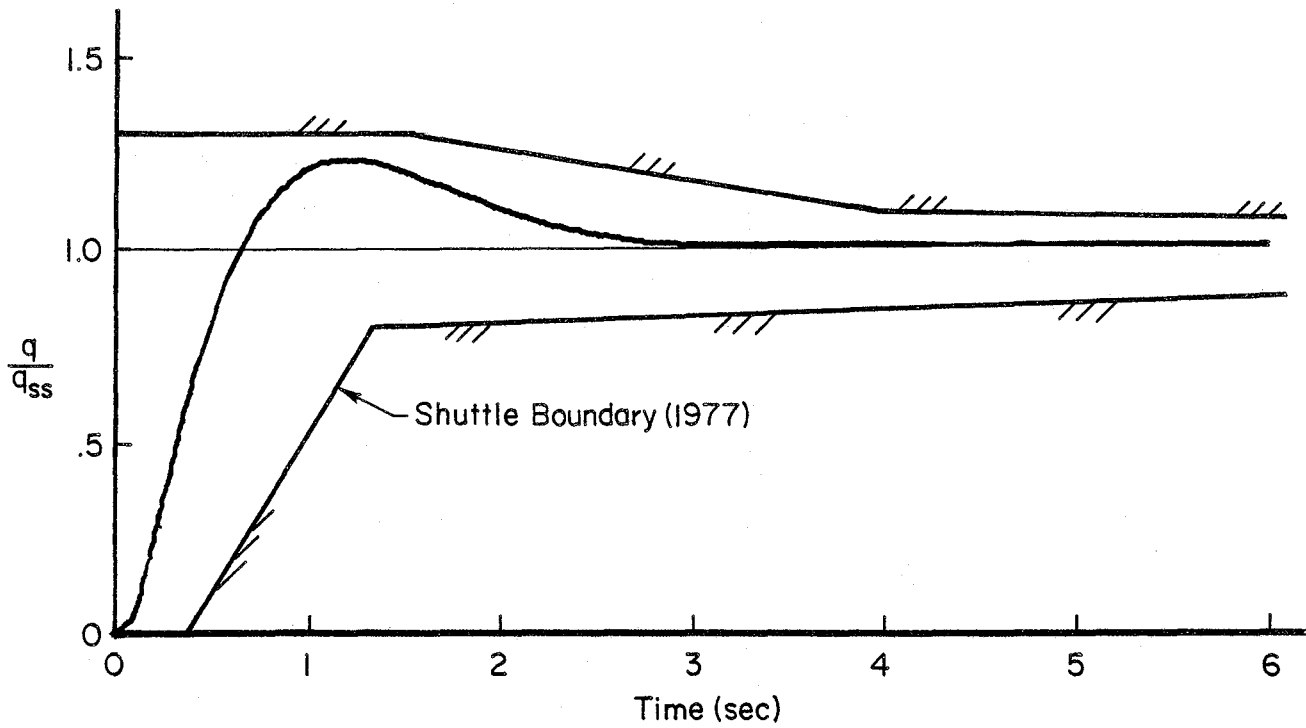


Figure 11. Normalized Indicial Pitch Rate Response to Stick Force, Ref. 5 Short Aft Tail, Extra High  $K_q$ ,  $T_q = 0.5$  Configuration

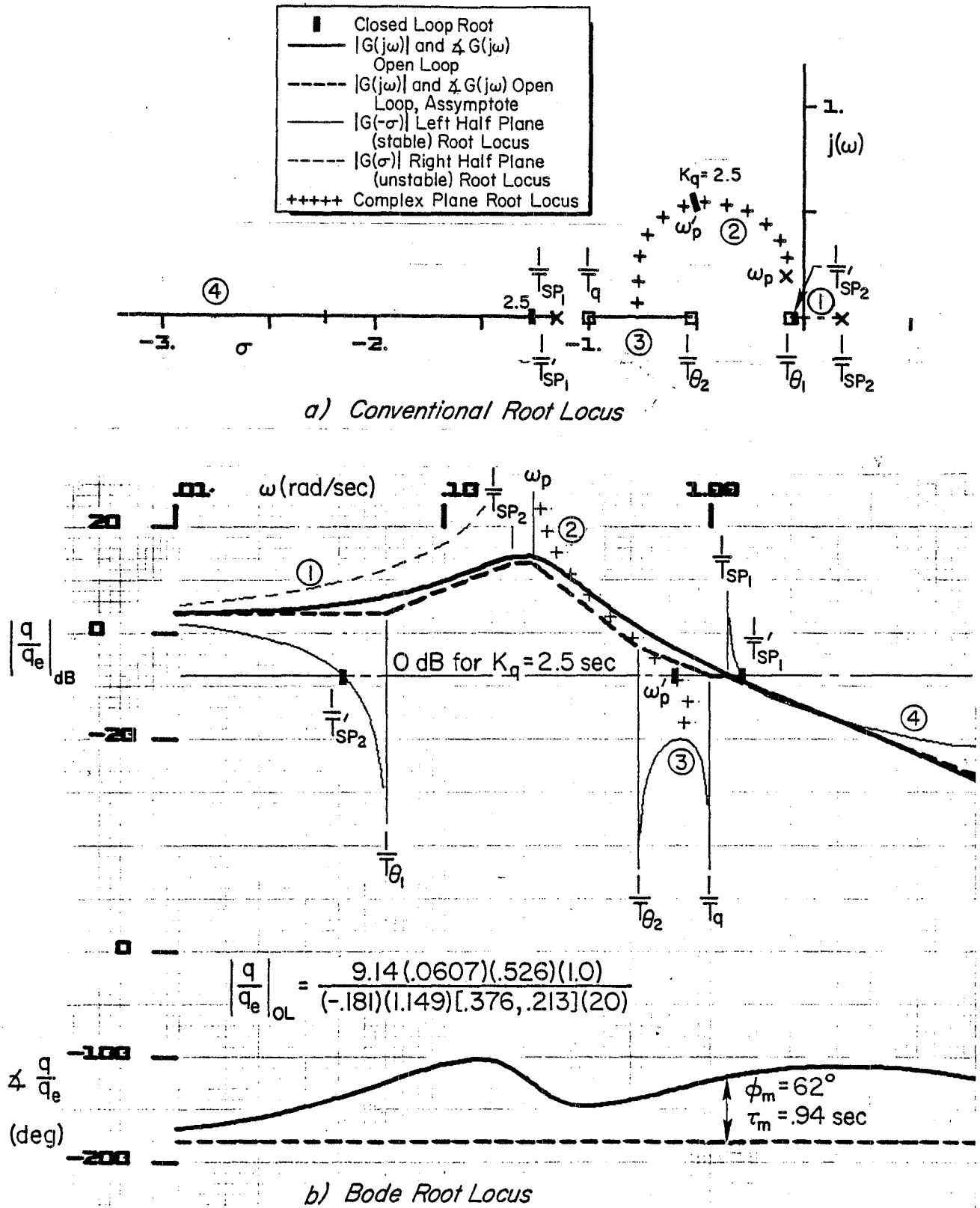


Figure 12. System Survey for Ref. 5 Short Aft Tail, High  $K_q$ ,  $T_q = 1.0$  sec Configuration

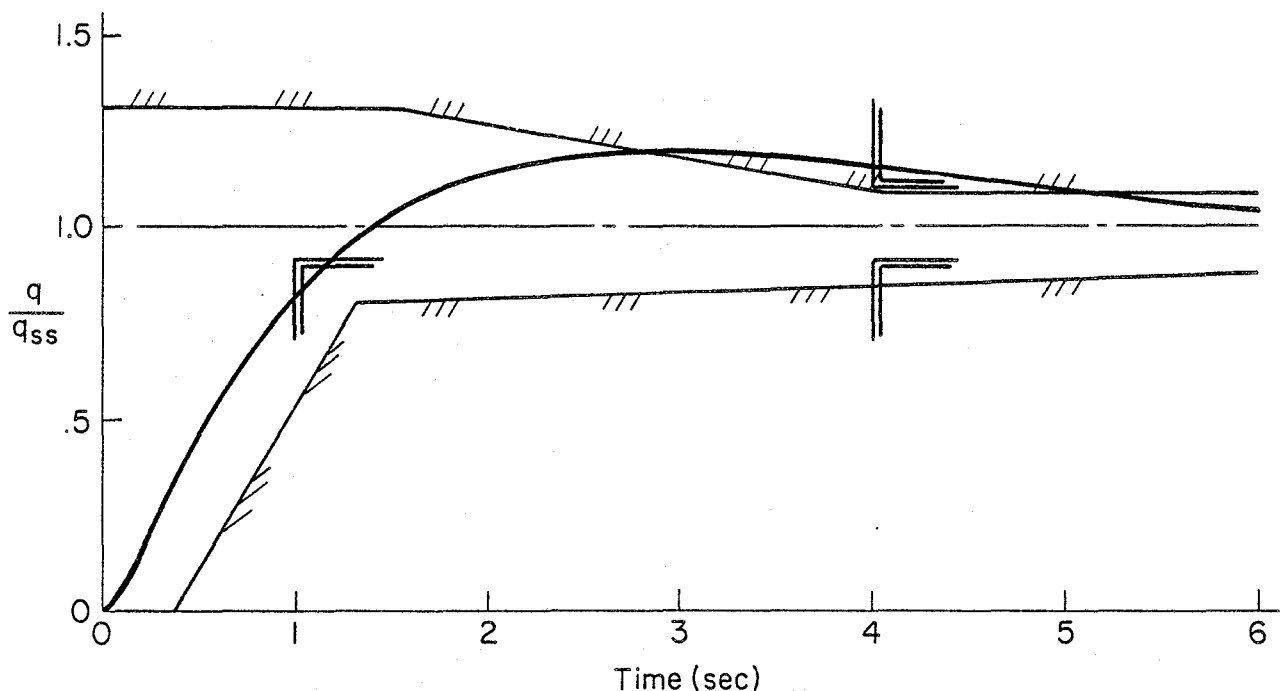


Figure 13. Normalized Indicial Pitch Rate Response to Stick Force, Ref. 5 Short Aft Tail, High  $K_q$ ,  $T_q = 1$  sec Configuration

its second evaluation by one pilot it was given a Cooper-Harper rating of 1 which is extremely unusual (the same pilot initially evaluated it as 4). The pilot commentary indicates initial problems in trim, basically in attempting to "Keep the airspeed and attitude organized." After familiarization, however, the same pilot noted that "Airspeed control is excellent. Once I get it trimmed up it virtually holds the airspeed, holds attitude, and stays trimmed in turns." The other pilot indicated that "airspeed control was good, predictable." His summary comment was "No major problems, an excellent airplane." From these comments it would appear that in precision path control, a superaugmented configuration may indeed exhibit good flying qualities. There does appear to be a potential familiarization problem, although this is rapidly overcome. This one flight data point goes a long way toward justifying a position that heavily augmented RSS aircraft, especially as they approach the superaugmented condition, cannot satisfactorily be judged by criteria or compared with data from conventional aircraft.

### C. PATH DYNAMICS

The previous discussions have focussed on pitch attitude and speed response to stick (RHC) inputs. Path response to attitude,  $h/\theta$ , has been treated through the basic, but generally valid, approximation in Figs. 1 and 2. We will now consider path dynamics in somewhat more detail to examine issues specific to the Shuttle and its Ref. 13 specification.

The complete path-to-attitude transfer function is more complex than indicated in Figs. 1 and 2, i.e.,

$$\frac{h}{\theta} = \frac{N_{\delta_e}^h}{N_{\delta_e}^\theta} = \frac{A_h (1/T_{h1})(1/T_{h2})(1/T_{h3})}{A_\theta (1/T_{\theta1})(1/T_{\theta2})} \quad (5)$$

The low frequency attitude zero ( $1/T_{h1}$ ) is an indicator of operation on the "front" or "backside" of the  $\gamma$ -V curve. This issue is addressed in the only path control spec for the Shuttle -- paragraph 3.4.3.5 in Ref. 13.

#### Flight Path Stability

Considering changes in airspeed by means of the pitch control only, with all other lift, drag, or thrust devices held constant, the change in flight path angle versus airspeed shall be negative in the approach operational range. In other words, the Shuttle is intended to be on the "front" side of the  $\gamma$ -V curve in equilibrium glide conditions.

The high frequency zeros, ( $1/T_{h2}$ ) and ( $1/T_{h3}$ ), for altitude at the pilot station, are determined by the relative location of the pilot and the instantaneous center of rotation (ICR) for elevator inputs. These zeros are unconventional and unfavorable for the Shuttle but are not covered in the Ref. 13 specification.

The Ref. 5 "million pound airplane" study provides some of the best available data concerning pilot/ICR location effects on the Shuttle. The configurations of interest are the three airframes (long aft tail,

short aft tail, and canard) with the "high  $K_q$ " pitch rate system. These configurations all had essentially the same pitch attitude response. The primary difference was in the airframe  $Z\delta_e$  values and therefore in ICR location. The effective pilot location was then further varied with respect to the ICR for each airframe configuration.

Figure 14 shows Cooper-Harper pilot rating (CHPR) plotted against the pilot location relative to the ICR ( $\Delta l_p$ ). While there are some large rating variations for several of the configurations, there does seem to be a definite degradation of pilot rating for the two short aft tail configurations in which the pilot was less than 10 ft ahead of the ICR.

The fact that the short aft tail configuration with  $\Delta l_p = 50$  ft is consistent in CHPR ratings with the canard and long aft tail configurations indicates that it is pilot location with respect to the ICR rather than instantaneous center location per se that is relevant to path control problems.

The dynamic effects of pilot/ICR location on path loop closure were investigated (as in Ref. 1) by examining the pilot station altitude-to-attitude transfer function,  $h_p/\theta$ , for different pilot locations with respect to ICR. For example, for the short aft tail configurations:

$$\frac{h_p}{\theta}(s) = \frac{10.2(-0.00256)(-3.27)(4.25)}{(0)(0.0607)(0.526)} \quad \Delta l_p = -10 \text{ ft (aft)} \quad (6)$$

$$\frac{h_p}{\theta}(s) = \frac{10.2(-0.00255)[0.024, 3.82]}{(0)(0.0607)(0.526)} \quad \Delta l = +10 \text{ ft} \quad (7)$$

$$\frac{h_p}{\theta}(s) = \frac{50(-0.00252)[0.150, 1.70]}{(0)(0.0607)(0.526)} \quad \Delta l_p = +50 \text{ ft} \quad (8)$$

(fwd)

It may be seen that the differences lie in the location of the high-frequency zeros. At  $\Delta l_p = -10$  ft all poles and zeros are real and one high-frequency zero has non-minimum phase. As the pilot is moved

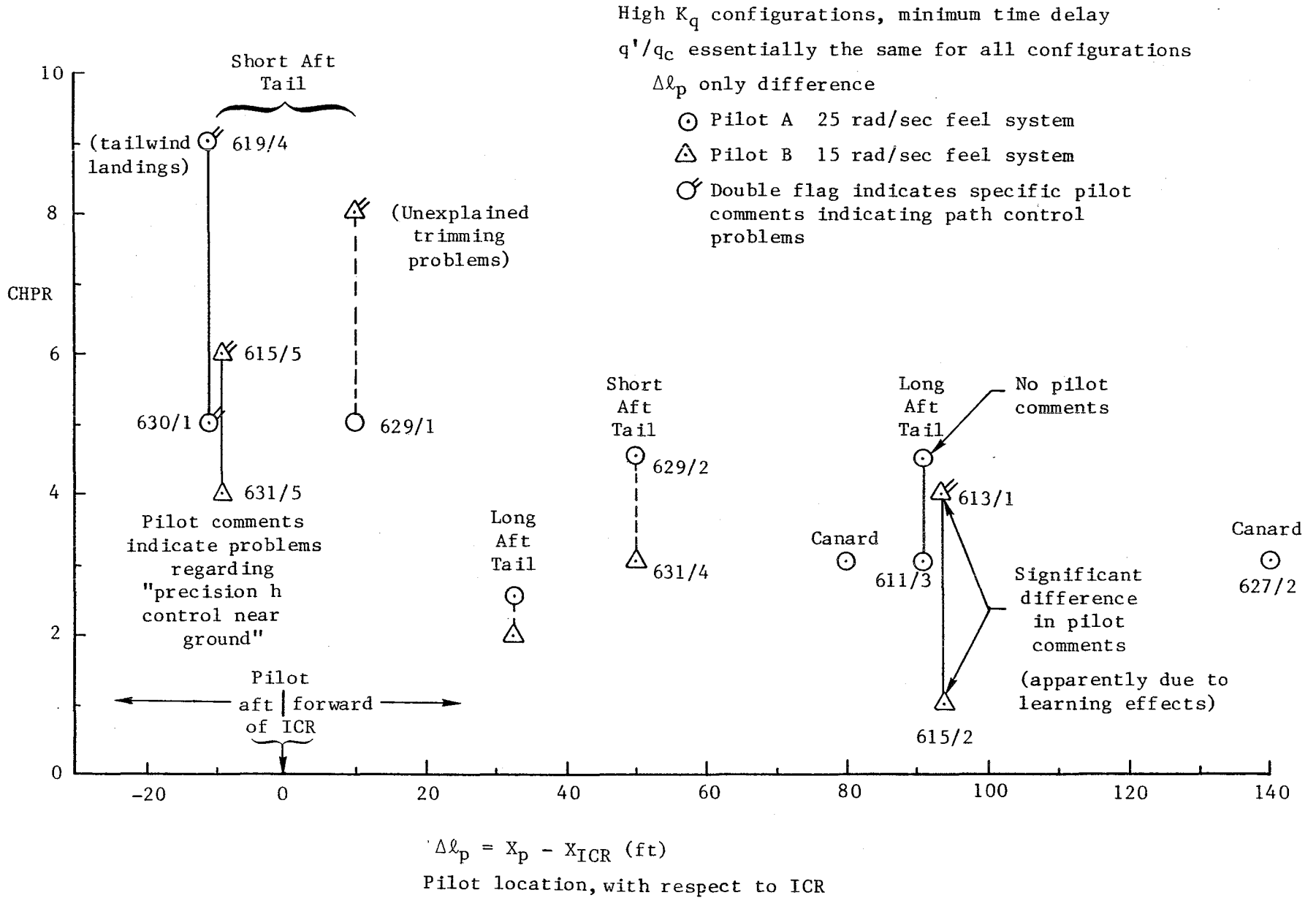


Figure 14. Variation of Pilot Rating with Relative Pilot/ICR Location, Ref. 5 Data

forward the high-frequency zeros become complex. The sensitivity of the high frequency  $h_p$  zero to pilot location can be visualized with the aid of the root locus of Fig. 15. This shows that, as the pilot station is moved forward from the c.g., the high-frequency zeros initially move out along the real axis until they couple and then move in roughly along the  $j\omega$ -axis toward the attitude roots. The zeros for  $\Delta l_p = -10, +10, \text{ and } +50$  ft are shown.

The pilot station path-to-attitude frequency response is shown in the Bode plots of Fig. 16 for the 3 pilot locations. The key differences in phase angle occur near the altitude zeros, i.e., above 1 rad/sec. However, the pilot will normally close the path loop at or below  $1/T\theta_2$  which results in a minimum of 45 deg phase margin for a pure gain closure. It is apparent from Fig. 16 that in the frequency band below  $1/T\theta_2$  there is no significant amplitude or phase difference between the three pilot locations. Thus, it is concluded that the Fig. 14 degradation in pilot rating with pilot located at or behind the ICR is probably not due to variations in the achievable path loop bandwidth.

Examination of the  $n_z$  and  $h$  time responses (Fig. 17) indicates the more likely explanation is that the non-minimum phase effect of an aft pilot location creates an effective time delay in the motion cues used by the pilot to assess path response. This same conclusion is reached in Ref. 5.

The preceding analysis is based on the conventional assumption of small perturbations about an operating point. However, because the Shuttle is a glider it decelerates rapidly in approach and landing compared to conventional jet transports. This situation leads to some unusual characteristics for the Shuttle with implications for manual control. These are analyzed in the next section.

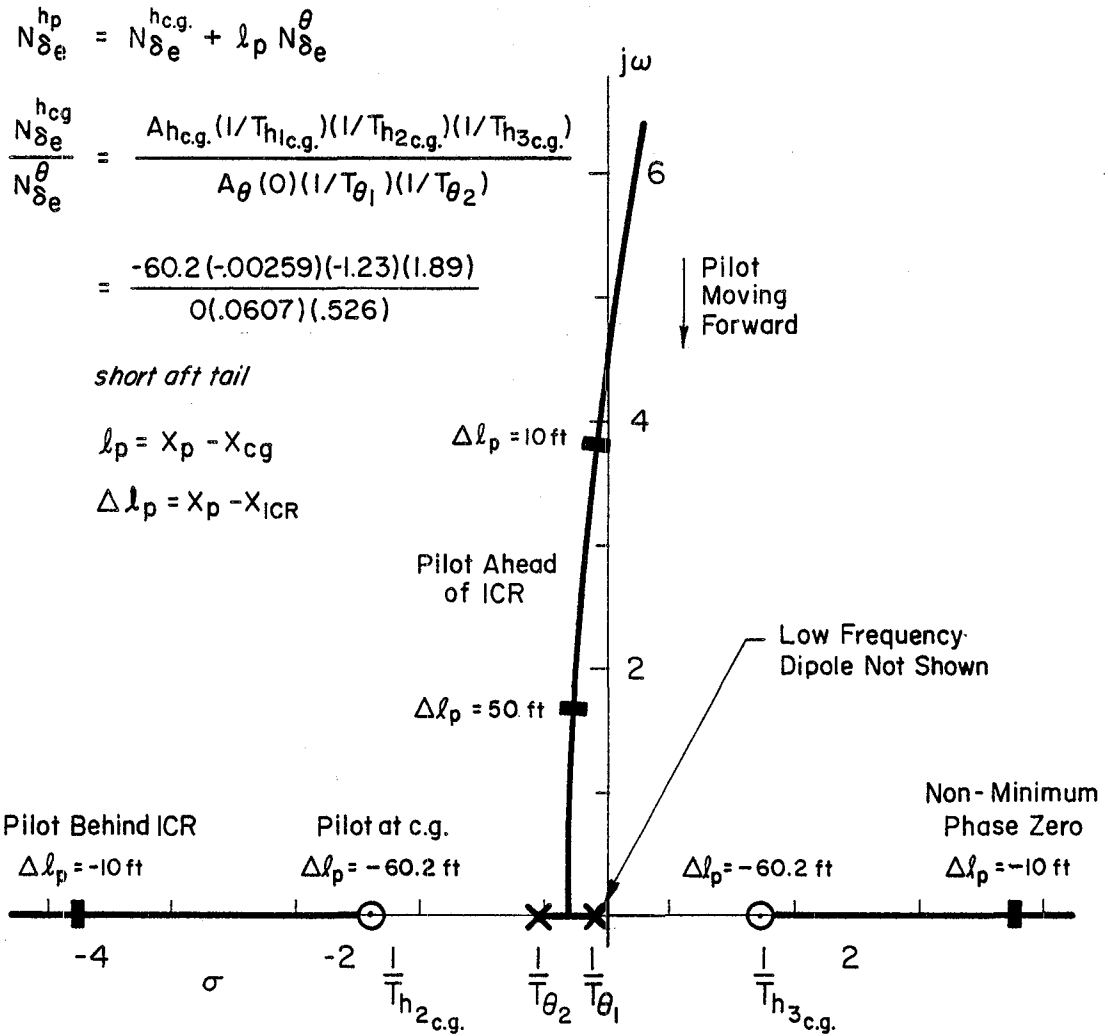


Figure 15. Migration of High Frequency Altitude Zeros at Pilot Station as Pilot is Moved Forward from c.g., Short Aft Tail Configuration

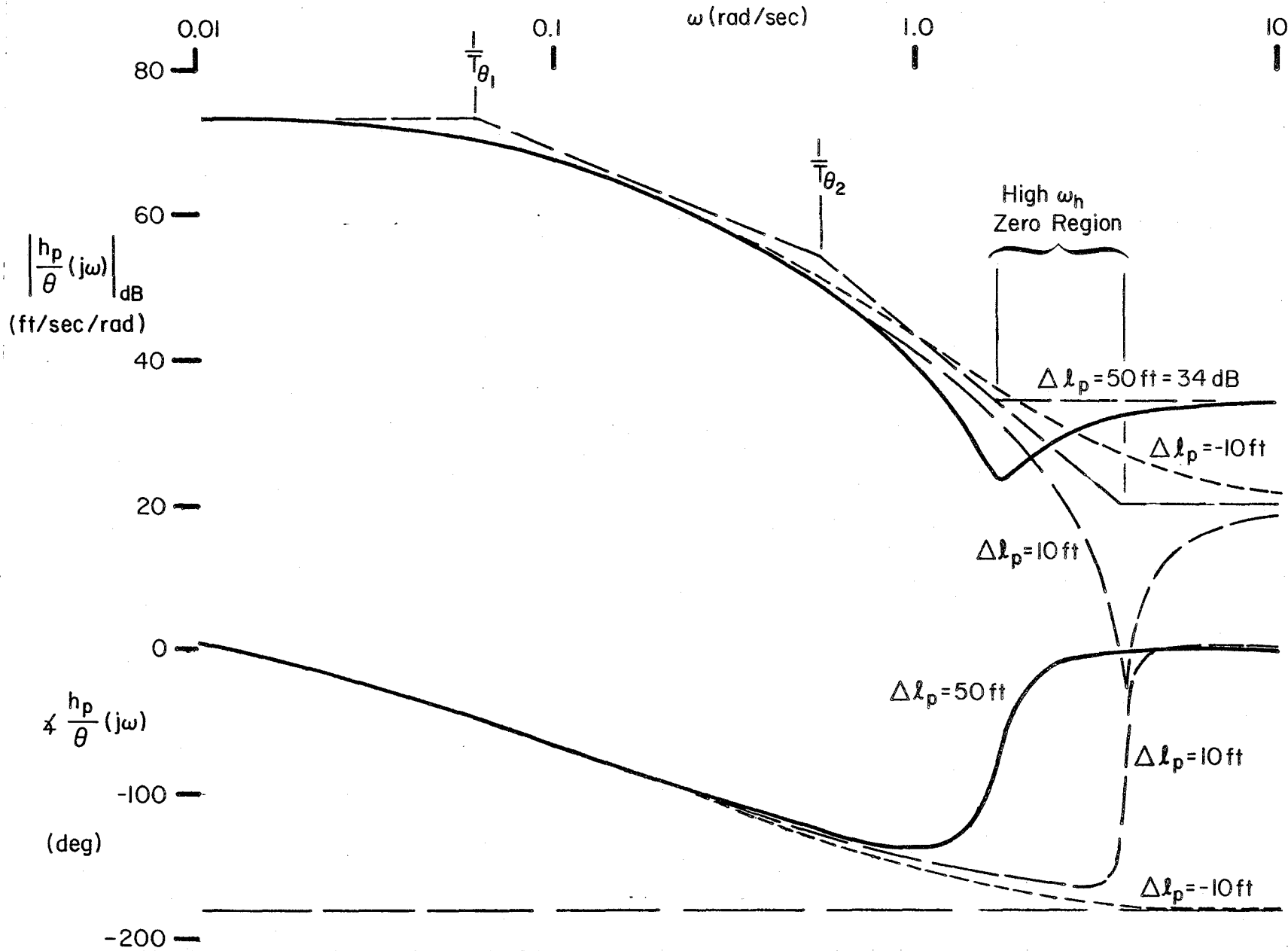


Figure 16. Path-to-Attitude Frequency Response for 3 Pilot Positions, Short Aft Tail Configurations

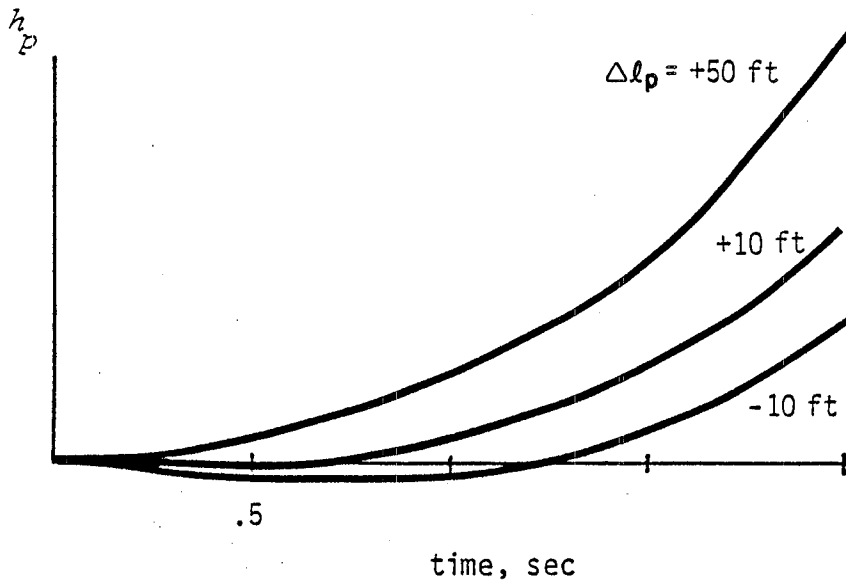
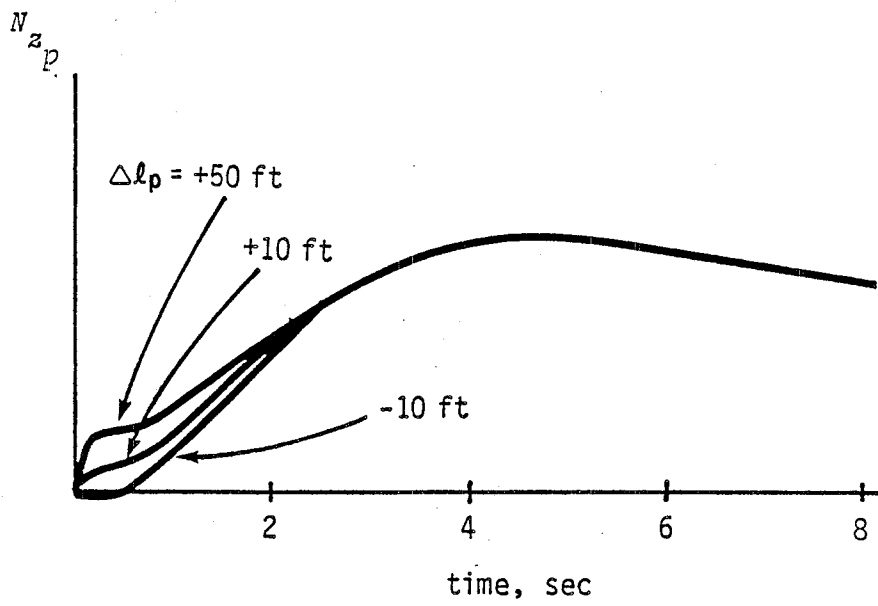


Figure 17. Normal Acceleration and Altitude at Various Pilot Stations in Short Aft Tail Configuration, High Augmentation,  $T_1 = A$  (From Ref. 5)

## **D. SHUTTLE FLIGHT MECHANICS FOR MANUAL APPROACH AND LANDING**

### **1. Nominal Trajectory for Manual Approach and Landing**

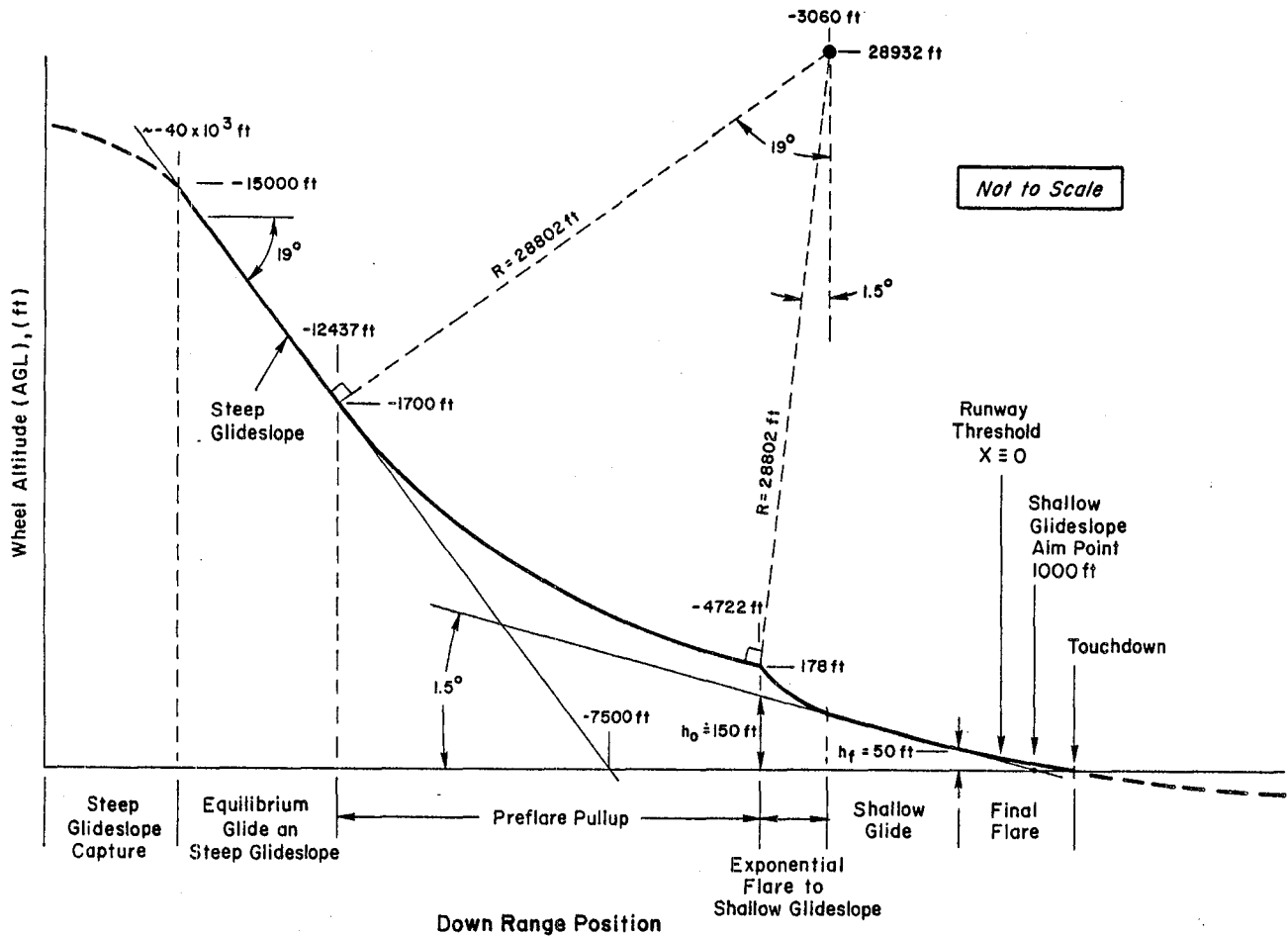
Figure 18a shows a nominal trajectory for considerations of manual control for the Space Shuttle approach and landing. Figure 18b shows the corresponding nominal airspeed variation. This nominal reference trajectory has been drawn based on considerations of basic flight mechanics (Appendix A), autoland system design data (Ref. 21) and flight data from STS-1 through 4. While actual trajectories will, of course, vary depending on pilot technique, disturbances, etc.; Fig. 18 will serve as a reference for developments to follow.

### **2. Steep Glideslope Capture**

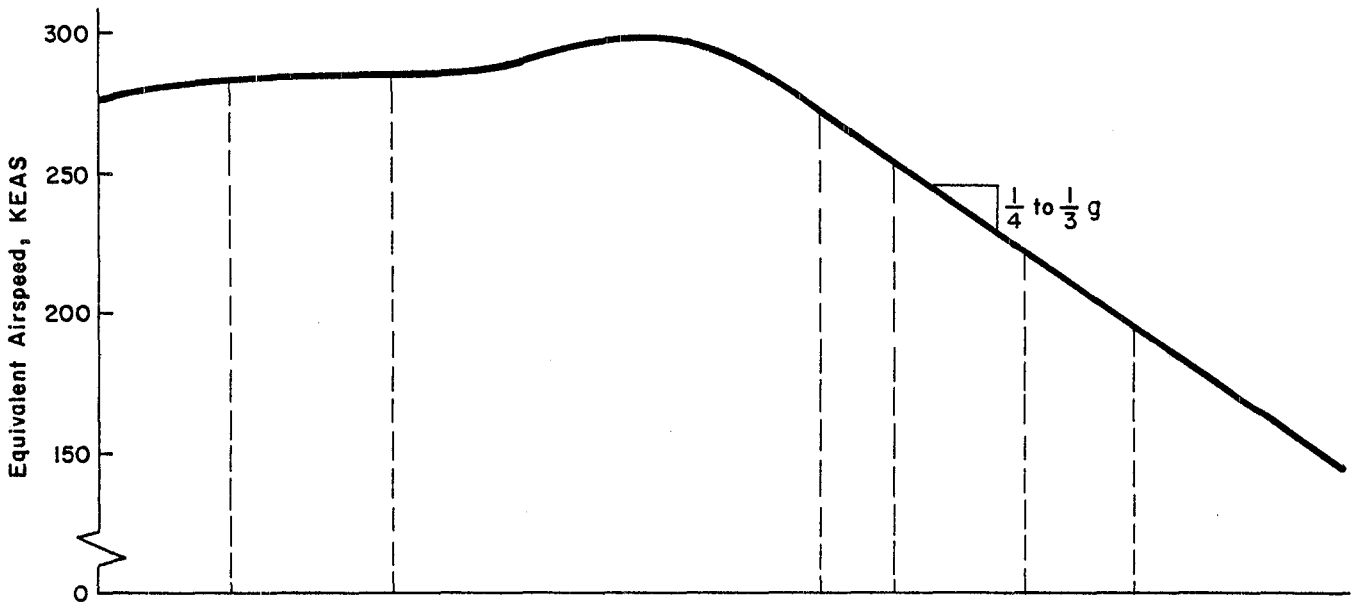
The approach and landing phase begins with capture of the steep glide slope shortly after leveling the wings following the HAC turn -- nominally at 15,000 ft altitude and approximately 40,000 ft from the runway threshold. For the first four Orbiter flights this maneuver has been performed manually.

### **3. Equilibrium Glide on the Steep Glideslope**

The primary purpose of the steep glideslope portion of the approach is to set up a constant equivalent airspeed (i.e., constant dynamic pressure). The steep flight path angle is selected such that the gravity component balances the drag. Precise control of airspeed is then achieved through modulation of the speed brakes. While the equivalent airspeed remains constant during the equilibrium glide, the true airspeed decreases due to the variation of atmospheric density with altitude. This effect is analyzed in Appendix A and shown to produce an approximately 10 percent error with respect to the classical ( $\rho = \text{constant}$ ) glide equation:



a) Trajectory



b) Equivalent Airspeed Variation

Figure 18. Nominal Trajectory and Airspeed Variation for Shuttle Approach and Landing

$$\tan \gamma = - \frac{C_D}{C_L} \quad (9)$$

Figure 19 shows typical  $\gamma$ -V curves based on the STS-4 weight ( $w = 210,000$  lb) and computed from Eq. A-27 in Appendix A. The difference between the solid and dashed lines indicates that the effect of atmospheric density change is roughly equivalent to the L/D increase accompanying a 10 deg reduction in speed brake deflection. For comparison, the nominal STS-4 glide condition ( $\gamma = -17.5$  deg,  $V_E + 290$  KEAS,  $\delta_{SB} = 10-15$  deg) is indicated based on Fig. 15 in Ref. 25.

#### 4. Preflare Pullup

At an altitude of approximately 1700 ft, a preflare pullup maneuver is initiated which "circularizes" the trajectory. The pullup is terminated when the flight path angle matches that for the shallow glideslope -- nominally -1.5 deg. Speed change during the preflare pullup is very slow until the flight path angle departs significantly from the equilibrium value. Therefore, the pullup may be considered a constant speed maneuver to a first approximation. This was done in Ref. 13 and may also be seen to be reasonable from examination of flight traces.

#### 5. Glide on the Shallow Glideslope and Final Flare

Most of the variation in approach and landing piloting technique will probably occur in final glide and flare. Nominally, as indicated in Fig. 18a, after the pilot performs the preflare maneuver, he should have achieved the proper flight path angle but be somewhat above the desired shallow glideslope. Thus he must perform a flare to acquire the shallow glideslope followed by a constant  $\gamma$  glide and a final flare. Conversely, the maneuver might consist of one continuous flare without a noticeable constant  $\gamma$  glide. The flight data indicates the first situation, although there is considerable variation in initiation of the final flare.

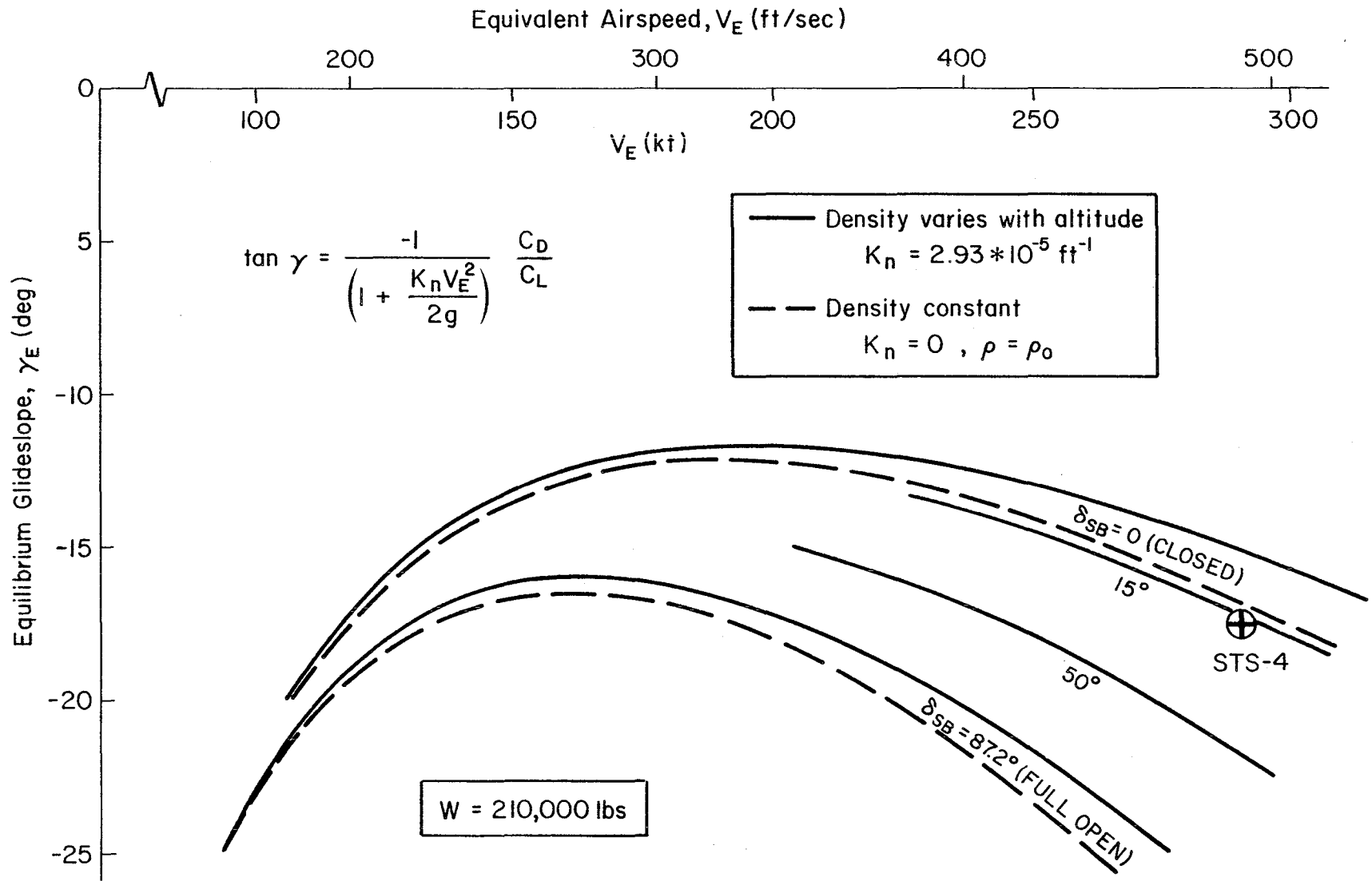


Figure 19. Equilibrium Glideslope-Airspeed Curves for the Shuttle on Steep Glideslope

A simple model which accommodates the various possibilities is indicated in Fig. 20 in which the details of the shallow glideslope capture are ignored. Rather it is assumed that, at the end of the preflare pullup, the pilot selects a shallow glideslope,  $\gamma_0$ , at some distance,  $X_0$ , with some initial conditions on altitude and velocity. He then maintains a constant  $\gamma_0$  glide down to the flare height,  $h_f$ , at which point he begins an exponential flare to touchdown. In the exponential flare, the pilot schedules sinkrate proportional to altitude with a bias,  $h_B$ , to insure nominal sinkrate at touchdown,  $\dot{h}_{TD}$ . The effective control law is thus

$$\dot{h} = -\frac{1}{T_f} (h + h_B) \quad (10)$$

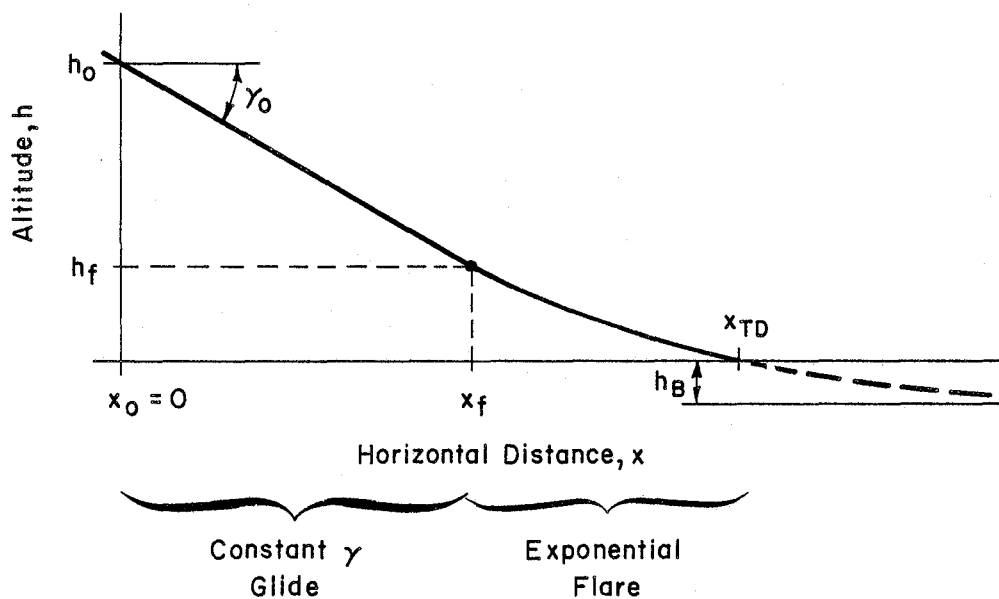


Figure 20. Idealized Shallow Glide and Final Flare Under Manual Control

The above simplified model is assumed to be a reasonable first approximation of pilot behavior since:

- 1) It corresponds to pilot comments (e.g., STS-4) concerning technique
- 2) It provides the simplest outer loop pilot model, i.e., a pure gain
- 3) It is also used by the Shuttle Autoland system which was specifically designed to be consistent with manual landing strategy

For this model,  $\gamma_0$  and  $T_f$  become the pilot's two primary control variables to establish acceptable values for the three primary controlled variables: touchdown sinkrate, touchdown speed and touchdown point. The flare height,  $h_f$ , could function as a third control variable in that variations in  $h_f$  can accommodate various techniques. That is, as  $h_f$  goes to  $h_0$ , a continuous flare occurs and at the other extreme, as  $h_f$  goes to zero, a continuous glide with no final flare occurs. It appears from flight data, however, that neither extreme is used and that the crews use a preselected value of flare height.

As indicated in Fig. 18b, most of the deceleration in approach and landing occurs during the shallow glide and final flare. The development in Appendix A shows that

$$\dot{V} = a + bV^2 + cV^{-2} \quad (11)$$

where  $a$ ,  $b$ , and  $c$  are constants. Furthermore, it is shown that the  $b$  and  $c$  terms roughly cancel and  $\dot{V}$  is approximately constant ( $-1/4$  to  $-1/3$  g). This may be confirmed by examining flight traces.

Using this basic assumption, the pilot's landing control problem may be viewed in a particularly simple way from Fig. 21 based on equations in Appendix A. In Fig. 21, the controlled variables -- sinkrate ( $\dot{h}_{TD}$ ), speed ( $V_{TD}$ ) and distance ( $X_{TD}$ ) at touchdown -- are shown as contours in the  $\gamma_0 - T_f$  plane. Important limits and design values, from Ref. 13, are also shown in Fig. 21:

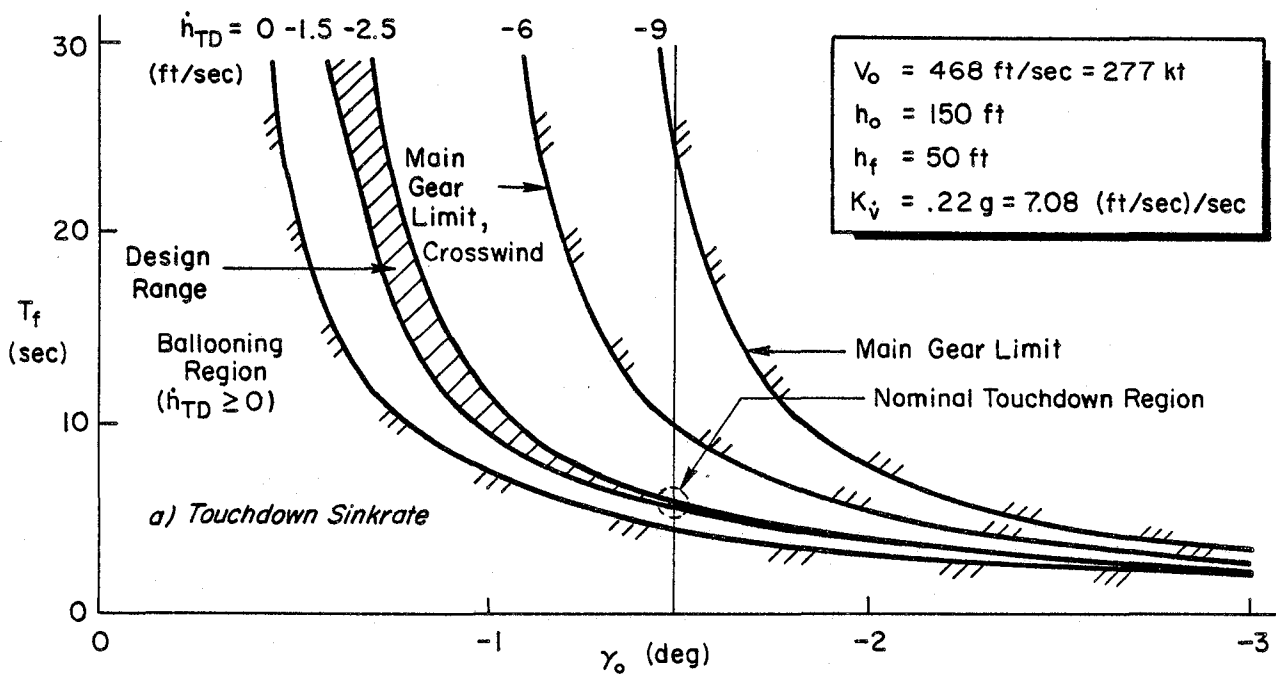
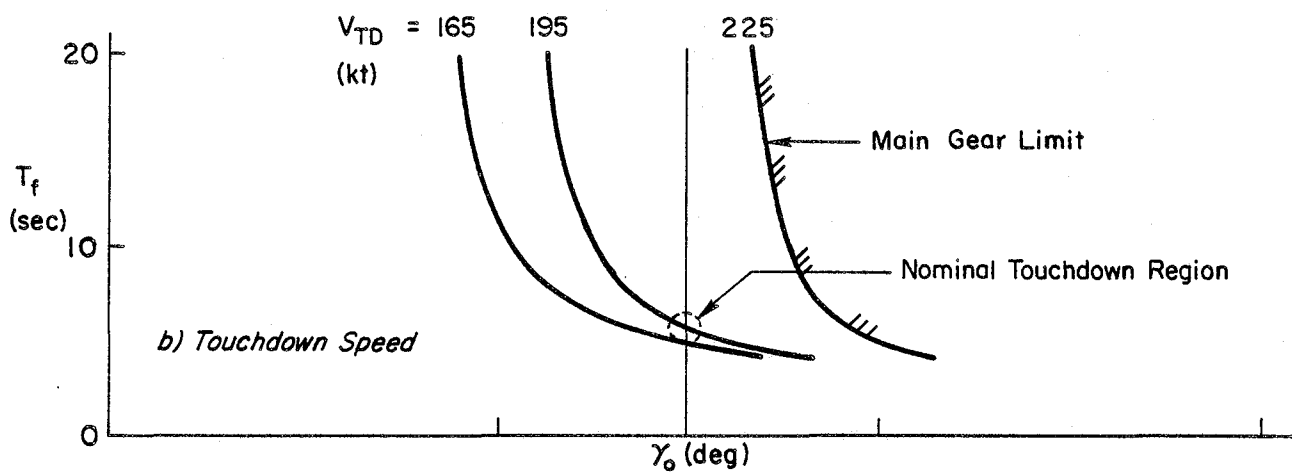
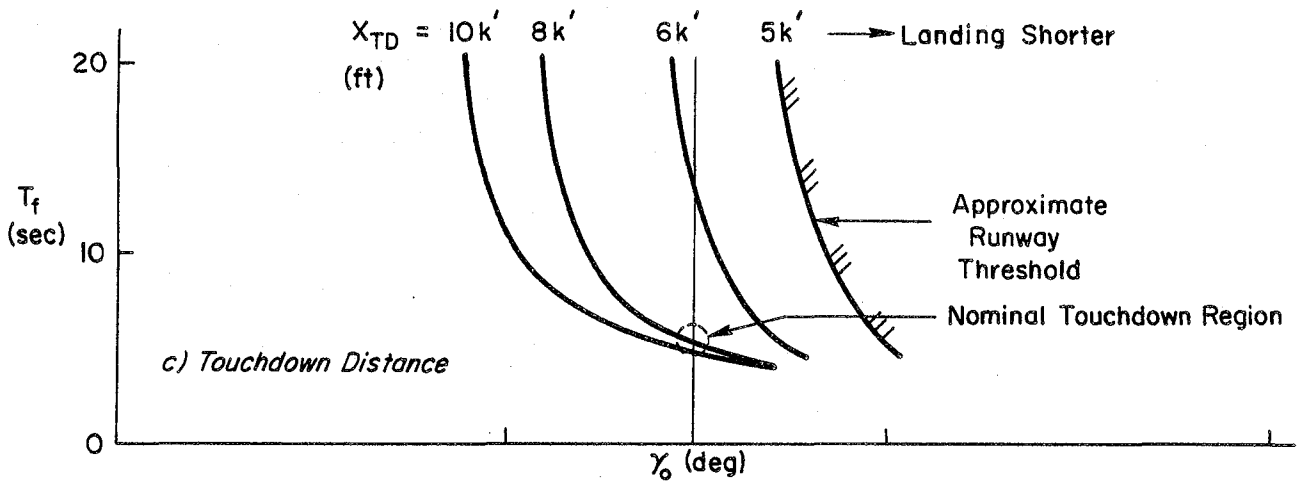


Figure 21. Variation of Touchdown Variables in the Pilot's  $T_f - \gamma_0$  Control Plane

- Design sinkrate at TD:  $-1.5 \text{ fps} \geq \dot{h}_{TD} \geq -2.5 \text{ fps}$
- Maximum sinkrate at TD:  $\dot{h}_{TD} = -9 \text{ fps}$
- Maximum sinkrate at TD, crosswind:  $\dot{h}_{TD} = -6 \text{ fps}$
- Nominal  $V_{TD} = 195 \text{ kts}$
- Maximum  $V_{TD} = 225 \text{ kts}$
- Minimum  $X_{TD} \doteq 5000 \text{ ft}$

Understanding of the trends in Fig. 21 is complicated by the fact that  $\gamma_0$  effects the initial conditions for flare. From Eq. A-53 in Appendix A, the touchdown sinkrate is

$$\dot{h}_{TD} = V_f \gamma_0 + h_f/T_f \quad (12)$$

The speed at the start of flare,  $V_f$ , is a function of  $\gamma_0$  alone as shown in Fig. 22. For glideslopes steeper than about  $\gamma_0 < -1$  deg, the Shuttle reaches flare height,  $h_f$ , before much speed is lost so  $V_f$  is roughly constant (with  $\gamma_0$ ) and approaches  $V_0 = 468 \text{ fps}$ . Thus, from Eq. 12, it may be seen that, for a given  $T_f$ , touchdown sinkrate increases with glideslope steepness as seen in Fig. 21. For increasingly steep glides, the pilot must flare more rapidly (smaller  $T_f$ ) and more precisely (smaller  $T_f$  error). For shallower glides,  $\gamma_0 > -1$  deg,  $V_f$  decreases and the flare must be slower to maintain a given  $\dot{h}_{TD}$ . Furthermore, the sensitivity to  $T_f$  decreases rapidly.

The equations in Appendix A for touchdown speed and distance are more complex than Eq. 12, however, the  $V_{TD}$  and  $X_{TD}$  contours are similar to the  $\dot{h}_{TD}$  contours. From Fig. 21b and 21c, steepening  $\gamma_0$  produces faster, shorter landings.

Perhaps the most important implication of Fig. 21 is that very precise control of flare ( $T_f \doteq 5.5 \text{ sec}$ ) is required to achieve the nominal touchdown situation. This may help explain why so many STA training flights are required, i.e., the pilot must achieve a precognitive skill level in this task. Other important conclusions are:

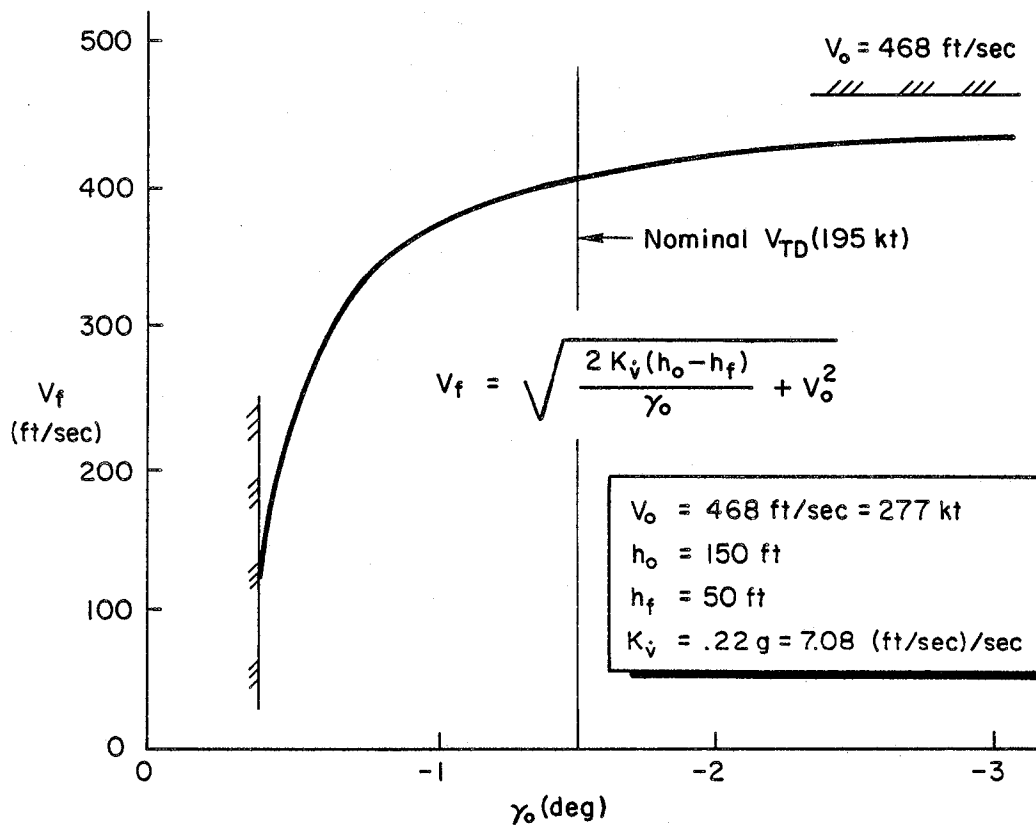


Figure 22. Variation of Speed at Flare Initiation with Glideslope

- The adequacy of the Appendix A approximations is indicated by the fact that, in Fig. 21, the nominal values for touchdown speed, touchdown sinkrate and touchdown position converge on the nominal  $\gamma_0$  of  $-1.5$  deg to form the nominal touchdown region indicated.
- For a given  $\gamma_0$  near nominal, the pilot has very little margin on  $T_f$  below the nominal  $T_f \approx 5.5$  sec to avoid  $h_{TD} > 0$  (ballooning). However, there is considerable margin for larger  $T_f$  with respect to the main gear  $h_{TD}$  limit. If the pilot uses a slow flare (long  $T_f$ ) strategy he will tend to land short and fast.
- For a given value of  $T_f$ , shallow  $\gamma_0$  leads to ballooning ( $h_{TD} > 0$ ). This is consistent with STS-3 crew comments that low, flat approaches in the STA are prone to ballooning (see Sec. III).
- For  $\gamma_0$  values near nominal, the pilot's  $T_f$  margin is reduced greatly in crosswinds due to the reduction in the crosswind  $h_{TD}$  limit.
- If the pilot executes a slow flare, i.e.,  $T_f > 10$  sec. the importance and roles of  $\gamma_0$  and  $T_f$  are reversed.  $T_f$  no longer makes significant difference (except for touchdown sinkrate in a crosswind) and touchdown speed and position are essentially determined by  $\gamma_0$ . In this situation  $T_f$  adjustments can not make up for an improper  $\gamma_0$  decision made earlier unless the pilot reverts to a "fast  $T_f$ ," precise flare strategy.
- Control of speed at touchdown is essentially a matter of how soon the pilot touches down. Touching down quickly implies high touchdown speed and vice versa. The speed stability issue is effectively removed by the  $V = \text{constant}$  assumption. But, even with a more complete model, touchdown speed control will probably be dominated by control of touchdown time.
- The touchdown distance varies inversely with the touchdown speed, i.e., landing fast implies landing short. Figure 21 indicates that  $\gamma_0$  errors of  $-0.25$  to  $-0.5$  degrees (i.e.,  $\gamma_0$  steeper than the nominal  $-1.5$  deg) could cause touchdown before reaching the runway threshold.

While the above view is a gross simplification of pilot technique, it does indicate some of the basic flight mechanical constraints, sensitivities, non-linearities and above all the effect of rapid deceleration.

#### **E. SUMMARY OF SHUTTLE FLYING QUALITIES AND FLIGHT CONTROL SYSTEM ISSUES**

The OEX plan to be developed in Section IV-VI has been created to address specific flying qualities issues identified in the work to date. Review of STS flights 1-4 (to be discussed in Sec. III) indicates that the primary flying qualities regime of interest is approach and landing, starting with acquisition of the steep glideslope (following the HAC turn) and ending with touchdown and rollout. Pilot stress reportedly increases as altitude decreases. During these flights longitudinal flying qualities have been the primary interest, with lateral directional control basically a secondary task related to regulation against disturbances. However, future crosswind landings may alter priorities somewhat.

In the following summary, issues related to flying qualities design criteria and specification problem areas for shuttlecraft in general are considered first, followed by a listing of issues directly concerning the flying qualities and manual control characteristics of the current Space Shuttle. The latter will be summarized on a three level priority basis. First, issues now considered to be flying qualities problems; second, characteristics which are unconventional but not necessarily problems; and finally potential problems considered previously, but now (following review of flights STS-1-4) of less immediate concern.

##### **1. Issues Relevant to Relaxed Static Stability Shuttlecraft with Rate Command, Attitude Hold Dynamics**

Extensive review of Shuttle flying quality and control system requirements and comparison of these with other flying quality requirements and data reveal several areas of disagreement and possible deficiencies in the Shuttle specification requirements. Most important of these are:

- a. Pitch rate requirements -- Shuttle time response upper boundary specification may be misplaced, being too tight on pitch rate overshoot allowable (or even desirable). Alternatively, the existing flying qualities data, and perhaps parameters based on conventional aircraft, may be inappropriate for heavily augmented, relaxed-static-stability, aircraft.
- b. Allowable dead time on the Shuttle time response specification for pitch rate and roll rate is probably too large.
- c. There is no specification of path-to-attitude dynamics (i.e.,  $h/\theta$  in Figs. 1 and 2) except for the implicit requirement on  $1/T_{h1}$ , ( $\partial\gamma/\partial V < 0$  requirement in Paragraph 3.4.3.5, Ref. 13). There is no consideration of other important path/attitude parameters (e.g.,  $1/T_{\theta 2}$ ,  $1/T_{h 2}$ ,  $1/T_{h 3}$ ).
- d. There is no explicit consideration of neutral speed stability in Ref. 13. Paragraph 3.4.3.5 "Controller-Speed Characteristics" probably has little practical effect.
- e. The form of the stability requirements for control of structural modes -- i.e., gain-stabilize with filters -- may increase effective time delay for manual control beyond that of alternative requirements (e.g., phase stabilization).
- f. Because superaugmented aircraft flying qualities are less constrained by airframe characteristics, the response may be tailored (especially for digital implementations) to specific missions, mission phases or tasks. This implies that design criteria and specs should be more task-specific. Further, the extrapolation of empirical flying qualities data from past designs may not be adequate. Accordingly, greater use of explicit pilot-vehicle-task models may be needed to formulate design criteria and specs.

## 2. Existing or Likely Shuttle Flying Qualities Problems

Comparison of Shuttle closed-loop dynamic characteristics with existing flying quality criteria, data, and design guides (all developed since the Shuttle specifications were finalized years ago) indicates several likely or existing problem areas:

- a. Large Longitudinal Effective Time Delay which leads to
  - 1) Lowered effective vehicle bandwidth and hence reduced pilot-vehicle and autopilot-vehicle attainable closed-loop bandwidth in path control functions
  - 2) Tendency for PIO under high stress, precise control conditions
  
- b. Large lateral effective time delay which leads to
  - 1) Lowered effective vehicle bandwidth and thus reduced pilot-vehicle and autopilot-vehicle attainable closed-loop bandwidth in rolling and path control functions
  - 2) Tendency for PIO under high stress, precise control situations
  - 3) Increased time to bank ( $\phi_{30}$  is 8785C Level 2, due entirely to the lateral effective time delay)
  
- c. Pilot location effects -- while well ahead of the c.g., the pilot is aft of the instantaneous center of rotation for longitudinal control inputs (whereas on most large aircraft the pilot is ahead of the ICR). This location has consequences on:
  - 1) Longitudinal path control -- possibly quite unfavorable for precise control situations due to "delay" in acceleration cues
  - 2) Lateral acceleration at the pilot station which is possibly deleterious
  
- d. The RHC displacement/force/electrical command combined characteristics possibly result in larger pilot control latencies (due to near isotonic properties). This can affect the control bandwidth and contribute to control difficulties in urgent tasks.

### 3. Unconventional Flying Qualities Issues

A number of issues which, while not necessarily problems, are unconventional and warrant further study:

- a. The effective pitch attitude numerator zero for RHC inputs is essentially set by the ELFBK filter and is much higher in frequency than  $1/T_{\theta_2}$ , the path inverse time constant.

- b. The mechanization of the pitch control system produces neutral speed stability (zero RHC force/speed gradient).
- c. Proper manual control procedures for the speed brakes is unclear (equilibrium glide).
- d. Use of the PIOS filter as a long term solution to the PIO problem, especially when the HUD becomes available.

#### 4. Lower Priority Issues

Comparison of possible or conceivable Shuttle dynamic characteristics with analyses, limited data, and tentative design guides has focused attention on several conceivable problem areas:

- a. Controllability of lateral coupled roll subsidence-spiral oscillation (lateral phugoid)
  - 1) In the  $1.5 > M > 1.2$  regime an effective lateral phugoid exists (1.4 Hz)
    - a) Divergent oscillation, yaw jets off
    - b) Stable, yaw jets firing
  - 2) Damping (effective  $[\zeta\omega]_{RS}$ ) is 8785C marginal with jets on, unsatisfactory with jets off
- b. Possibly marginal bank angle control in the  $3.4 > M > 2.5$  area if some aerodynamic characteristics approach the extremes of critical variation sets.
- c. Coordination in rolling maneuvers and sideslip trimming characteristics for "bent" airframe and laterally off-center c.g. effects -- especially above  $M = 3.5$  (where rudder is inactive and yaw jets provide coordination and trim).
- d. Reduced pitch and roll surface rates with 2 failed APUs
  - 1) Possible deficient control with crosswind, runway landings
  - 2) Increased PIO potential with such landings
- e. Possible deficient rudder surface rate with crosswind, runway landings (no failed APUs).

### SECTION III

#### REVIEW OF FLYING QUALITIES INFORMATION FROM SPACE SHUTTLE FLIGHTS 1-4

The following discussion summarizes information on Space Shuttle flying qualities derived from the first four Shuttle flights. This information has been obtained from various sources including articles in Aviation Week and Space Technology magazine, preliminary analysis reports prepared at DFRF for STS-1-4 (Refs. 22 through 25), transcripts of relevant portions of the STS-3 and STS-4 debriefings sessions obtained from DFRF, and the STS-4 crew report by Mattingly and Hartsfield (Ref. 26). A formal pilot questionnaire has been developed, see Appendix B, and was given to the STS-4 crew following their flight; however, a reply to this questionnaire has not yet been received and face to face meetings with any crew specifically for discussion of flying qualities issues have not yet been arranged. The available pilot comments have been combined with review of flight traces to form the following summary. Our concern is primarily with manual control but the information was also reviewed with an eye towards problems the crews might have encountered in monitoring the FCS in the AUTO mode. No major problems were indicated in this monitoring role.

The Space Shuttle is unique in having been flown manually at a more extreme flight condition than any previous aircraft, e.g., Mach 24 at 260,000 ft on STS-2. While many manual maneuvers have been performed during entry there is as yet little flight-based evidence of control characteristics which could reasonably be considered significant flying qualities problems at hypersonic or supersonic speeds. A number of questions about vehicle response above Mach 1 do remain to be answered but the primary area of interest from a flying qualities standpoint is the subsonic region from the HAC turn down through touchdown and roll-out. The emphasis on flying qualities indubitably increases as touchdown is approached. The subsonic TAEM region has been flown entirely in CSS (manual) only on STS-1. Subsequent flights involved some use of automatic control, in particular, for the equilibrium glide region on

the outer glideslope. Manual versus automatic control of pitch and speed brake in the subsonic regime is summarized in Table 5.

## **A. INDIVIDUAL FLIGHTS**

### **1. STS-1**

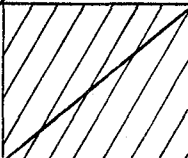
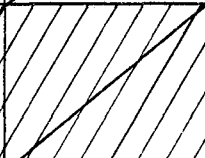
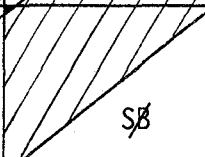
The first manually controlled maneuver of the Shuttle orbiter flights occurred at Mach 5 and 115,000 ft when Mission Commander John Young took control of the orbiter and flew the next to last roll reversal maneuver. The final roll maneuver was also performed manually at Mach 2.5 and the Shuttle was then returned to AUTO. Manual control was again started at 35,000 ft with a 1.3 g left turn around the HAC and continued through touchdown and rollout.

The most unexpected event during the approach and landing was a speed increase during the pre-flare pullup in which the airspeed reached 305 knots. This occurred as part of a long period speed oscillation beginning near the end of the equilibrium steep glide. Some significant activity in the manually controlled speed brakes occurred during the later half of the equilibrium steep glide phase and appears to correspond to the initiation of the low frequency speed oscillation. The excess energy ultimately caused the vehicle to land 2,000 ft longer than the nominal touchdown point; however, because the touchdown point was not tightly constrained in this initial flight this did not produce a flying qualities problem per se. The higher than expected energy was indicative of a higher than expected L/D ratio and the fact that speed brakes were retracted somewhat sooner than necessary. Winds and turbulence were quite light and the final flare and landing were very smooth with the touchdown sinkrate being 1 fps or less as compared to the anticipated 2.5 fps. There was very little action in the PIO's filter during the landing.

### **2. STS-2**

Manual control in the second orbiter flight began much earlier when Mission Commander Joe Engle flew the first roll command to about 80 deg of bank at Mach 24.5 and 260,000 ft. A number of additional manual

TABLE 5. SUMMARY OF MANUAL PITCH AND SPEED BRAKE CONTROL, STS-1-4

FLIGHT SEGMENT \ STS	1 APR 81	2 DEC 81	3 APR 82	4 JUL 82
HAC Turn	P SB	P SB	P SB	P SB
Steep Glideslope Capture	P SB	P SB	P SB	P SB
Equilibrium Glide on Steep Glideslope	P SB			P SB
Preflare Pullup	P SB	P SB		P SB
Shallow-Glideslope Capture and Glide	P SB	P SB	P SB	P SB
Final Flare and Touchdown	P SB	P SB	P SB	P SB
Slapdown and Rollout	P SB	P SB	P SB	P SB

P = Manual Pitch Control, SB = Manual Speed Brake Control

SB = Speed Brake Retracted,  Auto

maneuvers were flown as the entry continued, but (as in the first orbiter flight) none of these maneuvers above the TAEM region produced any concerns for flying qualities problems even though winds were considerably higher than for the first flight. The STS-2 commander was impressed with the "tightness" of the rate command system relative to the Shuttle training simulators. He further noted that in the training simulators he had seen attitude drifts at the end of maneuvers, as well as oscillations and overshoots which did not occur in flight. The STS-2 crew also felt that the Shuttle's gust tolerance was better than expected. It was remarked that the workload connected with the manually performed inputs for aerodynamic data extraction was very high and it was recommended that the number of such inputs be reduced for upcoming flights.

The high winds encountered during entry dictated somewhat more manual flight than originally anticipated and the HAC turn was flown manually. This allowed the crew to account for wind during the turn and thus avoid a high-g final correction to achieve proper alignment with the runway -- a strategy that would not have been used by the automatic guidance system. After completing the HAC turn, the steep glideslope was acquired and control switched to the autoland mode. The craft was flown in autoland down to the preflare altitude of 1,750 ft at which point the commander again took manual control of the aircraft. At manual takeover the airspeed was approximately 15 knots below the nominal of 285 KEAS due largely to energy loss during a speed brake sweep on the HAC turn. A smooth landing was again made but with lower than nominal energy. As with the first flight, little PIO's activity occurred during the landing.

### 3. STS-3

The STS-3 flight is possibly the most interesting of the four flights from a flying qualities standpoint. This flight was unique for several reasons. In particular, the final manual takeover before landing was very low (around 140-120 ft altitude) and was followed by some off-nominal pilot/vehicle response. Before the final landing the

vehicle was flown in a right turn around the HAC which restricted the commander's visibility. Only the pilot could actually see the runway and thus he gave the signal to initiate the turn. High winds required the speed brakes to be initially deployed to the full open position; but by the end of the HAC turn they were partially closed and modulated manually to maintain the desired 285 KEAS.

Following the turn the vehicle was lined up with the steep glide-slope and the auto guidance engaged at about 12,000 ft with transition to the autoland at around 10,000 ft. The craft continued in AUTO through the steep glide, the preflare pullup, and the initial acquisition of the the shallow glideslope whereupon final manual takeover occurred. The commander indicated that, on the inner shallow glide-slope, the aircraft appeared to be flying "low and flat." Based on his STA experience he felt that the craft was prone to "ballooning" and possibly a PIO in this condition. At this point, the pilot requested the commander to "hold the aircraft up" and allow airspeed to decrease before touchdown. The commander gave the vehicle a nose-up command and to him the response felt like the ballooning previously observed in the STA. He then gave a nose down command to stop this perceived ballooning and the craft immediately touched down. This was unexpected and prompted concern for exceeding the limits on the landing gear.

After main gear touchdown, the commander felt that the craft was maintaining the desired pitch attitude initially but later began to pitch down. This prompted a nose up RHC command which did not seem, to the commander, to generate much pitch response and thus a second nose up command was put in. A rapid nose up response occurred which seemed excessive and the commander immediately reversed the RHC command. However, by this point elevator rate limiting had begun which interfered with effective manual control. The result was that the nose came down quite rapidly and the pilot, using full back stick, was unable to prevent the nose gear from touching down. Postflight analysis discussed in Ref. 24 concluded that the problem experienced during the maneuver was almost entirely due to inadequate rate limit and that such saturations are quite easily obtainable with the control authority available. It

was further concluded that such an occurrence might be quite likely in an operational environment and that the handling qualities are not adequate to perform a satisfactory landing in a routine manner under these conditions.

#### 4. STS-4

STS-4 was the first landing on a restricted (15,000 ft) runway. This flight also produced some detailed crew comments concerning flying qualities. As with the previous 3 flights no distinct flying qualities problems were indicated above Mach 1. Specific indication of this occurred in the flight debriefing when Commander T. K. Mattingly was asked to comment on the Orbiter's handling qualities at Mach 2.8 where he did a roll reversal. The commander replied that there was nothing worth commenting on. He indicated that he was very satisfied with the Orbiter's handling qualities during the HAC turn and that it flew just as he had expected. This view may be influenced by the lack of significant winds, which allowed the HAC turn to be flown manually according to the nominal guidance commands.

After completing the HAC turn and acquiring the outer glideslope, the craft was switched to AUTO pitch/roll/yaw but the speed brakes were retained under manual control. The commander remarked that airspeed varied between 282 and 287 knots and "that it was not obvious what to do with the speed brake." CSS was re-engaged at 2,500 ft and maintained through rollout in a near-nominal landing. The preflare was initiated on a radar altimeter cue and the ADI pitch rate was used to aid in executing the pullup. It was remarked that the nominal preflare initiation altitude is too high for the commander to execute repeatably (as opposed to safely) using "out-the-window" perspective only. A point of particular interest is the commander's remark that he relied more on the pilot's altitude calls than he did on his perception of altitude during the final flare and, at touchdown, the commander felt he was actually higher than what the pilot was calling out.

Concerning the details of flare strategy the commander remarked that he "could not fly  $\dot{h}$  or  $\ddot{h}$  in the Shuttle -- you have to fly pitch attitude." However, he indicated that his method for landing was to estimate  $\dot{h}$  from the pilot's altitude call cadence and then control pitch attitude based on this estimated sinkrate and the pilot's airspeed calls. He felt that if the pilot had not been able to call out this information, as would have been the case if he was trouble shooting some system problem, the landing strategy would not have worked as well. He stressed the need for more timely information transfer and believes that the HUD will help. The landing occurred earlier and faster (200 KEAS) than the commander had anticipated. No major problems were encountered in the rollout, although the commander felt frustrated in his inability to obtain either the target deceleration or even a smooth level of deceleration.

In summary comments, the commander indicated that he felt the Orbiter is a difficult aircraft to land and an excessive amount of training is necessary to learn how to fly the Shuttle. He emphasized that small discrete attitude corrections are necessary for the final stages of landing below 100 ft AGL. He further felt that the pitch control is very crisp and acts more like an attitude hold than a rate command system. This impression bears further consideration since it is at odds with the FCS concept and the comments of the STS-2 crew. The commander was aware of the effect of the pilot location relative to the ICR and felt that the characteristic is very undesirable because it prevents tight closure of the  $\dot{h}$  loop. It was noted that external trajectory cues are needed to aid the pilot in smoothly executing the preflare and that elimination of the 6 ft per sec landing sinkrate restriction is desirable as soon as possible.

## **B. SUMMARY**

The information extracted from the first four Shuttle flights may be summarized by considering it in relation to the specific flying qualities issues that have been identified in this program to date.

- No explicit reference to large effective time delays have been uncovered in crew comments. In this connection it must be remembered that the time delay in pitch attitude response only becomes critical in a high stress situation in which high bandwidth pilot activity occurs, i.e., situations bordering on PIO.
- Effects of pilot location with respect to the instant center of rotation were explicitly noted by the STS-4 commander and it was felt that these characteristics were very undesirable and limited tight closure of an h outer loop in landing flare.
- No explicit comments concerning RHC force/displacement characteristics were noted nor was there any explicit mention of the neutral speed stability (i.e., zero RHC force speed gradient.) There was, however, indication of speed control problems during the equilibrium glide on the steep glideslope under manual speed brake control.
- No direct influence of superaugmentation effects is readily evident, but the STS-4 commander's comments that the flight control system appears more like an attitude command system than a rate command system deserves further consideration.
- The impact of rate limiting on the STS-3 events indicate that rate limiting is an important consideration even without APU failure.

Thus in final summary of the information extracted from the first four Shuttle flights, it appears that the Shuttle flying qualities are adequate at higher altitudes and that the Shuttle can be landed adequately if the landing situation is sufficiently near nominal such that pilot's may fly in almost a preprogrammed manner. There is some indication, however, of potential difficulties in Shuttle landings in more extreme operational situations, in particular with winds and relatively tight constraints on touchdown point and rollout distance.

## SECTION IV

### OVERVIEW OF THE SHUTTLE OEX PLAN

This section presents an overview of the technical approach for the OEX flight experiment designed to produce (ultimately) flying qualities and flight control system design criteria and design guides for future space shuttle craft. The approach is an expansion and extension of the preliminary plan outlined in Ref. 1.

In any handling quality experimentation, it is highly desired to set up and assess a wide range of off-nominal flight and dynamic conditions and situations of increasing pilot stress from which to establish limiting boundaries. It is also desired that the experimental conditions be highly repeatable and assessed by a sufficient number of pilots to produce meaningful data in a statistical sense. The resulting boundaries then establish the maximum allowable off-nominal flight conditions and stress levels. Unfortunately, the Space Shuttle flight goals (e.g., normal operations involving the lowest possible stress) are the exact antithesis of the above flying quality research goals.

As a result, the overall plan presented herein is to extract the maximum possible information from the routine, ongoing STS flights with a minimum of special manual control inputs and maneuvers. This approach is based upon an unusual, recently developed, non-intrusive data and information extraction technique. This technique can be used to define pilot dynamic behavior in either flight or simulation. The resulting data will then be used as points of departure to validate and/or adjust flying qualities criteria or bounds obtained via ground and in-flight simulation.

This section begins with a summary of the elements of an ideal flying qualities flight experiment as a point of reference for considering problems anticipated for the Shuttle OEX (Subsection B). The proposed OEX approach is outlined in Subsection C with primary emphasis placed on an indirect approach which includes a simulation program correlated with

the flight experiments. The flight experiments and simulations would be linked by pilot model identification and the simulations would provide a means of producing flying situations not possible in Shuttle flights.

#### **A. ELEMENTS OF AN IDEAL FLYING QUALITIES FLIGHT TEST**

A number of limitations must be anticipated for Shuttle in-flight flying qualities studies. However, it is useful to begin by considering an ideal experiment as a point of reference for considering what may actually be done. The basic elements of an ideal experiment are as follows.

##### **1. Pilot Stress and Workload**

Identification of flying qualities deficiencies in landing generally requires that the pilot fly the aircraft in a high stress/high workload situation. Potential problems may not be uncovered and flying qualities may appear adequate if high stress flying is not examined. High stress situations may be created by:

- Off-nominal initial conditions, e.g., high speed and altitude at end of preflare
- Disturbances: a variety of crosswinds, shears and turbulence
- FCS failures: most probably 2 failed APU's
- Touchdown constraints: limits on touchdown sinkrate, speed and distance

##### **2. Vehicle/FCS Parameter Variations**

The ability to vary FCS parameters as well as basic airframe and aerodynamic parameters is desired to consider sensitivities and improvements and ultimately to define criteria. The first level of parameters of interest include:

- Manipulator (RHC) characteristics: force/displacement, gain (e.g.,  $q_c/\delta_{RHC}$ ), PIO's filter design, shaping

- Attitude dynamics: for the superaugmented Shuttle 3 parameters ( $T_q$ ,  $\omega_n$ ,  $\tau$ ) are basic
- Path dynamics: basic elements of  $h/\theta$  --  $T_{\theta_2}$ ,  $T_{h_1}$ ,  $T_{h_2}$ ,  $T_{h_3}$
- Speed dynamics: variations in speed stability

The basic experimental design is thus built around a 2-dimensional matrix in which one dimension consists of system parameter variations and the other consists of pilot stress/workload variations.

### 3. Tasks and Maneuvers

A variety of tasks and maneuvers are of interest beginning with nominal, operational tasks. These may be categorized as:

- Discrete maneuvers, e.g., transition from steep to shallow glideslope in the preflare pullup
- Tracking tasks, e.g., following the shallow glideslope
- Regulation tasks, e.g., maintaining constant speed in turbulence on the steep glideslope

In addition to nominal tasks, special maneuvers and inputs are of interest to explore the flight envelope and improve the measurement situation.

- Discrete maneuvers: sidesteps, pitch doublets, etc. for subjective flying qualities assessment
- Tracking or regulation tasks with special inputs (e.g., sum of sine waves) to allow describing function analysis, etc.

### 4. Performance Measures

When a task is flown, the variables which define the trajectory will depart from their nominal values and task performance measures may be defined in terms of the statistics of these variations. For the Shuttle landing task, for example, performance measures may be defined in terms of touchdown distance, speed and sinkrate. Acceptable performance is set by limits on landing gear loads, runway length, etc.

## 5. Workload Measures

Flying qualities of an aircraft cannot be determined from task performance alone but rather must consider the pilot stress and workload for acceptable performance. Thus there is a requirement for stress or workload measures as well as performance measures. Possible measures may be classified as:

- Objective and quantitative, e.g., the Cross Coupled Instability Task, CCIT (Ref. 27)
- Subjective and quantitative, e.g., Cooper-Harper pilot ratings
- Subjective and qualitative "measures" from pilot comments and questionnaire replies
- Implied from pilot model measurements, Ref. 28

## 6. Measurement Requirements

The above elements imply a requirement for a number of specific measurements. In addition, these must be obtained for a statistically significant sample of flights and crews. Primary measurement categories include:

- Vehicle state and state rate
- Control surface deflections
- Manual controller deflections (commander and pilot separate)
- Trim control inputs
- Selected FCS "discretes"
- Crew physiological data, crew conversation transcripts

## B. LIMITATIONS AND EXPECTATIONS FOR OEX FLIGHT EXPERIMENTS

A primary consideration that must be allowed for in planning the OEX is that every effort has and will continue to be made to minimize off-nominal, high stress situations for Shuttle flights. This is

operationally necessary, and makes assessment of flying qualities margins or problems difficult from flight data alone unless an extreme off-nominal condition develops accidentally.

This situation exists to some extent in any flight test program, but in normal flight tests (e.g., fighters) non-operational higher stress maneuvers can be employed intentionally to explore suspected problems. This procedure is not feasible for the Orbiter for several reasons:

- The Shuttle is in an "operational status" (even though extensive data acquisition will go on for some time) and will often be landing with valuable payloads on board
- There is now no ejection capability for the crew which is necessary for high risk flight test operations
- Even if crew ejection were feasible, the Shuttles are very few in number, very costly, and highly "visible" vehicles for which every effort must be made to minimize risk

There are a number of additional unusual considerations specific to the Shuttle, which make inflight experiments concerned with manual control and flying qualities somewhat difficult:

- Shuttle flights are relatively infrequent
- There is only "one pass" through each flight condition per flight and the flight conditions change continuously and rapidly
- There may be significant limitations on special inputs or maneuvers
- The need to evaluate the automatic flight control system conflicts with the need to study manual flight control
- It is not possible to vary Shuttle FCS parameters. On the other hand, uncontrolled changes in these parameters can be expected from flight-to-flight which further complicates interpretation of data.
- There is a different crew for each flight, crews are not necessarily closed-loop flying qualities oriented, and, in fact, are trained to exceedingly high precognitive skill levels
- It is difficult to obtain relevant information from the crews in a timely manner

Given the above limitations, the expectations for OEX flight experiments may be considered with respect to the ideal situation.

### **1. Pilot Stress and Workload**

Variation in pilot stress will occur during approach and landing, generally increasing as touchdown is approached. High workloads will occur, especially with manual PTI's. However, stress and workload will not be under direct experimental control and we must assume that critical levels (e.g., PIO) will occur rarely.

### **2. Vehicle/FCS Parameter Variations**

As with pilot stress, vehicle parameters will not be under direct experimental control. Some uncontrolled (from an OEX standpoint) variations in FCS ILOADS and software and vehicle mass properties is to be expected as the Shuttle matures. These changes may be expected to increase data scatter and hinder statistical analysis but to provide some trend information through flight-to-flight comparisons. The latter may be unreliable due to low sample size.

### **3. Tasks and Maneuvers**

Nominal approach and landing tasks including discrete maneuvers, tracking and regulation tasks may be expected. While efforts to obtain special flight maneuvers should be pursued, it cannot be assumed that these can be obtained and the OEX plan should accommodate this situation.

### **4. Performance Measures**

Because the instrumentation on the Shuttle is generally adequate, the possibilities for computing performance measures from actual Shuttle response data is good.

## **5. Workload Measures**

Use of pilot comments, special debriefings and questionnaires is feasible. Implied measures from pilot model measurements (to be discussed later) is also possible. Use of special on-board equipment (e.g., the CCIT hardware, Ref. 27) can be assumed to be much more problematical. Quantitative pilot ratings, widely used inflight testing, are problematical for the OEX because of the "one shot" nature of Shuttle flights and because the pilots (commanders) are not necessarily trained in flying qualities assessment.

## **6. Measurement Requirements**

The availability of the needed measurements is generally good with the present Shuttle instrumentation system. The situation will be reviewed in detail in Subsection J.

### **C. THE PROPOSED OEX PROCEDURE**

Having considered the limitations for OEX in-flight experiments -- in particular, limitations on variations of system parameters and pilot stress -- we may consider practical approaches. Two basic approaches are considered -- "direct" and "indirect."

The direct approach corresponds to typical flying qualities flight test procedures in which an aircraft is exercised by one or more pilots with risk and activities increasing as time goes on. Typically the pilots employ non-operational maneuvers (e.g., stalls, asymmetric loads) or fly near the limits of the flight envelope in an attempt to detect any flying qualities problems. Flight data is available from vehicle instrumentation and qualitative data is collected from the pilot in the form of comments, replies to questionnaires and pilot ratings. For the Shuttle, limitations on the direct approach come from the previously listed limitations on maneuvers and abnormal flight activities, and further, from the difficulties in the use of formal pilot ratings.

## 1. The Indirect Approach

The indirect approach is a somewhat unconventional procedure in which flight data is used to provide discrete reference data points and to validate one or more research (as opposed to training) simulations. Once a simulation is validated, the two-dimensional experimental design of the ideal program can be explored. The elements of this approach are:

- Measure pilot and vehicle response for each Shuttle flight, define piloting technique (i.e., a pilot model) using formal identification procedures (e.g., the NIPIP program) and other available data (e.g., crew debriefings), establish the degree of active manual control.
- Replicate the flight situation in simulator(s), identify pilot model as for flight data, validate the simulator based on the pilot model (i.e., the models must be essentially the same in flight and simulator).
- Conduct simulation studies under the 2-dimensional (pilot stress/system parameter) matrix, expand flight conditions to off-nominal situations, create high stress piloting tasks.

Having made the distinction between direct and indirect approaches, we can now say that these simply represent extremes of approach and as a practical matter both will be used in whatever mix is possible and useful. The essential point, however, is that because of limitations on the direct approach for the Shuttle, emphasis must be placed on the indirect approach to insure that useful flying qualities information will be obtained. Details of possible OEX simulations will be discussed in Section V.

## 2. Pilot Model Identification

The indirect approach makes use of pilot models as a "bridge" between flight and simulator. Traditional methods of pilot model identification have involved spectral or describing function measurements, Refs. 7, 29 and 30, of pilots performing tracking tasks involving specialized inputs such as a sum of sine waves. Thus, use of these

pilot identification procedures require an "active" flight test program involving special inputs. Recent work, Refs. 31 through 34, has developed "non-intrusive" pilot identification procedures which can provide useful results from normal flying tasks. These identification procedures are applicable to what have been referred to as "discrete maneuver models," Refs. 35 and 36. Discrete maneuvers comprise a class of flying tasks which include change of heading, altitude, airspeed, or landing flare. These relate more directly to operational mission oriented piloting tasks than the more abstract pure tracking tasks. Primary emphasis is placed on the non-intrusive approach here since it is the one approach which certainly can be applied to the Shuttle program. However, there are a number of conceptual and practical difficulties that must also be addressed.

Non-intrusive identification of pilot models for discrete maneuvers puts a new emphasis on explicitly modeling the task. Fortunately, for the highly structured Shuttle entry operations, discrete maneuver segments are quite well defined by the idealized trajectory and speed schedule in approach and landing (discussed and modeled in Subsection E and Appendix A). Given this new emphasis on explicit description of the piloting task it is appropriate to speak of a pilot-vehicle-task model rather than simply a pilot model. This system is reflected in Fig. 23.

The form of the pilot models is also important to the concept of the indirect OEX approach. This form is referred to as the structural isomorphic model to distinguish it from other possible model forms -- e.g., an algorithmic pilot model (see Ref. 37). An illustration of a structural isomorphic model will be provided in Subsection F through prototype models developed for this effort. For now we may define structural isomorphic models to be those which are consistent with inputs and modifications not only from formal computerized input/output pilot model identification programs but also pilot commentary and questionnaires. The ability of a model to accept inputs from a wide variety of sources is extremely valuable for a situation such as the OEX where no one procedure can reliably be expected to give the total answer and the "final" model must be pieced together from a number of sources. This, in turn, makes the structural isomorphic model an organizing concept for the OEX.

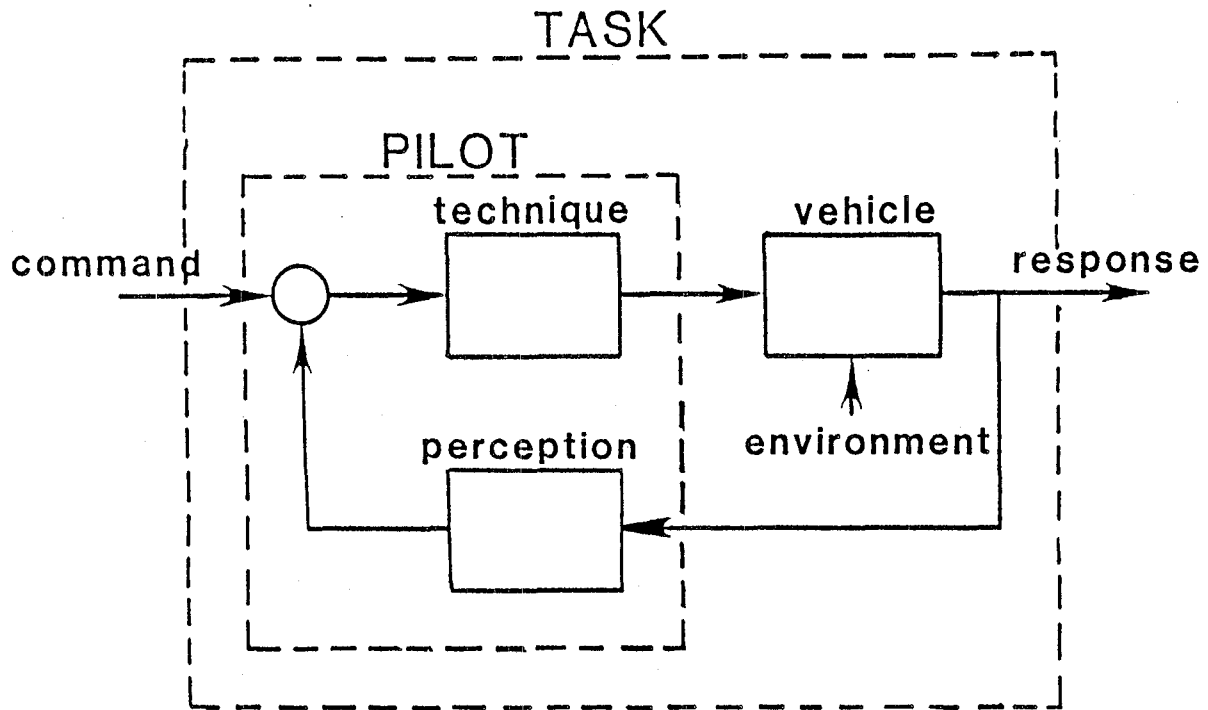


Figure 23. Block Diagram of Pilot-Vehicle-Task System

This view of the model's role is shown in Fig. 24 where it may be seen that the structural isomorphic pilot-vehicle-task model is formulated and modified on the basis of inputs from theory and analysis, from flight and simulator measurements and from crew experience. As will be discussed further in Subsection F, the model can be initially formulated from consideration of the flight mechanics of the task and manual control theory. Because the essence of the model is to allow ready physical insight to the piloting problem and thus accommodate diverse inputs, an essential step for theoretical inputs is simplification of the mathematical models. Illustration of this procedure is provided in Appendix A. The theoretical/analytical approach then employs a pilot-vehicle-task simulation and accompanying analysis. The simulation model could be in the form of a digital computer simulation, an analog computer simulation, or a hybrid combination, however, it would not be an elaborate "complete" simulation of the Orbiter, but rather a reduced order simplified simulation.

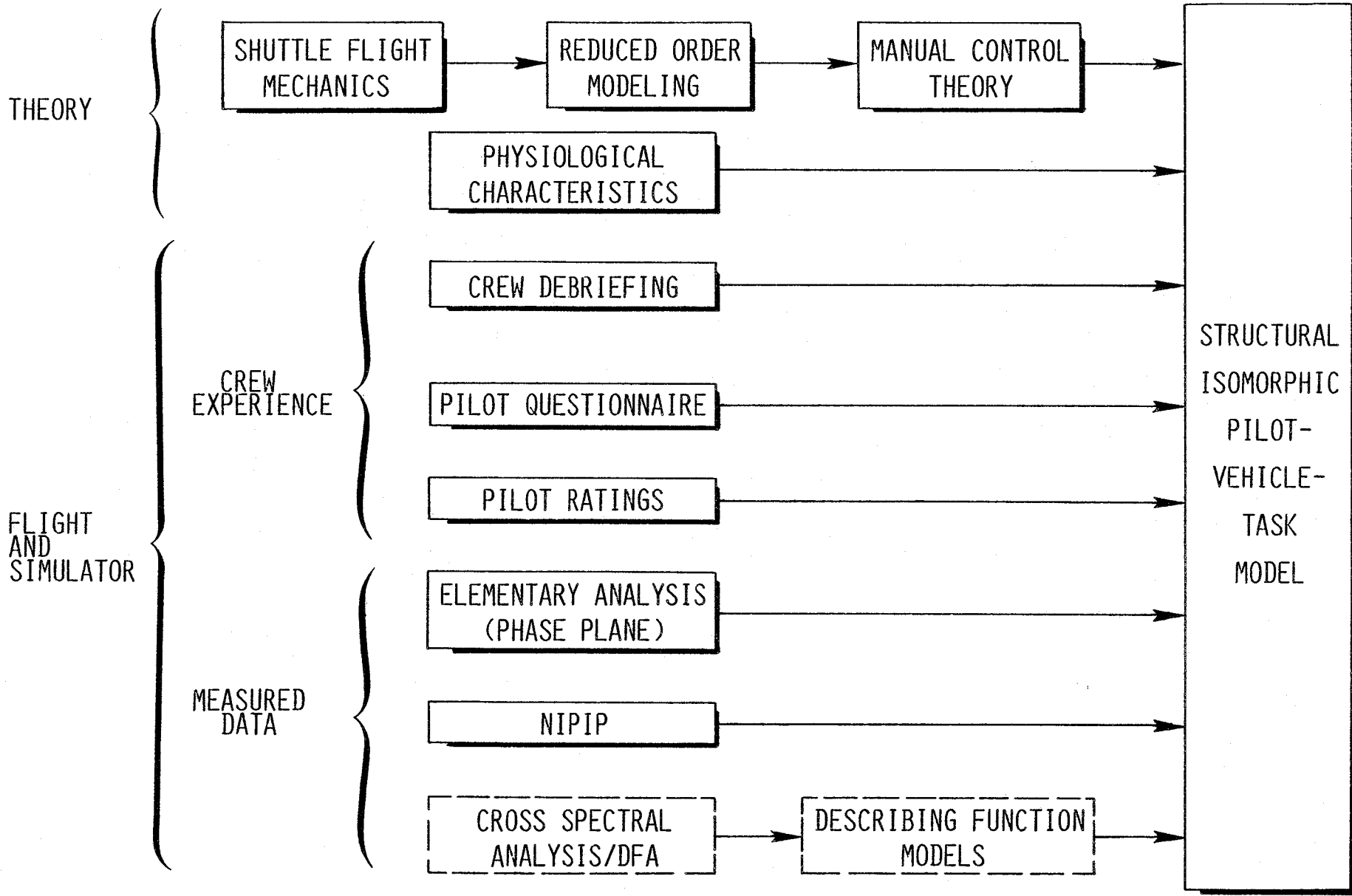


Figure 24. Development of the Structural Isomorphic Pilot-Vehicle-Task Model

The second general group of inputs for development of the pilot-vehicle-task model is crew (pilot) flight experiences. These inputs will come from three sources: comments, questionnaires, and non-intrusive model measurements. The latter would involve model identification efforts at various levels of sophistication based on measured Shuttle flight data. The most elementary level might involve simplified analysis procedures such as the phase plane procedure of Ref. 36. The simpler procedures are of interest because of the limitations on optimizing the inputs and experimental scenarios for more formal identification procedures. For more formal pilot model/vehicle identification, the primary procedure proposed is use of the NIPIP computer program presently available at DFRF and STI (Ref. 33). This program has been used in similar efforts and is considered the most appropriate for the OEX. Details of the use of NIPIP will be discussed in a later section. If an active experimental program allowing special inputs becomes feasible, it might be possible to use the previously noted cross-spectral or describing function procedures or other more elaborate identification procedures. These might lead to intermediate, higher order models which could then provide inputs to the structural isomorphic model.

### **3. Direct Flight Experiments for the OEX**

Having considered the indirect approach to the OEX, we may now consider the possibilities if any direct flight experiments become feasible. To examine the possibilities for direct flight experiments it is necessary to consider two additional categories: single-flight and multiple-flight experiments. In single-flight experiments a result concerning a specific issue is extracted from a single flight. In a multiple flight experiment data from several flights are required to accumulate a single data "point". The latter procedure take advantage of changes in the vehicle system or perhaps payload mass properties that would occur from flight to flight thus allowing some exploration of the system parameter dimension.

a. Active Single Flight Experiments

The distinguishing feature of these procedures is the presence of some special or non-operational maneuver or input to the FCS. The possibilities are somewhat limited for Shuttle flights. The most straight forward special inputs or maneuvers are those typical of conventional flying qualities flight tests such as pitch pulses or doublets, "bank-to-bank" maneuvers, side step maneuvers in landing approach, etc. Some precedent for these maneuvers exist in the small magnitude PTI test inputs that have been used for the purpose of "MMLE" identification of airframe aerodynamic coefficients. Because of crew complaints of high workload many of these inputs have now been automated; however the possibilities for a few select inputs for flying qualities studies, especially in the high subsonic region, may exist. These might include the use of tracking or regulation tasks involving external inputs to the vehicle. A tracking task could be formulated as follows: a high bandwidth (up to 2 rad/sec) quasi-random pitch attitude or flight path angle disturbance could be injected into the flight director signal on the commander's ADI (or on the HUD when installed). The commander would then actively track this disturbance signal. The pilot's display would not have the disturbance signal and thus he could function as a "safety pilot". This tracking task provides a potential for use of describing function analysis (DFA) procedures that would allow off-line identification of both a describing function pilot model and a model of the effective augmented vehicle.

A related procedure could be based on a regulation task. In this case a quasi-random disturbance (e.g., artificial turbulence) would be input to the Shuttle control surfaces by modifying the presently implemented program test input (PTI) capability. The pilot would then maintain the nominal flight trajectory while regulating against the artificial disturbance. This has advantages in that modifications to the flight software would not necessarily be required and the pilot's task would be to maintain the vehicle on the nominal trajectory.

An important consideration in direct, active flight experiments is the flight region where the maneuver is to be conducted. Since the approach and landing is of primary interest, it is desirable to perform any maneuvers as close as possible to the ground. However, from the flight safety standpoint just the reverse situation must be imposed. To some extent, it is feasible to conduct maneuvers at higher altitudes as long as the flight conditions are not significantly different. As a practical matter this specifies the subsonic flight regime which restricts the maneuver region to between initiation of the HAC turn and touchdown with the two most likely regions being the HAC turn and the equilibrium glide on the steep glideslope.

The possible flying qualities data to be obtained from such direct active experiments would primarily be measures of pilot dynamics, closed loop crossover frequency (control bandwidth) and phase margin (workload), and pilot commentary.

Finally, it is of interest to consider what specific flying qualities and design criteria issues could be considered using direct procedures. Obviously, the experiment can not focus on a particular issue but would rather provide data which is somewhat more general. Such experiments could reveal information concerning most of the high-stress related flying qualities issues, such as effective time delay. However, this data would not directly relate to specific sources of effective time delay (i.e., manipulator effects vs. those due to the structural filters).

#### b. Passive Single Flight Experiments

The distinguishing feature of these procedures is the absence of any special inputs or maneuvers. The only real possibilities are simply to conduct manual approaches and landings, define pilot behavior via non-intrusive measures, and interview the crew and/or have them respond to a questionnaire. If some unusual event happens to occur during the flight some insight may be gained but nothing can be planned before the flight.

c. Multiple Flight Experiments

Some additional data might be gathered in direct multi-flight experiments. For instance, for two flights with significant differences in payload mass properties there might be sufficient difference in the instant center of rotation to produce information about "pilot ICR location" effects. Similarly, variations in steady winds and wind shears during approach might provide some insight on the effect of neutral speed stability on flying qualities. However, there are fundamental problems in making flight-to-flight comparisons and extracting data on a multi-flight basis. These include the problems of using uncontrolled (from an experimental design standpoint) variations, working with different crews for each flight, and finally a very small sample in any reasonable period time.

Thus to summarize the situation for direct flight experiments it appears that the first priority should be given to arranging pilot briefings and formulating a very effective pilot questionnaire for use in the debriefing process. Planning of direct active experiments is necessarily limited until further contact with appropriate groups at NASA JSC, in particular the Astronaut Office, realistically establish what, if any, active maneuvers or special inputs are feasible for Shuttle OEX flights.

## SECTION V

### PROPOSED INDIRECT OEX APPROACH

Having introduced the overall concept of an indirect program based on the structural isomorphic pilot-vehicle-task model we may proceed to specifics which will help to refine some of the ideas. Prototype pilot-vehicle-task models for the Shuttle approach and landing will be developed first in Subsection A. Non-intrusive procedures proposed for use in the OEX will then be reviewed in Subsection B. Finally, instrumentation and software requirements for the OEX will be considered in Subsection C.

#### A. PROTOTYPE PILOT MODELS FOR SHUTTLE APPROACH AND LANDING

Prototype pilot models for the four primary segments of the approach and landing phase of the Shuttle entry are shown in Figs. 25-28. Each segment has a distinct set of loop structures: the equilibrium glide on the steep glideslope is shown in Fig. 25, the preflare pullup is shown in Fig. 26, the decelerating glide on the Shuttle glideslope is shown in Fig. 27, and the final flare is shown in Fig. 28. The capture modes for acquiring the steep and the shallow glideslopes are not shown explicitly, although, these features can be added to the pilot models without any major conceptual changes. The prototype pilot models shown in Figs. 25-28 are compatible with information from several sources: analysis of Shuttle flight mechanics in approach and landing, Subsection E; theoretical analysis of control law requirements with specific reference to manual control and to the autoland system (which was specifically designed to be compatible with the pilot); and the STS-1-4 flight data and pilot comments.



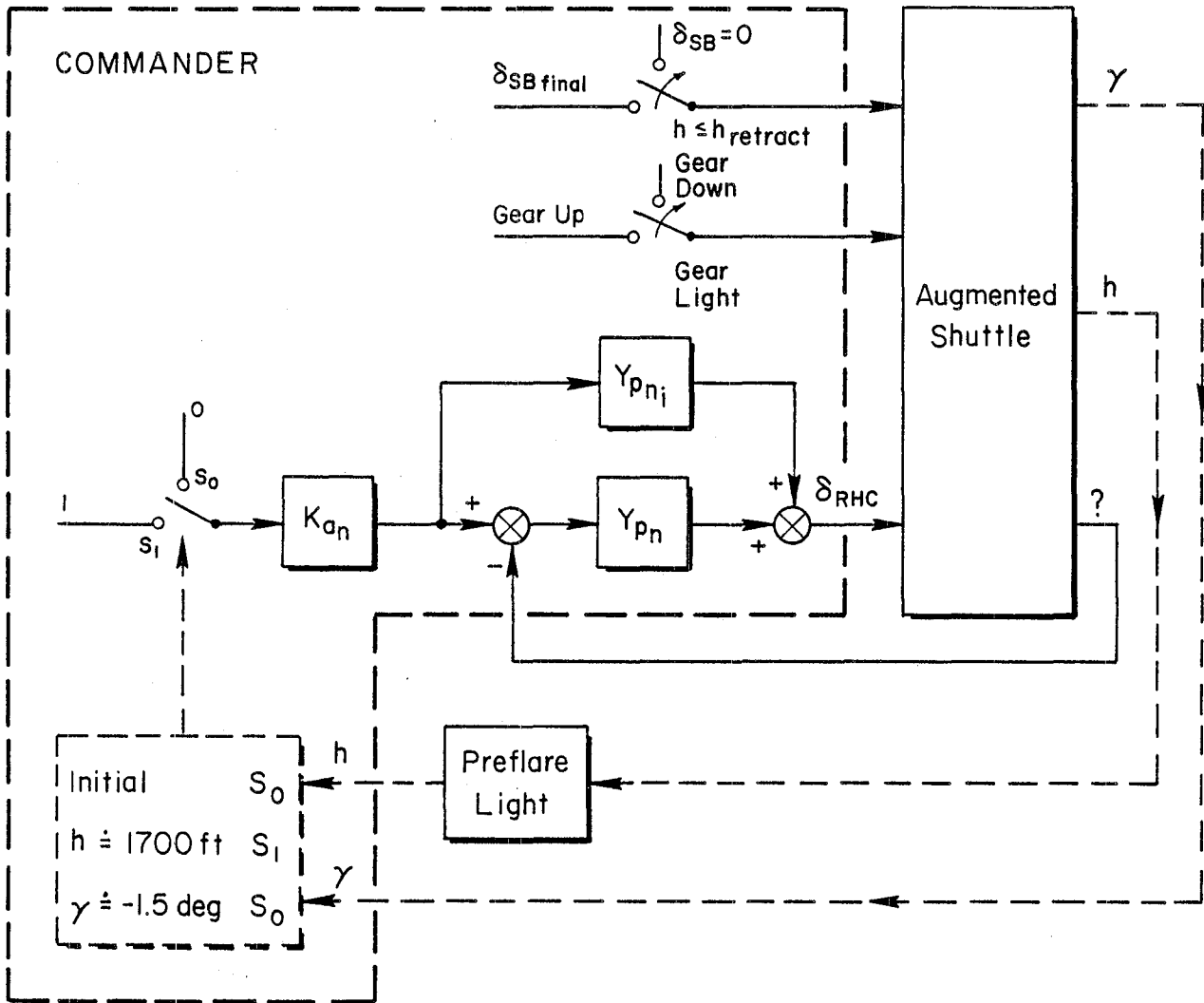


Figure 26. Preflare Pullup

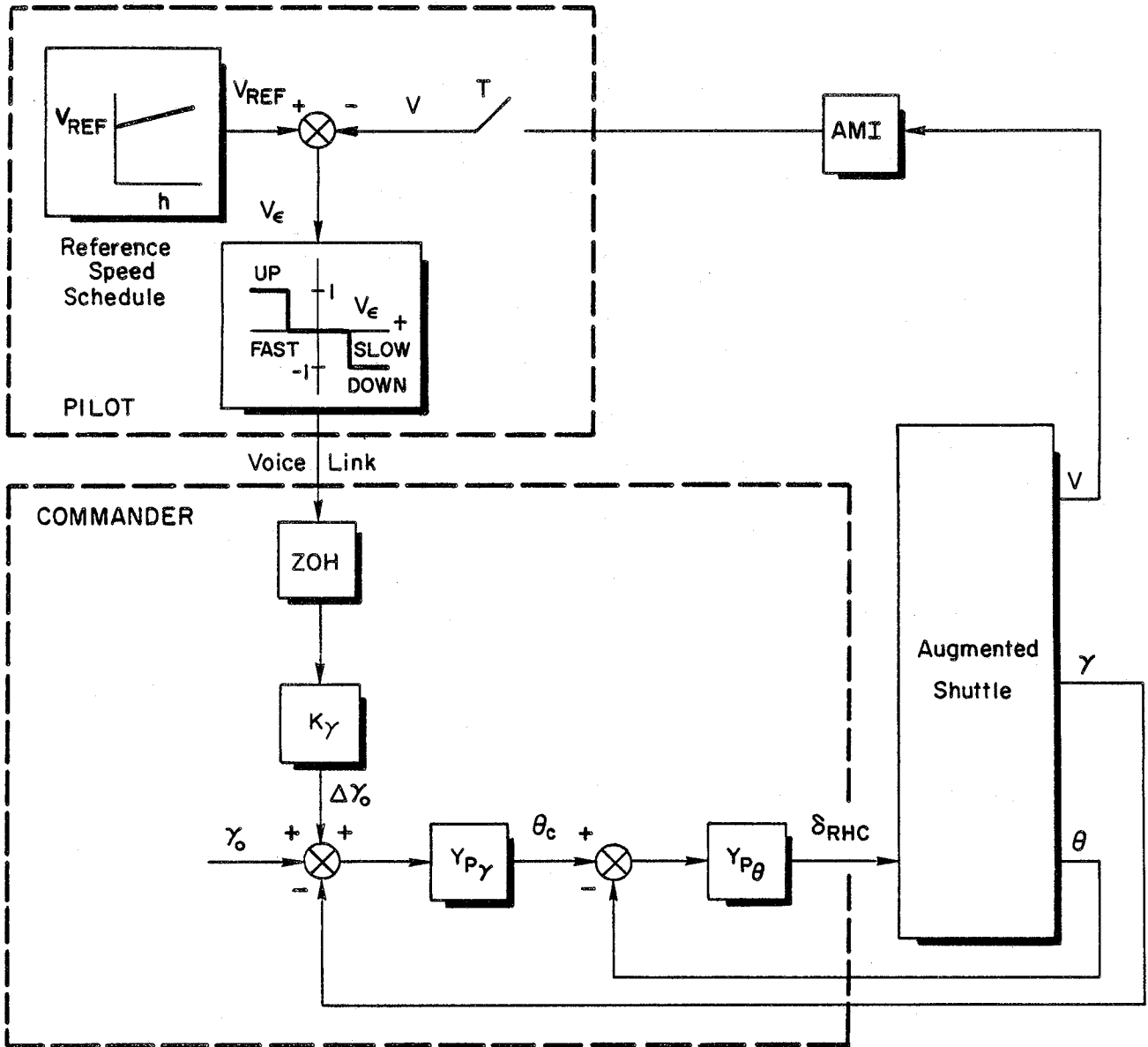


Figure 27. Shallow Glideslope

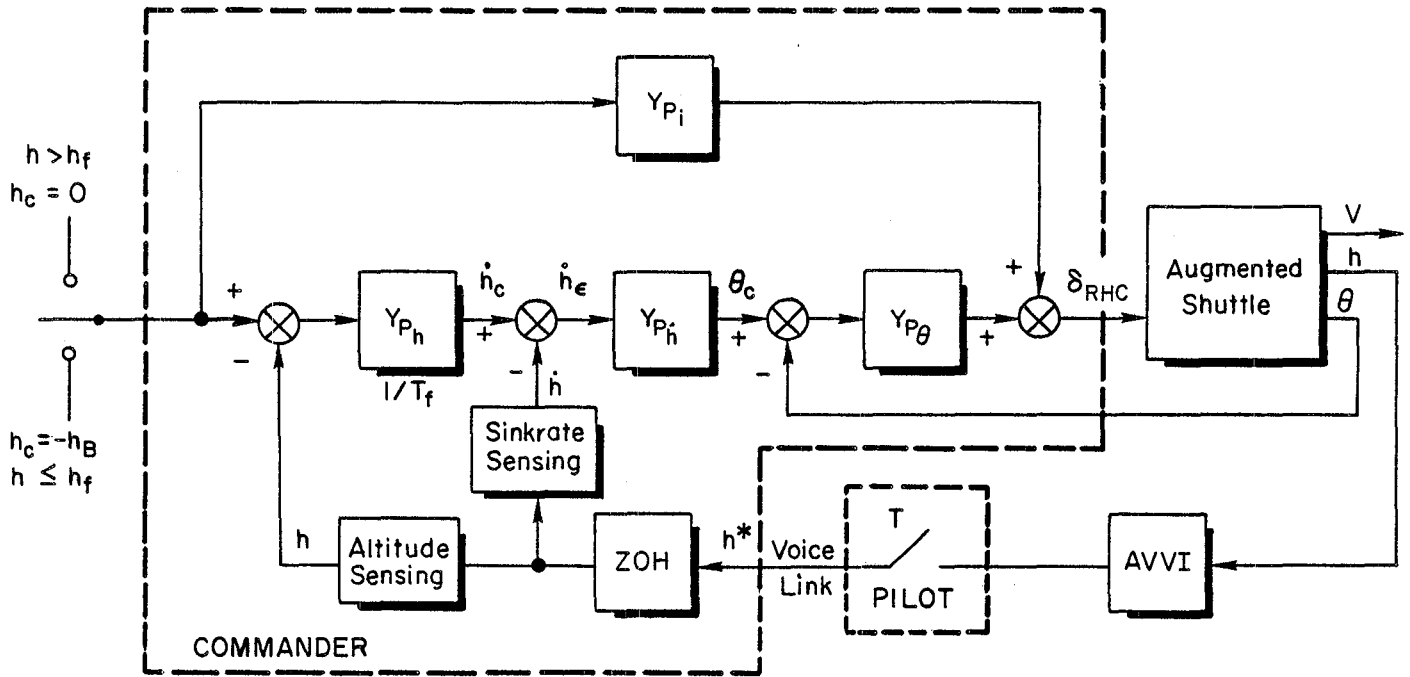


Figure 28. Final Flare

### 1. Inner Pitch Attitude Loop

All of the pilot models shown in Figs. 25-28 have an inner  $\theta \rightarrow \delta_{RHC}$  feedback loop except for the preflare pullup. This inner loop is needed for attitude control and regulation per se as well as for path damping and to relieve the anticipation (lead equalization) requirements of the outer (path deviation) loop(s). Consequently, attitude control is fundamental to the pilot's longitudinal manual control strategies in most situations. It will thus be considered first for application to several segments.

#### a. The Controlled Element, $\theta/\delta_{RHC}$

From the standpoint of pilot-vehicle control analysis, the first step in determining the nature of the inner loop pilot model,  $Y_{p\theta}$ , is to define the equivalent system model of the controlled element,  $Y_c$ , which in this case is  $\theta/\delta_{RHC}$ . The appropriate model is readily available in the "superaugmented"  $q/q_c$  transfer function discussed in Section II.

$$\frac{q}{q_c} \doteq \frac{\omega_n^2 T_q (1/T_q) e^{-\tau s}}{[\zeta, \omega_n]} \quad (13)$$

→ 1.0 in the steady state

In the Shuttle, the pitch rate command,  $q_c$ , is proportional to rotational hand controller deflection,  $\delta_{RHC}$ , with a gain (GPRHC) which is constant below  $M \leq 1.2$ . The only nonlinearities are those due to the PIOS filter and stick shaping. For the idealized pitch rate superaugmentation system of Table 2, the basic response parameters are set by the control system parameters  $T_q$  and  $\omega_{ca}$

$$\omega_n^2 \doteq \omega_{ca} / T_q \quad (14)$$

$$\zeta \doteq \frac{\omega_{ca} T_q}{2} \quad (15)$$

For the Space Shuttle, the time constant  $T_q$  is set by an elevator feedback filter such that

$$\frac{1}{T_q} \doteq 1.5 \text{ sec}^{-1}$$

The loop gain (GDQ) is set and scheduled with dynamic pressure such that

$$\omega_{ca} \doteq 1/T_q \quad (16)$$

Thus the effective equivalent pitch rate to pitch rate command response for the Orbiter in approach is

$$\frac{q}{q_c} \doteq \frac{1/T_q (1/T_q)}{[1/2, 1/T_q]} e^{-\tau s} \quad (17a)$$

$$= \frac{1.5(1.5)}{[0.5, 1.5]} e^{-0.25s} \quad (17b)$$

The corresponding attitude to rotational hand controller response is

$$Y_{\theta} = \frac{\theta}{\delta_{\text{RHC}}} = \frac{K_{\text{RHC}}}{s} \frac{q}{q_c} \quad (18)$$

b. Pitch Pilot Model,  $Y_{p\theta}$

The controlled element frequency response is shown in the Bode plot sketch of Fig. 29. According to the manual control theory of Ref. 28 we may expect that the pilot will provide lead equalization to make  $|Y_p Y_c|$  approximately  $|K/s|$  in the region of crossover,  $\omega_{c\theta}$ . Thus, we expect

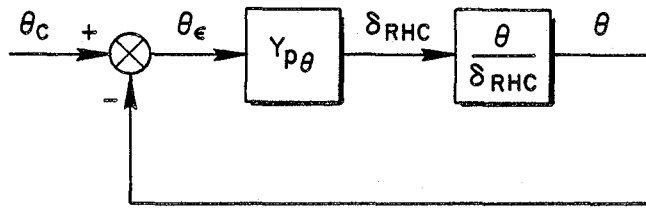
$$Y_{p\theta}(j\omega) = K_{p\theta}(j\omega + 1/T_{L\theta})e^{-\tau_p s}$$

where

$$1/T_{L\theta} \doteq 1/T_q \quad (19)$$

This equalization extends the -20 dB/dec region of the open loop pilot/vehicle system well past  $1/T_q$  and will therefore allow the pilot to achieve a closed loop bandwidth of approximately  $\omega_{c\theta} > \omega_n \doteq 1.5$  rad/sec. The effective time delay of the pilot will be a function of the lead required and the effective input bandwidth, however, we may expect that  $\tau_p$  is between 0.15 and 0.3 sec. The Shuttle effective dead time,  $\tau$ , must be added to  $\tau_p$  to compute the open loop phase angle (see Fig. 29). The pilot's lead equalization requirement, set by the net controlled element lag at  $1/T_q \doteq 1.5$  rad/sec, is more favorable (to workload) than the lower frequency lead which would be required with the conventional airframe attitude zero, i.e.,  $1/T_{\theta_2} \doteq 0.5$  rad/sec.

There is some indication from Shuttle pilot comments that pitch attitude is changed in discrete steps and held constant over brief periods of time. If required, this characteristic could be accommodated in the pilot model as shown in Fig. 30 by the use of a constant rate sampler and a zero order hold, ZOH. Such a model could be accommodated in a pilot identification program such as NIPIP without fundamental changes in procedure.



$$\frac{\theta}{\delta_{RHC}} = \frac{K_{RHC} q}{s} \frac{1}{q_c} = \frac{K_{RHC} \omega_n^2 T_q (1/T_q) e^{-\tau s}}{(0) [\zeta, \omega_n]}$$

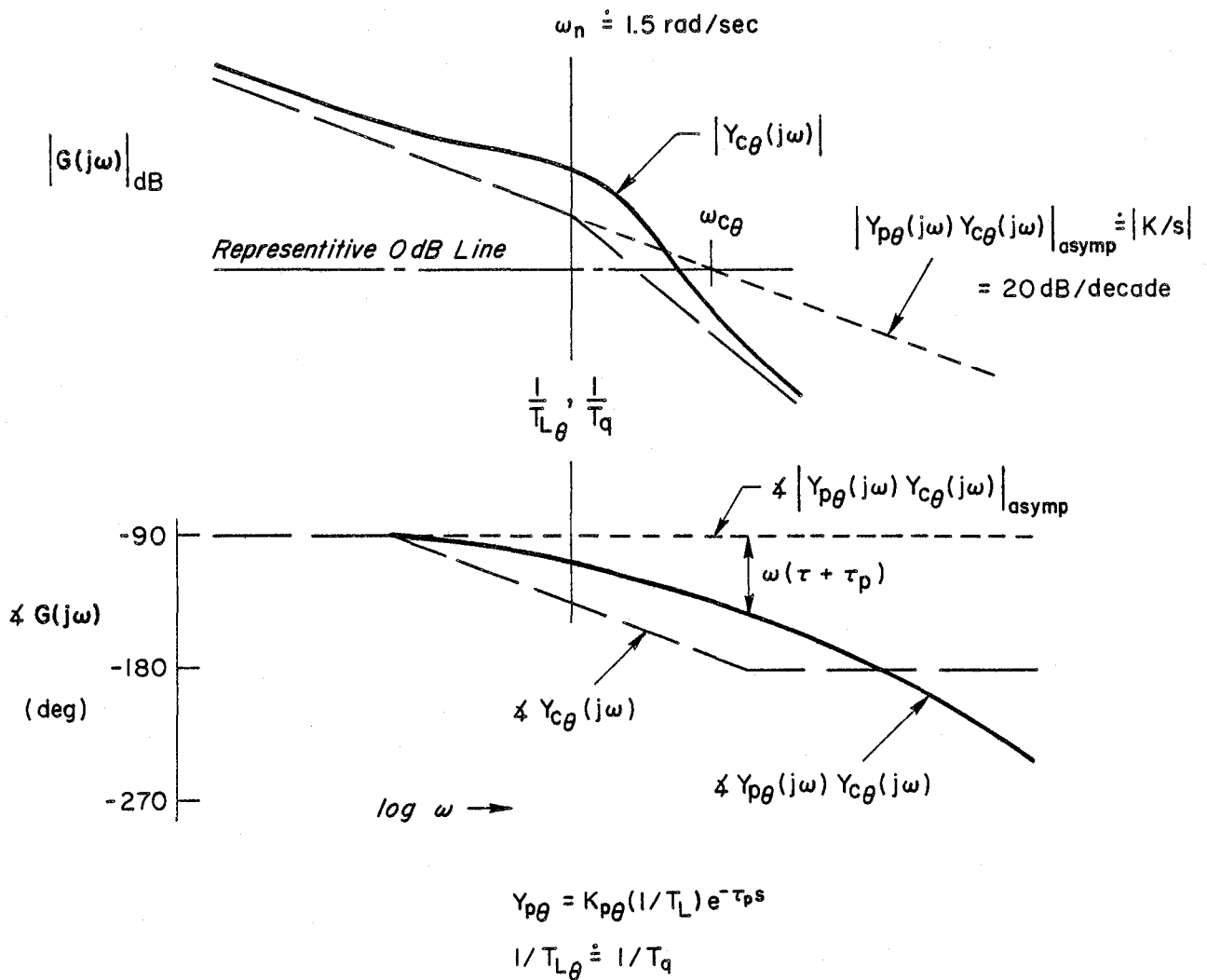


Figure 29. Determination of  $Y_{p\theta}$

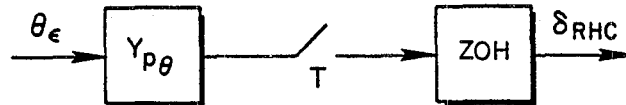


Figure 30. Sampled Data Model for Pitch Control

For considering closures of the outer pilot loops, an expression for the pilot's closed loop attitude-to-attitude command transfer function is needed. Making asymptotic approximations based on Fig. 29 gives

$$\frac{\theta'}{\theta_c}(s) = \frac{\omega_{c\theta} e^{-\tau's}}{(s + \omega_{c\theta})} \quad (20)$$

where

$$\tau' > \tau + \tau_p$$

and the prime indicates closure of the attitude loop.

## 2. Equilibrium Glide on the Steep Glideslope

There are two primary manual control tasks for manual flight on the outer steep glideslope: 1) regulation of the equivalent airspeed,  $V_E$ , to the reference value of  $V_E = 481$  fps, and 2) maintenance of the proper flight path angle of approximately  $-19$  deg. Since the flight on the steep glideslope is on the "front side" of  $\gamma - V$  curves (see Fig. 19) we can expect a "front side technique", that is, control of beam deviation with the rotational hand controller and control of speed with the speed brake controller. In the first 4 flights, the Shuttle was flown completely manually in this region only for STS-1, however, manual speed brake control was used on STS-4, with glideslope tracking in AUTO.

### a. Steep Glideslope Tracking

There are several sources of glideslope tracking information available for the pilot. First, deviation from the "synthetic" steep glideslope is available on the horizontal situation indicator, HSI. Secondly, a pitch flight director is available on the attitude director

instrument, ADI, where the display is essentially the  $n_z$  command from the autoland system. Thus, the pilot's use of the flight director is effectively equivalent to opening the autoland loop at the  $n_z$  command point and "inserting" the pilot between the flight director display and the rotational hand controller to close the beam tracking loop.

Finally, the pilot may perform the steep descent visually in "head-up" operation. This situation is accommodated in Fig. 25 by the head-up/head-down switch just upstream of the  $\theta_c$  point. There is indication, from training simulations, that the astronauts do fly the steep glideslope head-up and visual glideslope tracking aids are positioned near the ground intersection of the glideslope. The situation for visual glideslope tracking may be more complex due to the nature of the pilot's perceived error. As noted in Ref. 38, the perceived glideslope deviation for visual tracking is related to the actual glideslope deviation by

$$\frac{\text{perceived GS deviation, } d_p}{\text{actual GS deviation, } d} = \frac{1}{1 + R/A} \quad (21)$$

where

$R$  = actual geometric range

$A$  = perceived range of vanishing points in visual perspective, 0 (100m)

For the steep equilibrium glide of the Shuttle, we have

$$R = h \cos \gamma_0 \gg A \quad (22)$$

and

$$\frac{d_p/A}{d} = \frac{\epsilon_v}{d} = \frac{1}{R} \quad (23)$$

where the basic kinematics are indicated in Fig. 31. Equation 23 implies that human visual judgement of displacement tends to be angular when the range is much greater than A and thus varies inversly with altitude. Consequently, a time (altitude) varying element has been included in the beam deviation feedback of Fig. 25. Methods for treating such time varying elements in pilot identification problems are discussed in Ref. 38.

b. Speed Control With Speed Brakes

Regulation of the equivalent airspeed to the reference value is accomplished with a  $V_e$ -to-speedbrake feedback as shown in Fig. 25. The model includes provision for intermittent sampling of airspeed and a quantized output of speedbrake controller deflection. Similar models have been used for throttle control as in Ref. 31. The pilot must also

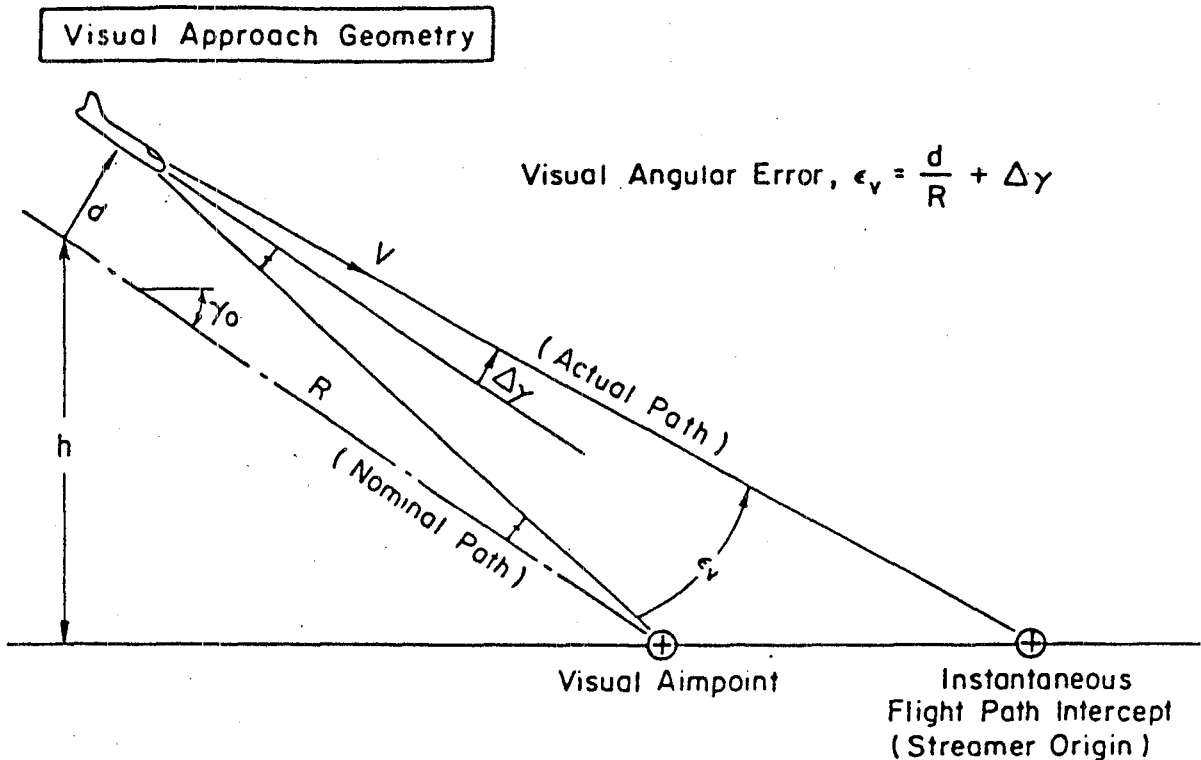


Figure 31. Visual Approach Geometry for Homing on an Aimpoint on the Earth's Surface (from Ref. 38)

monitor the average speedbrake deflection as a measure of the energy state and use this average value to define the altitude for retraction of the speedbrakes. This is similar to the speedbrake retraction logic used for the autoland system and should produce a retraction altitude between 4,000 and 1,000 ft.

### **3. Preflare Pullup**

The preflare pullup which accomplishes the basic transition from the steep to shallow glideslope appears to be largely a precognitive maneuver in which the pilot uses a steplike rotational hand controller input to maintain an incremental load factor between 1/4 and 1/2 g. This precognitive or open loop characteristic is represented by the feedforward element  $Y_{p_{n_1}}$  in Fig. 26. Initiation of the preflare pullup occurs at approximately 1750 ft altitude. A cue to the pilot is available through the preflare light but displayed altitude may actually be used.

The pullup is terminated when the flight path angle reaches approximately -1.5 deg at which point the vehicle should be above the shallow glideslope by approximately 30 ft. The precise cues and decision logic for termination of the pullup are not clear to us; they may involve visual assessment of glideslope angle, the verbal callouts of sinkrate to the commander or some combination of these cues. As indicated in Fig. 26, an inner feedback loop is to be expected especially at the end of the preflare and during capture of the shallow glideslope, however, the actual quantity fed back remains to be determined.

The speedbrake is generally retracted during the pullup at a specified retraction altitude. The main gear are deployed on an altitude schedule with a gear light cue available to the crew at 300 ft.

### **4. Decelerating Glide on the Shallow Glideslope**

Because of the 1/4 to 1/3 g deceleration on the shallow glideslope, a constant sinkrate does not imply a constant glideslope angle and vice versa. The autoland system flies a synthetic beam which implies that the glideslope angle is held constant which should also occur if the

commander uses the present flight director. If he uses the proposed HUD, Ref. 21 and 39, he would also probably fly constant  $\gamma$  since a flight path angle cue (but no sinkrate information) is available on the HUD. Headup visual control of the glide also probably implies constant  $\gamma$ , however, if the commander relied primarily on altitude calls from the pilot we would expect more nearly constant sink-rate. For purposes of initial consideration of the shallow glideslope phase, the pilot model shown in Fig. 27 assumes a constant flight path angle. Regardless of whether constant  $\gamma$  or constant  $\dot{h}$  is the best representation, the form of the effective pilot model element,  $Y_{p\gamma}$ , for this loop will probably be the same. Further, for purposes of establishing this form, it is reasonable to assume constant speed, recognizing that time variation of  $Y_{p\gamma}$  may have to be considered in the pilot identification process.

a. Expected Form of  $Y_{p\gamma}$

Concern with flight path control is in the frequency region for which a "short period" or quasi-steady speed approximation is appropriate. Thus, the flight path angle to pitch attitude transfer function is

$$\frac{\gamma}{\theta}(s) = \frac{1/T_{\theta 2}}{(s + 1/T_{\theta 2})} \quad (24)$$

In Eq. 24 it has been further assumed that the effects of the high frequency altitude zeros are negligible to a first approximation. The open loop transfer function for the flight path angle loop with the pilot's inner pitch attitude loop closed is thus

$$\begin{aligned} Y_{c\gamma} &= \left. \frac{\gamma'}{\theta_c} \right|_{OL} = \frac{\gamma}{\theta} \cdot \frac{\theta'}{\theta_c} \\ &= \frac{\omega_{c\theta}/T_{\theta 2} e^{-\tau's}}{(1/T_{\theta 2})(\omega_{c\theta})} \end{aligned} \quad (25)$$

An asymptotic sketch of the Bode magnitude plot for Eq. 25 is shown in Fig. 32. We would expect the pilot's closure of the path angle loop at a crossover frequency,  $\omega_{c\gamma} < 1/T_{\theta 2}$ , on the order of 0.1 sec. Thus, to achieve a "K/s-like" characteristic for the open loop transfer function, the pilot will have to provide low frequency lag equalization such that

$$Y_{p\gamma} = K_{p\gamma} \frac{(1/T_{L\gamma})}{(1/T_{L\gamma})}$$

where

$$\frac{1}{T_{L\gamma}} \doteq \frac{1}{T_{\theta 2}} > \omega_{c\gamma} \tag{26}$$

$$\frac{1}{T_{L\gamma}} \ll \omega_{c\gamma}$$

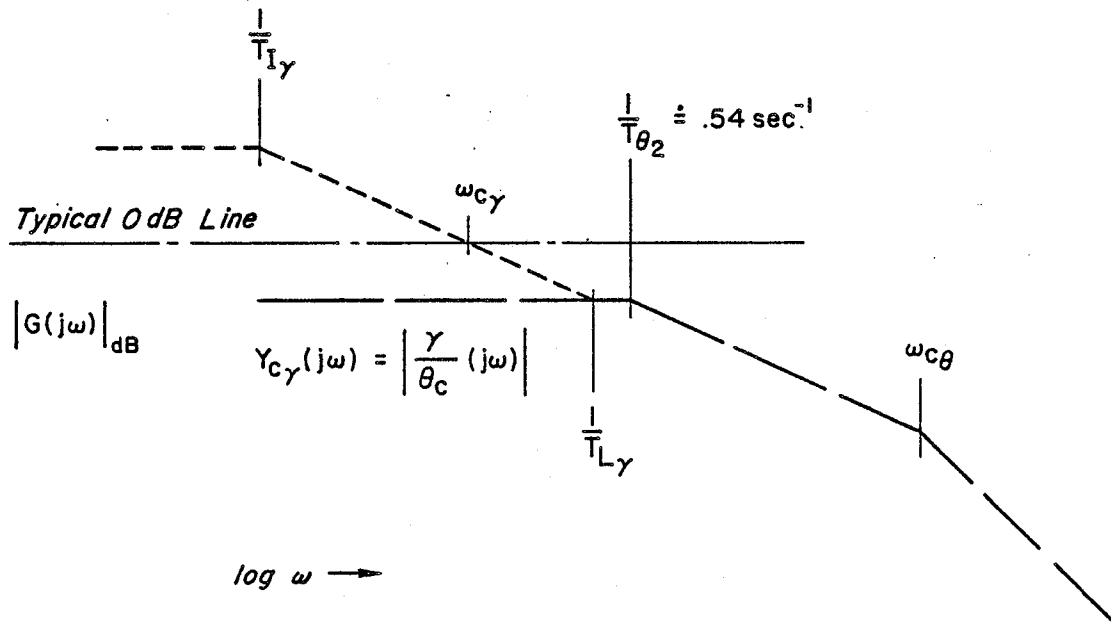


Figure 32. Determination of Form of  $Y_{p\gamma}$

It is possible that the pilot might track beam deviation (displayed on HSI) which is proportional to the integral of Eq. 25. This would remove the need for  $1/T_{L\gamma}$ , but probably would not effect workload since there is no significant workload penalty for lag equalization.

b. Touchdown Speed Control

The primary means of controlling Shuttle touchdown speed during the decelerating shallow glide is through control of touchdown time. Thus if the commander wishes to reduce the touchdown velocity he holds the Shuttle above the runway for a relatively longer period of time before touchdown. This speed control procedure is represented in Fig. 27 by the speed to path angle feedback which explicitly includes the commander and pilot in the loop with a voice link between them. The feasibility of such a control structure can be examined based on Eqs. A-41 through A-43 in Appendix A. Assuming a given value for the flare law time constant,  $T_f$ , the derivative of the touchdown speed with respect to shallow glide angle is given by

$$\frac{\partial V_{TD}}{\partial \gamma_0} = - \frac{\partial V_f}{\partial \gamma_0} = \frac{K_v \dot{X}_f}{V_f \gamma_0} \quad (27)$$

This relation may be used to estimate a path angle bias to modulate touchdown speed as

$$\Delta \gamma_0 \dot{=} - \left. \frac{V_f \gamma_0}{K_v \dot{X}_f} \right|_{\text{nominal}} * (V_{REF} - V) = \text{constant} * \Delta V \quad (28)$$

While Eq. 28 indicates the feasibility of a continuous speed controller, it appears likely from pilot comments that the actual situation corresponds more to the discrete controller indicated in Fig. 27. There the pilot monitors airspeed and issues "up," "down," or "no change" discrete vocal signals to the commander who uses the information to bias his  $\gamma_0$  reference. The pilot can monitor the AMI for actual airspeed, however, it appears that the time-varying reference speed is not available on any display and would therefore have to be a learned reference

for the pilot. The reference speed will be displayed on the proposed HUD (see Refs. 21, 39). The speed control concept shown in Fig. 27 is consistent with the crew actions on STS-3.

## 5. Final Flare

During the final flare it is likely that touchdown speed control is achieved in a manner similar to that shown in Fig. 27. However, for simplicity, this loop has not been included in the Fig. 28 final flare loop structure. The input to the Fig. 28 loop structure to initiate a final flare is modeled as a  $h_c = -h_b$  step input when the altitude reaches the flare height. As discussed in Subsection E, the final flare is probably achieved by scheduling sinkrate proportional to altitude. This implies an exponential flare with time constant  $T_f$  to an asymptote parallel to and  $h_b$  feet below the runway. Thus, the outer loop pilot element,  $Y_{p_h}$ , would be

$$Y_{p_h} \dot{=} 1/T_f \quad (29)$$

It is also possible that the commander may use a precognitive (feedforward) input to command a steady pitch rate for the flare. This would be similar to the feedforward used in some autopilots to avoid the delay in  $\theta_c$  while the  $h_c$  error builds up. The feedforward element would likely consist of a lag which would help to smooth the  $h_c$  step input to the rotational hand controller. The comments of the STS-4 crew indicate the sinkrate derivation shown in Fig. 28. Here the pilot reads the AVVI and verbally calls out altitude (alternating with the airspeed callout from the AMI). This is modeled in Fig. 28 as a sampler with sample period  $T$  approximately equal to the time between the altitude callouts which of course is only approximately a constant. The commander then derives sinkrate from the "cadence" of the altitude callouts.

### a. Expected Form of $Y_{p_h}$

If the sampled data effects are neglected for initial analysis, the sinkrate error is given by

$$\begin{aligned}
 h_{\epsilon} &= -\frac{1}{T_f} (h + h_B) - \dot{h} \\
 &= -(s + 1/T_f)h - h_B/T_f
 \end{aligned}
 \tag{30}$$

Making use of Eq. 25, the open loop transfer function for the outer loop exclusive of  $Y_{ph}^{\bullet}$  (with the feedforward open) is given by

$$Y_h^{\bullet} = \left. \frac{h_{\epsilon}}{\theta_c} \right|_{OL} = \frac{-\omega_{c\theta} V/T_{\theta_2} (1/T_f)}{(0)(1/T_{\theta_2})(\omega_{c\theta})} e^{-\tau's}
 \tag{31}$$

Figure 33 shows a Bode magnitude asymptote sketch for  $Y_h^{\bullet}$ , i.e., Eq. 31, as well as the equalized open loop describing function required to achieve a K/s-like characteristic in the crossover region near  $\omega_{ch}^{\bullet}$ . It may be seen that the implied equalization, i.e.,  $Y_{ph}^{\bullet}$  is

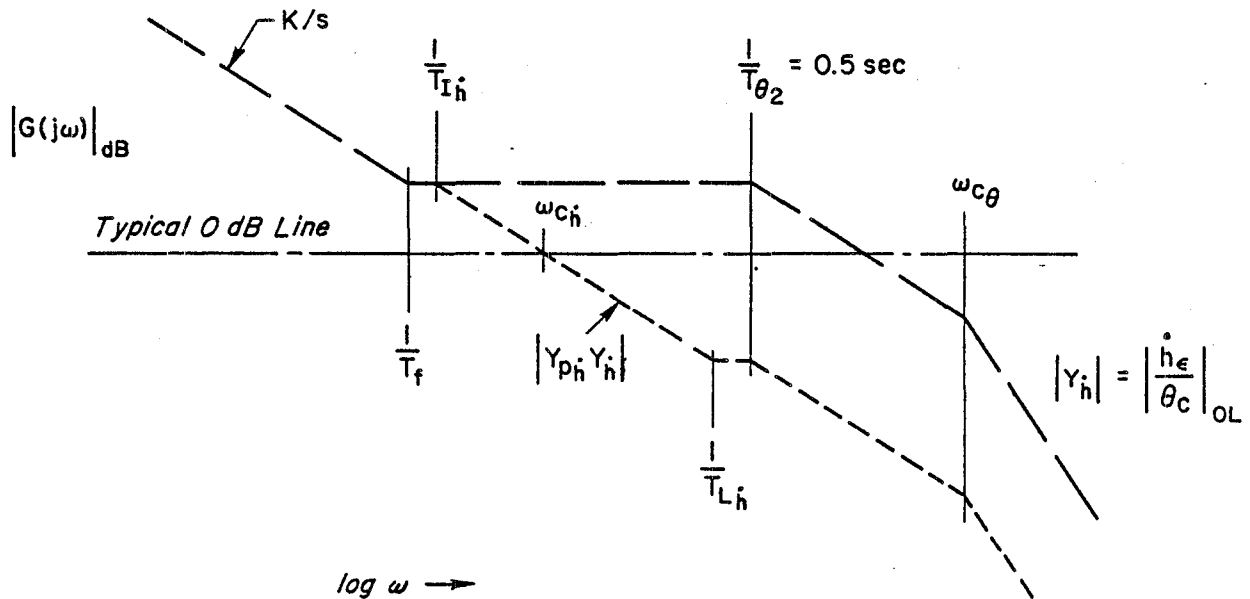


Figure 33. Determination of Form of  $Y_{ph}^{\bullet}$

$$Y_{ph} = \frac{K_{ph} \cdot (1/T_{Lh})}{(1/T_{Ih})}$$

where

$$\frac{1}{T_{Lh}} = \frac{1}{T_{\theta 2}} > \omega_{ch} \quad (32)$$

$$\frac{1}{T_{Ih}} = \frac{1}{T_f} < \omega_{ch}$$

Thus, the expected form of  $Y_{ph}$  is similar to the expected form of  $Y_{p\gamma}$  in Eq. 26.\* An interesting aspect of Fig. 33 is the relationship between the flare time constant  $T_f$ -which is largely set by fundamental flight mechanical considerations -- and the pilot equalization lag  $1/T_{Ih}$ . Thus, a pilot model quantity, which may be important to subjective flying qualities and pilot workload, is linked explicitly to a fundamental flight mechanical quantity associated with the task.

## B. NON-INTRUSIVE PILOT/VEHICLE/WORKLOAD MEASUREMENT METHODS

### 1. Use of NIPIP for Pilot Model Identification

#### a. Rationale

The NIPIP computer program, Ref. 33, is being proposed as a primary tool for use in the indirect approach to the flying qualities OEX for several reasons. First, NIPIP was developed by STI specifically for the type of identification effort being proposed and it has been used in several projects, Refs. 31, 23, and 34 to identify piloting techniques -- primarily from simulations but also to a limited extent from actual flight data, Ref. 34. Further, the NIPIP software is available at DFRF for coordinated flight analysis efforts. Finally, one of the primary desirable features of NIPIP with respect to the concept

---

\*If the shallow glide were to be modeled as a constant sinkrate region, it could be treated as a special case of Fig. 4 with  $1/T_f$  approaching zero.

indicated in Fig. 24, is that the pilot model forms required for NIPIP relate directly to the structural isomorphic pilot-vehicle-task models proposed as the central element of the indirect approach. Thus the pilot models may be used with NIPIP simply by transforming to a difference equation structure using z-transforms.

b. Pilot Model Identification

The theoretical basis for the NIPIP algorithm is presented in Ref. 33 and will only briefly be reviewed here. To consider the use of NIPIP for pilot model identification, we may refer to the multi-loop single controller pilot/vehicle system of Fig. 34 where the pilot model is the input/output relation between the error vector,  $\underline{X}_e$ , and the controller displacement,  $\delta$ . To use NIPIP, a  $Y_p$  is hypothesized in the form of a difference equation involving  $\delta$  and  $\underline{X}_e$  with undetermined coefficients. If the input (command),  $\underline{X}_c$ , can be specified (based on the task),  $\underline{X}_e$  is determined in terms of the state vector  $\underline{X}$ . Thus,  $Y_p$  may be represented as

$$\delta = f_1 c_1 + f_2 c_2 + \dots + f_j c_j + \dots + f_m c_m$$

or

(33)

$$\delta \equiv \underline{F} \underline{c}$$

where  $f_1, f_2, \dots$  are selected variables from the state vector  $\underline{X}$  or explicit functions thereof and past values of  $\delta$ , and the  $c_j$ 's are constant coefficients relating  $\delta$  and  $f_j$ . In Eq. 33,  $\underline{F}$  is a row-vector of the  $f_j$  and  $\underline{c}$  is a column-vector of the  $c_j$ .

If a minimum number of sets of discrete measurements for  $y$  and  $\underline{F}$ , exist, multiple linear regression may be performed using the NIPIP program to compute the coefficient vector  $\underline{c}$ . An important feature of NIPIP is the formulation of the estimator as a recursion equation so that each new measurement set may be directly combined with the previous estimate to form the new estimate. This eliminates the need to store old measurements. A  $\underline{c}$  vector inserted into Eq. 33 constitutes a measured pilot

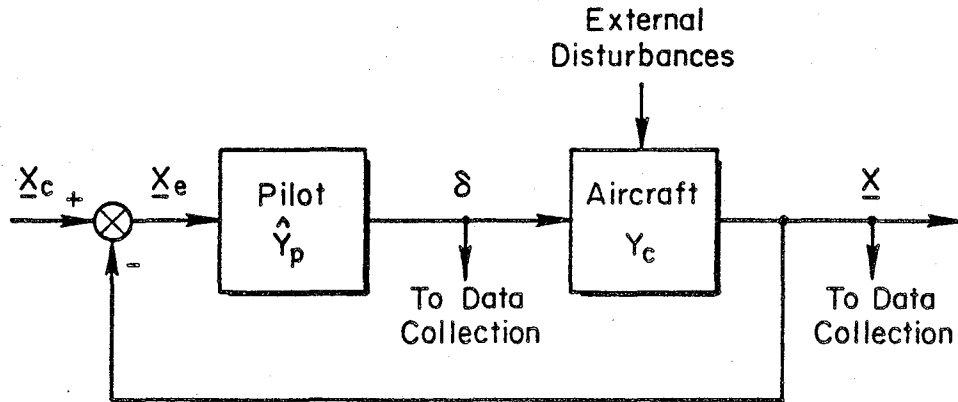


Figure 34. An Example of a Pilot-Vehicle System

model but does not guarantee its validity. Estimates of model validity may be obtained by correlation measures discussed in Ref. 32.

A major concern in using NIPIP (and many other schemes) for identification in closed loop systems, is that there can be confusion as to whether the correlation between  $\delta$  and  $X$  reflects more accurately functions describing the pilot,  $Y_p$ , or those describing the aircraft controlled element,  $Y_c$ . This problem is complicated by the presence of pilot remnant (noise) in the closed loop system. It is useful to compare the NIPIP method to classical cross-spectral methods (Ref. 28) applied to the single loop case, Fig. 35. Direct determination of  $Y_p$  using NIPIP is analogous to use of the cross spectral ratio

$$\frac{\Phi_{ec}(j\omega)}{\Phi_{ee}(\omega)} = \frac{Y_p \Phi_{ii}(\omega) - Y_c^* \Phi_{nn}(\omega)}{\Phi_{ii}(\omega) + |Y_c|^2 \Phi_{nn}(\omega)} \quad (34)$$

Equation 34 reveals that the above ratio yields a good measure of  $Y_p$  only if the terms involving the input power spectra,  $\Phi_{ii}(\omega)$ , dominate those containing the remnant spectra,  $\Phi_{nn}(\omega)$  -- otherwise the ratio approaches  $Y_c^{-1}$ . This problem has been minimized in the past by careful design of inputs and extraction of  $Y_p$  from "input-referenced" cross spectra, i.e.,

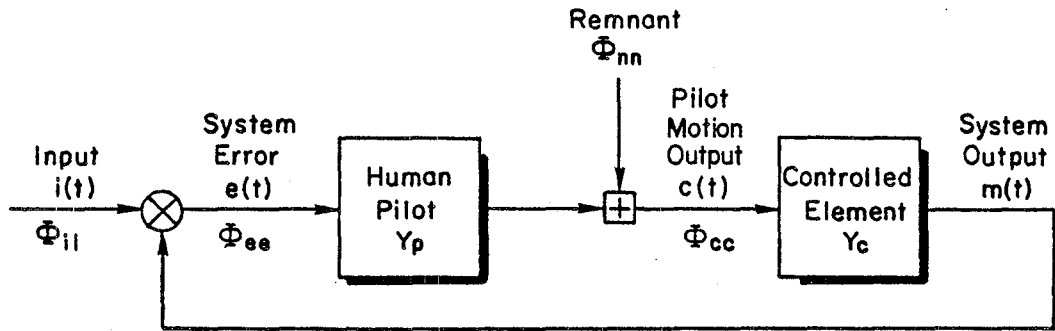


Figure 35. Single Loop Pilot/Vehicle System for Application of Cross-Spectral Methods

$$Y_p = \frac{\Phi_{ic}(j\omega)}{\Phi_{ie}(j\omega)} \quad (35)$$

These approaches have been very successful for compensatory tracking situations in the laboratory and also in flight, (Refs. 29, 40). However, for measurements in more general tasks, such as approach and landing, optimizing the input for measurement considerations is not possible and even adequate definition of the input may be difficult. Given these problems for general tasks, experience has indicated that NIPIP can identify pilot behavior. Further, even in those cases where the pilot's remnant dominates the input spectra (and the "measured"  $Y_p \rightarrow Y_c^{-1}$ ) useful information is provided -- i.e., the pilot is not using significant closed loop control.

c. Special Considerations for the OEX

The first step in the application of NIPIP to identify pilot models is formulation of appropriate loop structures. A "first cut" at this process is provided by the prototype loop structures previously discussed in Subsection F and shown in Figs. 25 through 28.

A very important consideration in application of NIPIP, or any identification procedure, is provision for switching which allows for

discrete changes in the model structure between flight segments. The basic switching between segments for the Shuttle approach and landing also has been included in the prototype models of Figs. 25 through 28. In addition, there are certain discrete changes which must occur during segments, i.e., landing gear extension and speed brake retraction. These events can be determined from flight records to make discrete changes in the controlled element model. A more problematical switch is the pilot's change from head-up visual flight to head-down instrument operation. One possible means of obtaining data on this "switching" activity would be through eye-point-of-regard measurements.

If explicit representations of the pilot's use of sampled data control is to be considered (as implied by the speed control model in Fig. 25), then an estimate of the sample time,  $T$ , must be made and used in the formulation of the pilot model. This was done in Ref. 32 by observing the average frequency of discrete changes in throttle position. For sampled data elements such as the altitude feedback of Fig. 28 in which the data is presented to the commander verbally, transcripts of voice records with appropriate time references would be useful.

Perhaps the most challenging aspect of attempting to extract pilot models from the Shuttle flight data comes from the fact that all three levels of the pilot's Successive Organization of Perception (SOP), Ref. 28, may be expected in the Shuttle approach and landing. Thus, the identification effort must be done using complex models which involve simultaneous feedforward and feedback elements to produce a specific input/output relationship.

d. "Tuning" the NIPIP Program for the Shuttle  
Flying Qualities OEX

Simulation and analysis of the identification problem. It is anticipated that the problem of identifying pilot models from the Shuttle flight data will be difficult given the previously discussed severe constraints. Thus, it is felt important to study the NIPIP identification applied to the Shuttle situation as a prelude to the OEX

effort. This point of view is supported by previous experience with the use of NIPIP in analyzing flight data, Ref. 34. An approach that has been used to study the problems associated with NIPIP identification is a simulation consisting of an aircraft model coupled to candidate pilot models. For use in studying the Shuttle OEX problem, the Shuttle model could (and should) be quite simple and in the spirit of the structural isomorphic model discussed in Subsection C. For initial work a longitudinal model based on the superaugmented pitch response (Eq. 18) coupled with the lift and drag equations as developed in Appendix A would be adequate.

Because the maneuvering and disturbance environment for the vehicle has a significant impact on the performance of the NIPIP algorithm, a simple atmospheric disturbance model will be needed. This could be based on the MIL-F-8785C low altitude model but the specific values of parameters would not be critical. The primary requirement would be the capability to vary steady wind, wind shear, and turbulence level.

The final important element in the simulation would be an elementary noise and measurement model which would include such important measurement factors as sample rate and sensor bandwidth, resolution and quantization elements, time skews and perhaps measurement noise. Finally, some provision for modeling system noise and pilot remnant would be desirable. The measurement model envisioned would be quite elementary and effects such as sample rate, resolution and time skews could be examined with simple additions to the PREPR subroutine which is specially coded for each NIPIP application.

On the simplest level, especially for situations in which a quasi-steady speed could be assumed, transfer function representations of the Shuttle and pilot model could be used. In this situation, no new software would be required since the necessary system time response files could be generated using the TRFN and USAM programs available on the STI computer system. These files could then be input to the NIPIP program for testing of the identification process.

Once suitable simulation models have been assembled, numerical experiments and analysis could be conducted using the synthetic data as an input to the NIPIP program. Among the most important issues to address in such tests would be to:

- Check the feasibility of pilot models including the provisions for discrete switching -- i.e., test the theoretical validity of the Figs. 25 through 28 models.
- Define a minimum level of disturbance necessary for obtaining adequate results from NIPIP and investigate the behavior of the NIPIP results as the disturbance level is reduced to zero. If the use of special inputs (such as special PTI's) appear to be feasible for OEX flights, their design could be tested using the simulation.
- Study the problems associated with identification of complex loop structures which involve simultaneous feedforward and feedback loops.
- Study the effects of measurement system factors including sample rate, resolution, quantization, time skews, system noise and remnant.
- Study the problems of identification of the controlled element versus identification of the pilot element (especially important if attempts are to be made to identify the effective augmented Shuttle using NIPIP).

Preliminary identification tests on pre-OEX Shuttle flight data.

Efforts to test the use of NIPIP for the Shuttle OEX by applying it to flight data obtained from the STS-4 DFRF MMLE data file are planned. These efforts have not yet been possible because of problems in transferring the necessary subset of the overall data file between the DFRF Cyber computer and the STI Hawthorne computer. This problem is expected to be resolved shortly and a continuation of this effort is proposed for Phase III. The basic effort would be to try the procedures proposed on actual Shuttle data to define problems which could then be further explored using simulation procedures noted above.

## 2. Phase Plane Methods

An altitude-sinkrate phase plane of the type used in Ref. 34 is shown in Fig. 36 based on STS-4 data. The plot was made from radar h

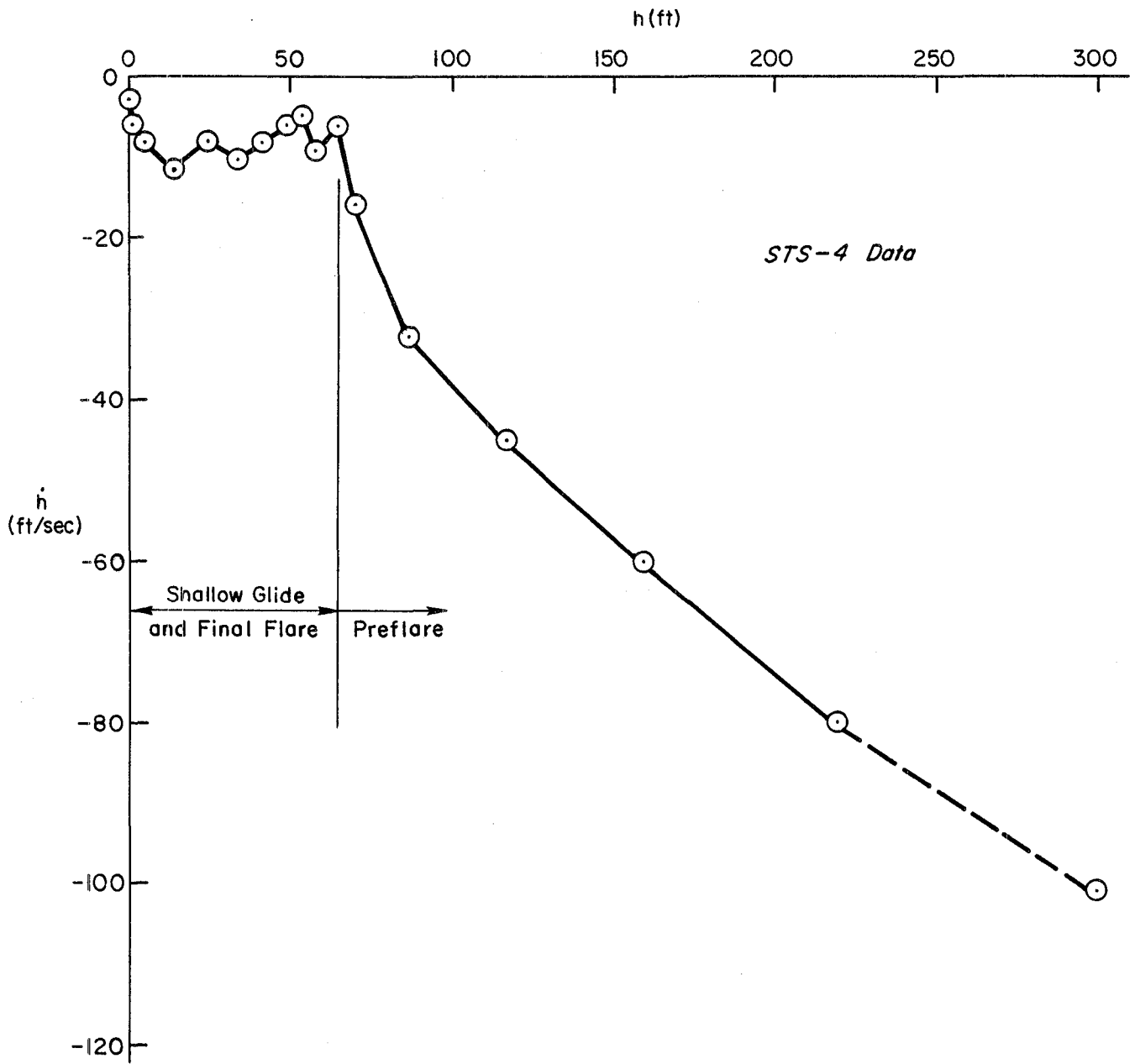


Figure 36. Altitude-Sinkrate Variation from Preflare through Touchdown

and  $\dot{h}$  time responses (Fig. 37) which were taken from Ref. 25. This hodographic presentation of data for landing is sensitive to the actual "control law" being used by the pilot. It has been particularly effective in showing the relative utilization of sinkrate cues in flight versus simulator comparisons. This is an anticipated role for the hodograph in the OEX. At this juncture, however, the primary value of the Fig. 36 plot is in illustrating certain data problems. For instance, the "scatter" in the shallow glide and final flare region is probably due primarily to inaccuracy from manually reading Fig. 37 at a very poor scale. This is fundamentally a dynamic range problem that is best handled by making all plots by machine using digital data files.

There are additional problems that would be encountered even with this procedure. For the rapidly changing altitude data, the one-sample-per-second data leads to  $h$  increments greater than half the value of the instantaneous altitude below 25 ft. Additional data problems and possible solutions will be discussed in Subsection J.

### **3. Flying Qualities Questionnaire**

A preliminary flying qualities questionnaire (Appendix B) has been developed for use in the OEX program based on the Ref. 1 work. This preliminary version was given to the STS-4 crew. While awaiting the reply, work such as development of the prototype pilot models has provided insights for refining the questions and possibly the format of the questionnaire. The latter emphasizes a "multiple-choice" format in which no written reply is required. A prototype for this format is shown in Appendix C which also incorporates revisions to the content of the questions. One modification which ties the revised questionnaire more closely to the prototype pilot models is the more specific reference to flight segment. A further step that might be considered is inclusion of pilot model block diagrams (suitably simplified versions of Figs. 25 through 28) for reference in questions with respondents invited to markup the drawings. The final questionnaire format has yet to be established.

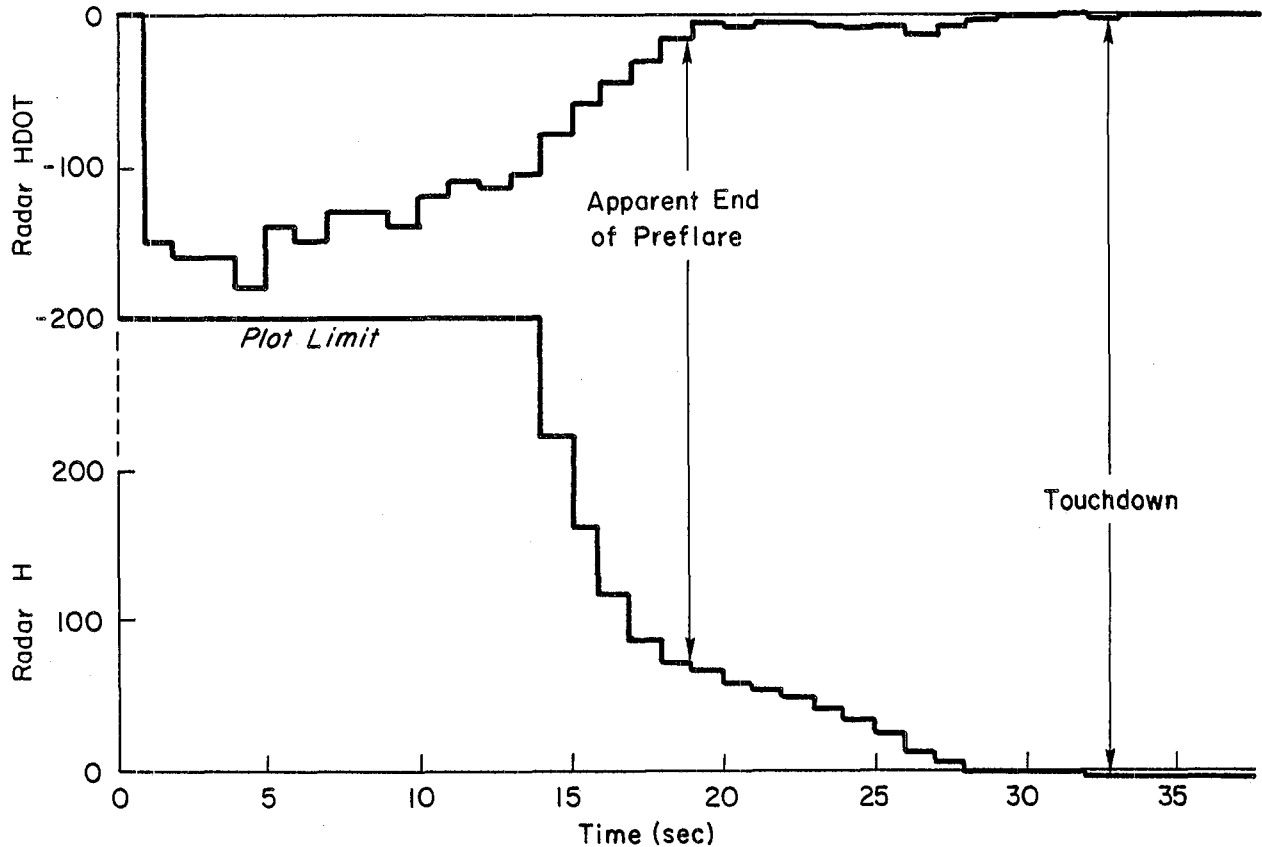


Figure 37. Radar Altitude and Sinkrate Time Responses from Ref. 25

**C. INSTRUMENTATION AND SOFTWARE REQUIREMENTS FOR DATA PROCESSING**

**1. Present Availability of Flight Data**

**a. Present Instrumentation and Data Processing**

The onboard instrumentation for the Space Shuttle is summarized in Fig. 38, taken from Ref. 41. While this figure was constructed to represent the ALT instrumentation system, it is still generally representative of the present Orbiter system. There are two primary instrumentation systems: the Operational Instrumentation, OI, and the Aerodynamic Coefficient Identification Package, ACIP. The ACIP package is a special

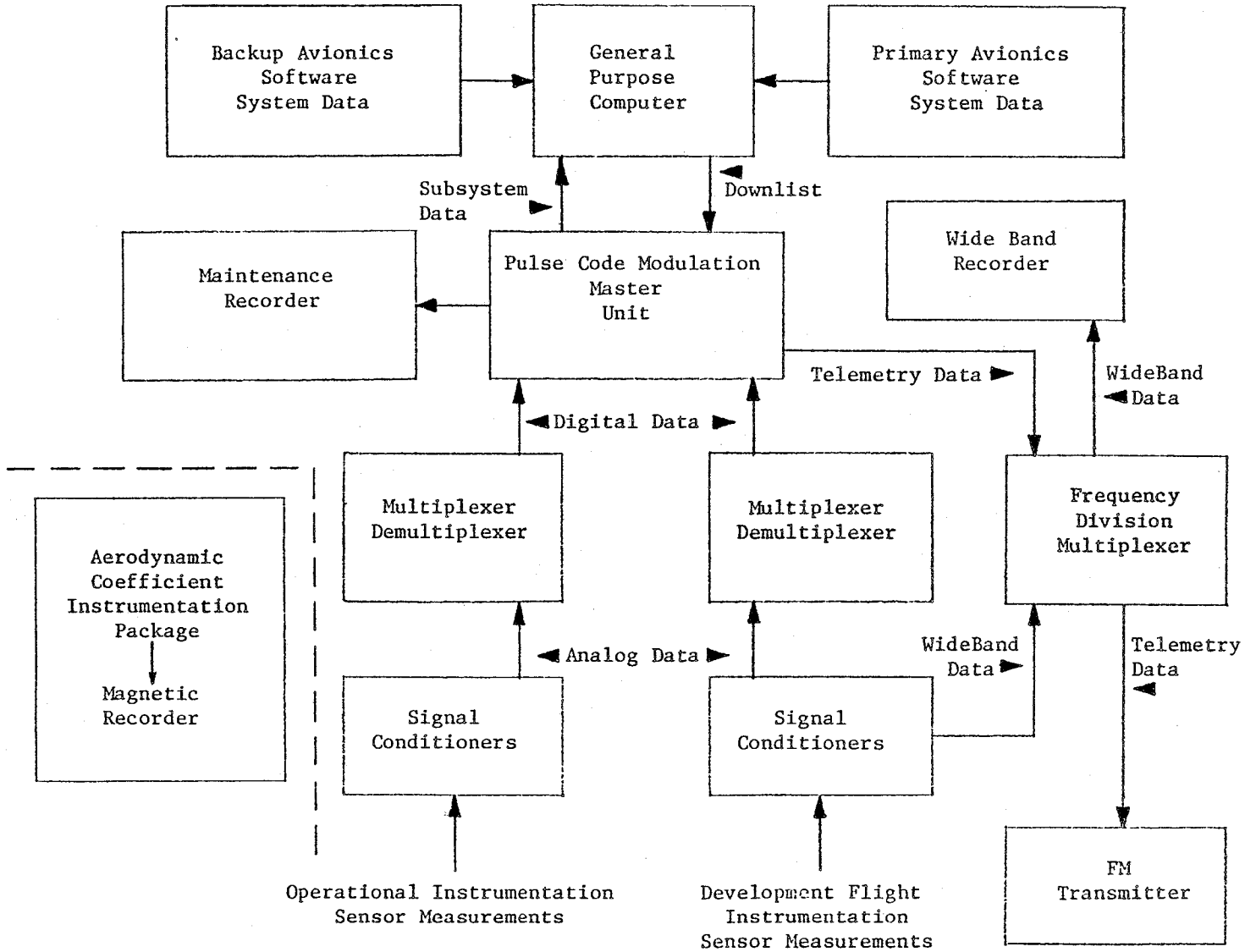


Figure 38. Instrumentation System Block Diagram (from Ref. 41)

purpose instrumentation system developed specifically for generation of data adequate to identify airframe aerodynamic derivatives. The package contains high resolution/high sample rate sensors for acceleration and rate quantities as well as rudder and elevon surface panel deflections. The inclusion of surface deflection data with the response data helps to reduce time skew problems in the data.

The Operational Instrumentation is actually a group of components which receive inputs from several sources. This system includes the Developmental Flight Instrumentation, DFI, and is to remain on all Orbiters at all times. Some of the data is taken from the FCS sensors including the inertial measurement unit, IMU; the rate gyro assembly, RGA; and the air data system, ADS. Other inputs come from special sensors whose outputs are not used by the general purpose computers. The first group of variables are considered "GPC-provided data" and form what is referred to as the "downlist." Those data not passing through the GPC form the "downlink" data set.

Most of the data of interest for flying qualities experiments is processed through a pulse code modulation, PCM, system and recorded both directly on board and through telemetry to ground recorders. As indicated in Figs. 38 and 39, the OI and ACIP packages have separate dedicated recorders. The processing procedures for orbiter data are indicated in Fig. 39 where it may be seen that the OI and OEX (i.e., ACIP) data are initially processed by different groups at NASA JSC. This data is ultimately combined with meteorological and Best Estimated Trajectory, BET, data to form a final complete data tape available from NASA JSC to various users.

b. Future Plans for Shuttle Instrumentation

The operational instrumentation is intended to be used on all orbiters over their operational lifetimes while the ACIP package was originally intended to be used just during the developmental flight test. However, it now appears that the ACIP will remain on the Orbiters at least through STS-12 and perhaps indefinitely. The package is now on the Columbia (Vehicle 101) and the Challenger (Vehicle 99) and plans are

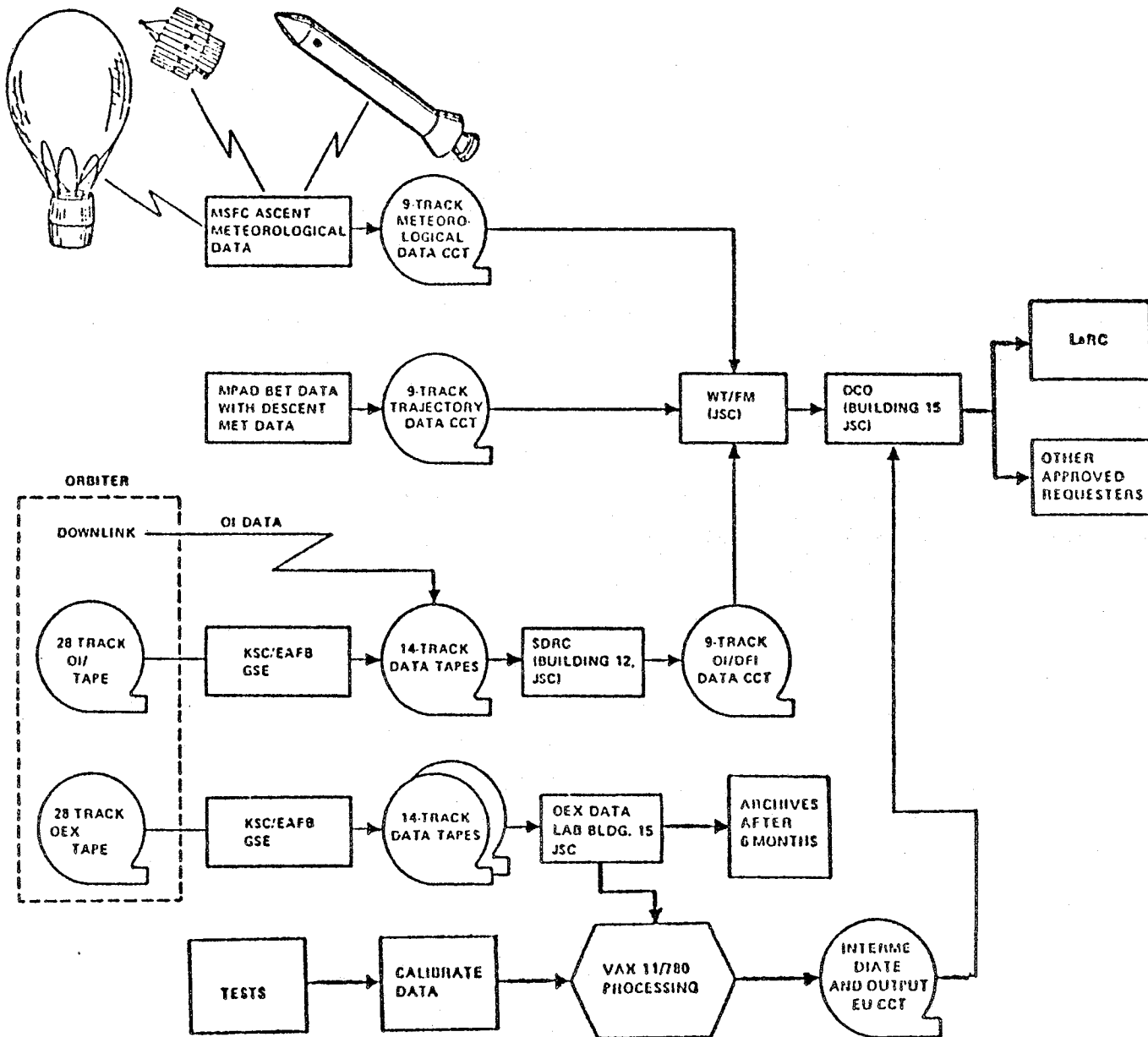


Figure 39. OEX Data Flow Diagram from Ref. 42

being made for installing it on vehicles 102 and 103. Two improvements are presently being made to the ACIP package. These include the "HIRAP" project to add higher resolution accelerometers, Ref. 42, and the "WIRE" project to add additional reaction control system sensors to the unit.

For planning the flying qualities OEX, details of the instrumentation hardware are less important than a good understanding of what data is available and the characteristics of this data. Contact with appropriate groups at NASA JSC has indicated that most of the data needed for the flying qualities experiment is presently being recorded in a useable form. The main instrumentation and data processing problem thus appears to be one of extracting the needed data from the large amount of available data for the flight regime of interest and organizing that into an edited computer file with the necessary preprocessing.

c. DFRF MMLE Data File

Specialized data files have been generated for STS-1 through 4 for use in the NASA DFRF effort for identification of aerodynamic coefficients. These files form an excellent starting point for flying qualities OEX data files. Of particular value is the fact that these files are available on the DFRF Cyber computer and may be accessed over phone lines and transferred to remote computer facilities such as the STI Hawthorne facility. Efforts to make this process operational have begun at STI and, while data has been transferred between the STI computer and the NASA DFRF Cyber computer, complete data files have not yet been transferred. The primary value of this approach is that it avoids physical transfer of magnetic tapes which past experience at STI has shown can require considerable time and expense.

The flight variables available on the DFRF MMLE file are indicated in Table 6. Since the primary use of this data file is in extraction of airframe aerodynamic coefficients, the primary emphasis is on airframe response and control surface deflection variables; however, limited data is available on manual controller deflections as well as some flight control system discrete data. It is recommended that the effort to create flying qualities OEX data files be correlated with the DFRF MMLE effort to take maximum advantage of this available data.

TABLE 6. SUMMARY OF DATA AVAILABLE FROM THE NASA DFRF MMLE FILE

VARIABLE	SOURCE												
	ACIP				GPC			OI		BFCs		COMPUTED	
	CHANNEL	ACCURACY % F.S. (Ref. 45)	RESOLUTION (Ref. 42)	SAMPLE RATE Hz	CHANNEL	ACCURACY (Ref. 45)	SAMPLE RATE Hz	CHANNEL	SAMPLE RATE Hz	CHANNEL	SAMPLE RATE Hz	CHANNEL	RESOLUTION (Ref. 42)
Translational Acceleration	A <sub>x</sub>	7	0.5	150 $\mu$ g	174								
	A <sub>y</sub>	19	1.1	50 $\mu$ g		65		25					
	A <sub>z</sub>	5	0.4	300 $\mu$ g		66		25					
Angular Acceleration	P	20	1.7	240 $\mu$ r/sec <sup>2</sup>									
	Q	6	1.7	120 $\mu$ r/sec <sup>2</sup>									
	R	21	1.7	120 $\mu$ r/sec <sup>2</sup>									
Translational Rate	$\alpha$					1,87	0.5 deg	1				72	
	$\beta$					16		5				73	
	H					103		5					
	V <sub>TRUE</sub>					3	2%	1				71	
	V <sub>EAS</sub>					101	2%	1					
	M					15	4%	1				70	
Angular Rate	P	17	0.2	0.003 o/s	174	62		25					
	Q	2	0.5	0.001 o/s		63		25					
	R	18	0.5	0.001 o/s		64		25					
Euler Angles	$\psi$					86		5					
	$\theta$					4		5					
	$\phi$					12		5					
Altitude	H					13,102		1					
Control Surface Deflection	$\delta_e$											8	2.9°
	$\delta_a$											22	2.9°
	$\delta_r$	23	1.0	2.7°									
	$\delta_{SB}$					9		6.25	26	1			
	$\delta_{BF}$												
Manual Controls Commander/Pilot	$\delta_{QRHC}$					95*		1			93**	12.5	
	$\delta_{PRHC}$					94*		1			92**	12.5	
	$\delta_{PED}$								88-91	1			
	$\delta_{SBC}$												
	$\delta_{BFC}$												

\* Pilot's input

\*\* Sum of commander's and pilot's inputs

## 2. Data Considerations for the Flying Qualities OEX

### a. Primary Data Characteristics

The primary sensors used in the orbiter instrumentation system are analog devices, thus, the two most important characteristics are their accuracy and resolution. Accuracy refers to the instrument's deviation from the "true" value for controlled conditions and is often specified as a percent of full scale. Resolution refers to the smallest change in input that may be detected. Resolution has been a problem for identification efforts as noted in Ref. 34.

The data processing elements downstream of the sensors are also of concern, in particular with regard to the digital nature of the system. There are three primary considerations: the sample rate, quantization, and time skews. In general the minimum sample rate is set by the highest data frequency of interest. An absolute minimum of two samples per cycle is necessary to identify a given frequency component, however, practical requirements indicate a much higher sample rate. Aliasing is a particular concern and occurs when high frequency signals (or power spectra) are "folded" onto the lower frequency region at the Nyquist frequency

$$f_N = \frac{1}{2T}$$

where

$$f_N = \text{Nyquist frequency, Hz} \tag{36}$$

$$T = \text{inter-sample period, sec}$$

There are two basic approaches to dealing with aliasing problems. The first, is to make the sample rate very high such that there is no significant signal (power) above the Nyquist frequency and the second is to apply a low pass filter for the frequency regime of interest before digitizing the signal. There are various "rules of thumb" available for selecting sample rate. Reference 43 recommends a sample rate 3 to 4 times higher than the maximum frequency of interest and STI experience

in spectral analysis indicates a factor of 5. A rule used for the NIPIP program, Ref. 33, is

$$\frac{1}{T} > \frac{20 \omega_c}{2\pi} \quad \text{Hz} \quad (37)$$

where  $\omega_c$  is the loop crossover frequency in rad/sec. This rule is based on the idea that the crossover frequency is a relevant measure of the maximum frequency content in a closed loop system. Table 7 summarizes the Eq. 37 requirement based on the typical crossover frequencies for manual control of various longitudinal loops.

Quantization errors arise from finite digital word lengths and effectively amount to a change in resolution. Although complete specs have not been uncovered, quantization does not presently appear to be a problem with the Shuttle instrumentation system.

Time skews, on the other hand, have been and continue to be of particular concern for the Shuttle instrumentation system. The time skews arise because not all data is sampled at the same instant within a sample period due to a lack of synchrony between the several instrumentation systems. An even more complex problem, referred to as a "rolling time skew," occurs when digital signals are sampled at other than integral multiples of the original sample time.

TABLE 7. MINIMUM SAMPLE RATES BASED ON NIPIP CRITERION

LOOP	NOMINAL CROSSOVER FREQUENCY, $\omega_c$		MINIMUM SAMPLE RATE, $T^{-1}$
	rad/sec	Hz	Hz
Attitude ( $\theta, q$ )	2.	0.32	6.4
Path ( $h, \dot{h}$ )	0.2	0.032	0.64
Speed ( $u$ )	0.08	0.013	0.25

b. Required Data for the Flying Qualities OEX

The primary variables needed for the Shuttle flying qualities OEX are the vehicle state vector and state rates, the control surface deflections, and the primary manual controller deflections. These are summarized in Table 6. In addition, for flying qualities experiments, trim inputs are also of interest and are summarized in Table 8. Because of the great complexity of the switching and gain scheduling logic of the Shuttle FCS, a number of switch positions and other discrete variables are needed to define the actual configuration dynamics present. A minimum set of these discretely are summarized in Table 9.

Certain other data which is not readily available from the Shuttle instrumentation system is of interest such as sinkrate at the pilot station, however, the variables listed in Tables 7-9 should be adequate for computation of such needed auxiliary variables. In addition to the data

TABLE 8. MANUAL TRIM INPUTS DESIRED FOR THE OEX

TRIM INPUT	FCS NAME	FCS SAMPLE RATE, Hz
Pitch Panel Trim	DETM-PAN	6.25
Pitch RHC Trim	DETM-RHC	6.25
Roll Panel Trim	DATM-PAN	6.25
Roll RHC Trim	DATM-RHC	6.25
Yaw Trim	DRT	6.25

TABLE 9. SWITCHES AND FCS DISCRETES DESIRED FOR THE OEX

Body Flap Auto/Manual
Speed Brake Auto/Manual
Pitch Gain Enable
Pitch Control Stick Steering
Pitch Auto
Roll/Yaw Gain Enable
Roll/Yaw Control Stick Steering
Roll/Yaw Auto
Preflare Light
Gear Light
DAP Rate Gain -- Pitch
DAP Rate Gain -- Roll/Yaw
DAP FWD Loop Gain -- Pitch
DAP FWD Loop Gain -- Roll/Yaw
PIO Filter (PIO-ON)
(WOWLON)
(ROLLOUT)

above it may be desirable to obtain certain display variables directly from the data stream. It would probably be useful to directly obtain flight director inputs (and later HUD) inputs. These could be computed from other data if necessary, but obtaining these directly could greatly reduce computational efforts.

c. Data Available from the DFRF MMLE File

The present MMLE file, as summarized in Table 6, has no trim controller or display data. There is some limited discrete variable data and some data for manual controllers. Surface deflection, but not controller inputs, are available for the speedbrake and bodyflap and separate data for the commander and pilot's controls are not available in all cases.

Based on information in Refs. 42, 44, and 45, the ACIP and other data used for the airframe aerodynamic identification effort (i.e., the MMLE programs) should be adequate for the flying qualities OEX. However, certain data in the Table 6 listing should (and could) have increased sample rate. These include angle-of-attack, altitude, the speed brake deflection, as well as the rotational hand controller and rudder pedal deflections. With respect to resolution, the ACIP data is also expected to be adequate. There is some uncertainty, however, concerning resolution for the attitude angle data. Resolution in attitude data has been a problem in other identification efforts, Ref. 34. As shown in the diagram in Fig. 40, the pitch and roll angle signals from the IMU, are sampled at approximately 1 Hz. To make attitude data available to the FCS at a higher sample rate, the IMU data is combined with inputs from the rate gyros using appropriate filtering and integration to interpolate between the IMU samples. It is not presently clear at what point in the system the attitude data is taken for recording and well documented resolution specifications have not been found.

d. Obtaining Adequate Data for the Flying Qualities OEX

Contact with various groups at NASA JSC has indicated that desired data which is not presently available or adequate in the DFRF MMLE file

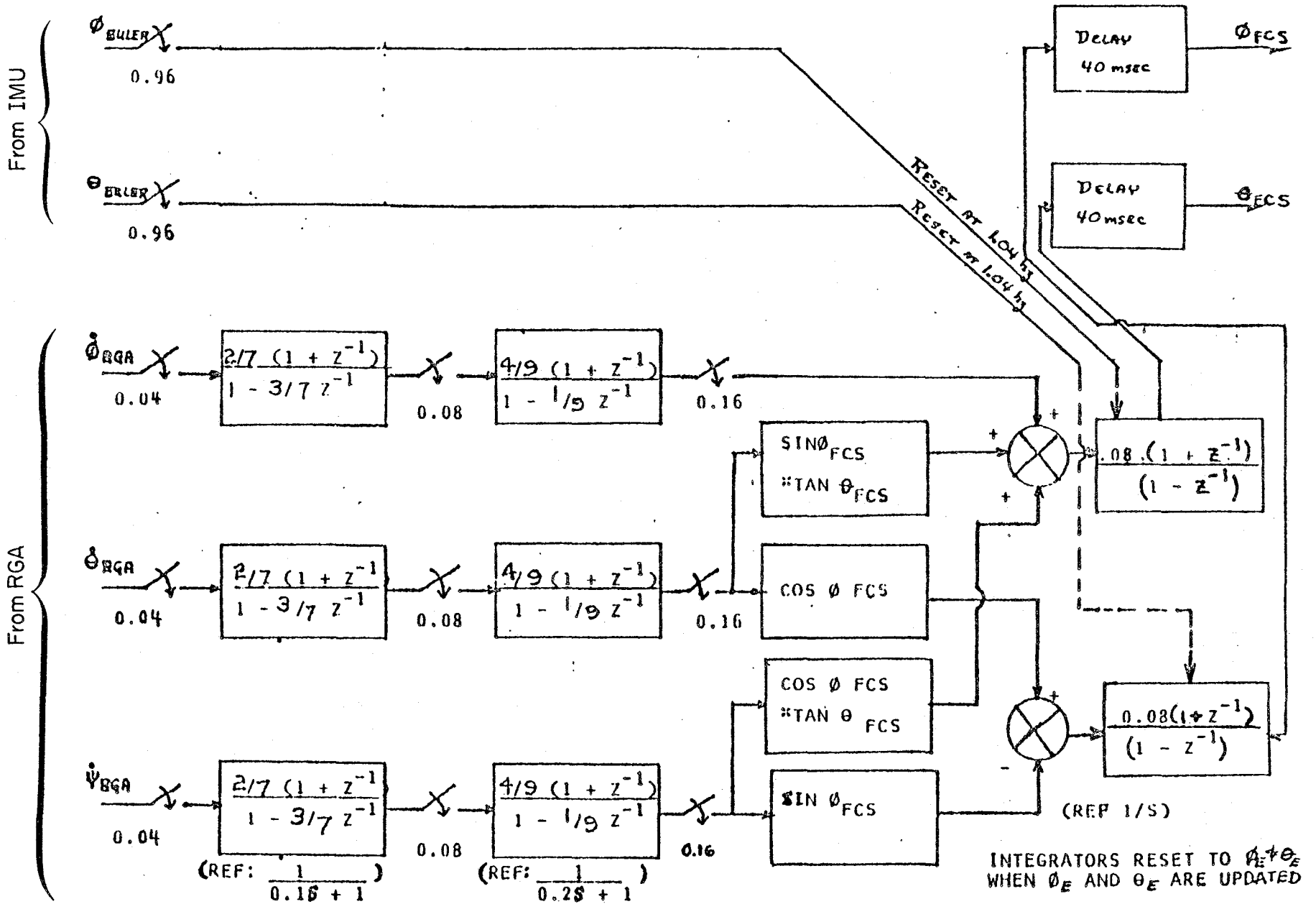


Figure 40. Simplified Block Diagram of Shuttle Attitude Processor (from Ref. 46)

is probably available in the complete data set at NASA JSC. A complete catalog of available data and data characteristics is summarized in the "Master Data Products List" published by the Avionics Systems Division of NASA JSC and arrangements have been made to obtain a copy of this document. This group will supply specialized tapes to users if a subset of the master list is specified for time periods of interest. It appears that the best way to proceed would be to identify the data necessary for the OEX from the Master Data Products List and then coordinate the effort of obtaining this additional data with the effort to create MMLE data files at DFRF.

Much of the data obtained from the present OI system will be available at the sample rates used for the actual flight control system computations. Thus, while it is in principle possible to change the sample rate it would be extremely difficult and probably unnecessary anyway since we will be dealing with actual digital FCS data as opposed to digitized data from an analog FCS. There may, of course, still be time skew problems arising from differences between the sample rate of the PCM system and the Shuttle FCS.

e. Additional Data Not Presently Available

There is, in addition to the data above, certain data which is highly desirable for the flying qualities OEX that is not presently available. Because crew comments have indicated the importance of verbal callouts of airspeed and altitude from the pilot to the commander, transcripts of voice communication during the approach and landing phase with proper time references would be desirable. Because of the importance and uncertainty regarding head-up versus head-down operation; eye-point-of-regard, EPR, data from appropriate devices would be of great interest. When the HUD becomes operational it is of course expected that head-up operation will be the dominant mode, however, there are still questions of interest concerning when the pilot explicitly uses the HUD and when he is actually focussing on the outside visual scene. Finally, other physiological data -- e.g., heart rate, respiration rate, etc. -- might be of interest if it could be made readily available with minimal effort.

### 3. Data Handling and Software Requirements

As noted above it appears that the ideal way to proceed with data analysis for the flying qualities OEX would be to create an augmented OEX file in coordination with the DFRF MMLE file. As with the present MMLE file, the OEX flying qualities file would be accessible on the DFRF Cyber computer. Thus, all analysis could be done by reading subsets of data from this file directly from the computer, thus avoiding the physical handling of data tapes. This is feasible since the DFRF Cyber computer can be accessed from remote facilities such as the STI Hawthorne computer.

There are at least four software "packages" or computer programs needed for the data analysis proposed in the OEX flying qualities plan.

- A data handling program is necessary to read the primary OEX file and to select a subset of the data for the relevant altitude, Mach number or time "slice" of interest to set up a working file to be used in the actual data analysis. Relevant software now exists at DFRF and is also being developed at STI for use on the STI Hawthorne computer.
- Data plotting programs are needed for time response and phase plane plotting. Time response plotting is available at DFRF presently and, at STI, software for both time response and phase plane plots is available in the RESP and PTIME programs.
- Pilot identification programs are needed for the indirect procedure. The primary candidate for this activity is the NIPIP program currently available at DFRF and STI. If spectral analysis procedures prove to be feasible and desirable, analysis software is available at STI in the FREDA and MFP programs. Support software for such activities as frequency response plotting is available on the STI USAM2 package.
- Simulation programs are needed for testing and tuning the identification procedures. The requirements for these programs were previously discussed in Subsection G. Certain programs which might be used are already available (e.g., the USAM2 package).

Additional software and computer graphics capabilities may be found to be desirable as the program progresses. The possibilities are well summarized in Ref. 34. However, it is felt that any additional efforts should be postponed until further experience is gained with the proposed programs outlined for the OEX plan.

## SECTION VI

### POSSIBLE OEX SIMULATION EXPERIMENTS

As noted in the discussion of the indirect approach to a flying qualities OEX, the severe constraints on Shuttle flight tests greatly increases the need for a coordinated research simulation program. A great deal of simulation has been done and will continue to be done on the Shuttle program. However, much of this effort is devoted to system development and training goals and does not directly address many of flying qualities issues of interest in the OEX. A dedicated OEX research simulation program (which might, however, be coordinated with some Shuttle developmental/training simulation) is needed to exercise the 2-dimensional pilot stress/system parameter matrix to address the specific flying qualities issues and ultimately generate design criteria.

Based on the STS-1-4 flight experience, the primary region of concern for Shuttle flying qualities is approach and landing (end of HAC turn through touchdown). Consequently, first consideration will be given to longitudinal manual control but lateral-direction control will be of interest e.g., crosswind landing. As a second priority, stability and control in the low supersonic region will be of interest from the standpoint of FCS development. Specific issues for first consideration are (from pages 56 and 57):

- 2a, 2b - Large effective time delay
- 2c - Pilot/ICR location effects
- 2d - RHC characteristics
- 3a - Superaugmentation effects,  $\theta/\delta_{RHC}$
- 3b, 3c - Neutral speed stability, manual use of speed brakes

## **A. SIMULATION POSSIBILITIES FOR SPECIFIC FLYING QUALITIES ISSUES**

### **1. Effective Time Delay**

There has been considerable study of effective time delay especially in pitch control, e.g., the Ref. 5 and Ref. 47 studies. Thus another simulation (especially with less face validity than the Ref. 5 study) of time delay alone is probably not warranted. A study of specific sources of time delay, in particular that due to structural filters designed to particular specs is of interest; however, more analytical work should proceed any pilot-in-the-loop simulation of this latter issue. Effective time delay must be a variable in any simulation considering other issues. One possible study that could be accomplished even on a very simple (e.g., Ref. 48) setup would be to vary both pitch time delay and time delay in path response to attitude. The path time delay would represent a first approximation to the effect of pilot location aft of the ICR (see Section II-C).

### **2. Pilot Location with Respect to the ICR**

Because of the involvement of motion cues, inflight simulation is highly desirable and such a study has been performed for a Shuttle-like configuration in the Calspan TIFS, Ref. 5 -- although not under the urgency of a glider landing. Further, since it is unlikely that the basic phenomenon can be changed on the Shuttle, the primary interest is in developing spec formats. This might be done efficiently with the two time delay simulation proposed above. A more relevant approach for the Shuttle would be a study of the effects of the HUD/flight director in this issue.

### **3. Manipulator (RHC) Effects**

The basic approach would involve direct comparison of the Shuttle RHC to one or more alternatives. The simulation could be quite simple -- a CTT or Ref. 48 type. However, to the extent that arm-bob weight effects are important, motion or inflight simulation is needed.

Combining these studies with a more general program as proposed in Ref. 49 is recommended.

#### **4. Superaugmentation Effect ( $1/T_q > 1/T_{\theta_2}$ )**

A basic study of this issue might best be accomplished on a simple fixed-base simulator (e.g., of Ref. 48 type) in which the controlled element dynamics are modelled in the superaugmented LOES form (i.e., Eq. 18). This would probably be more satisfactory than attempting to modify a complete Shuttle FCS simulation. Various tasks (simple tracking, simulated landing, etc.) could be studied as  $1/T_q$  and  $1/T_{\theta_2}$  are varied independently. Measurement of pilot compensation would be of interest to verify the expected form of Section IV-F-2.

#### **5. Neutral Speed Stability**

This issue will probably require a relatively high fidelity simulation, or at least a detailed simulation of the task, since the stick force/speed gradient's primary use is as a airspeed or angle-of-attack "monitor." Its usefulness is often most apparent in unattended operation and thus probably of reduced importance for the Shuttle. There is a general interest in the issue for superaugmented aircraft and studies of alternative mechanizations ( $u$  and/or  $\alpha + \delta_e$ ) to produce  $[\partial F/\partial u]_{SS} = 0$  are of interest.

#### **6. Manual Control of Speed Brakes**

The primary region of interest is the equilibrium glide on the steep outer glideslope where problems in manual use of speed-brakes have been noted in STS-4. The primary variables would be speed brake linearity and effectiveness, and turbulence levels. The DFRF STS simulator would be a good facility for initial studies which should be coordinated with the stick force/speed gradient study. The crew's speedbrake retraction logic may also be worth study.

## **7. HUD/Flight Director**

Further information on the Shuttle HUD system is needed before possible studies can be defined. However, the effectiveness of the HUD in reducing pilot workload induced problems and the long term need for the PIOS filter will be of interest. It would be useful to coordinate this effort with any ongoing Sperry HUD studies such as discussed in Ref. 21.

## **8. Control Surface Rate Limiting**

Perhaps the best approach to this issue would be through use of multiple APU failures as a means of inducing pilot stress in other studies.

## **B. EXPERIMENTAL DESIGN**

The experimental design for any OEX simulator will, of course, depend on the simulation facility and the particular issues to be addressed. However, the fundamental design for all simulations will be the 2 dimensional pilot stress/system parameter matrix discussed in Section IV-C. While in theory it is much easier to vary system parameters in a simulator than in flight, the ease with which this may be done in practice may vary greatly among facilities. In particular, high fidelity simulators with detailed models of the Shuttle FCS may not be appropriate for examining variations in a LOES model parameter. For example,  $1/T_q$  for the Shuttle is set by the 'ELFBK' filter but changing this filter in a Shuttle simulator may not be an acceptable way to study  $1/T_q$  variations. It might well be that a simulation with the superaugmented LOES model (i.e., Eq. 18) implemented directly would be much more useful.

There may as well be problems in changing parameters required to vary pilot activity and stress on a high fidelity simulator. For instance, it may be desirable to vary initial conditions (altitude, speed, etc.) for any flight segment (e.g., the start of the preflare pullup). These requirements must be factored into simulator selection.

## **1. Flight Segments, Maneuvers, and Tasks**

Consistent with the previously noted emphasis, approach and landing will be of primary concern. The HAC turn will be of secondary concern and ultimately some of the lower supersonic region might be of interest.

## **2. Performance Measures**

The primary performance measures will be derived from the statistics of the aircraft state at the termination of a particular flight segment. Primary among these will be the touchdown dispersion statistics including the means and variances for touchdown distance, speed and sinkrate. The terminal parameters of previous segments (HAC turn) equilibrium steep glide, etc.) are also of interest because they define the initial condition statistics for the following segment.

## **3. Workload/Stress Measures**

Subjective and objective workload measures may be obtained by the procedures proposed for OEX flights, (Section IV-C). In addition, for simulations it should be possible to obtain quantitative subjective measures, i.e., pilot ratings, since the possibilities for acquiring statistically significant data samples will be much better than in flight. Objective measures may be approached through the pilot model identification efforts. For example, pilot parameters such as crossover frequency, phase margin, and effective lead extracted using NIPIP may be related to workload.

## **4. Possible Simulation Facilities**

A wide variety of simulators are of interest, from simple simulations allowing easy variation of parameters to high fidelity inflight simulators. A basic list is as follows.

### **a. Simplified Special Purpose Simulators**

These would be special purpose setups to focus on specific issues. An example of such a simulation is that used in the Ref. 48 study of

Shuttle approach and landing. This setup used a chair mounted, two-axis control stick; an EAI 1631-R analog computer; a PDP-11 minicomputer and a dual-beam oscilloscope display. The airframe and control system models were considerably simplified and implemented on the analog computer. The task was an abstraction of a landing task in which one oscilloscope beam presented the horizon (for a pitch cue) and the second beam presented the ground plane (for an altitude cue).

Even simpler "simulations" could be employed. For example, manipulator effects on pilot control latency could be examined by comparing several controller types using the STI Critical Task Tester (CTT), Ref. 50. This device requires the operator to control a display indicator with a hand control (one of the controllers to be compared). The CTT display indicator responds to an inherently unstable task analogous to balancing a broomstick on a fingertip. As the experiment session proceeds the "broomstick" becomes shorter (i.e., the task dynamics become more unstable). The point at which the operator loses control has been shown to be a very sensitive measure of the operator's effective time delay. For this application the effect of various manipulators on effective time delay could be defined.

b. DFRF Fixed-Base Shuttle Simulator

This simulator is a likely candidate because of ready access. This facility is presently being updated with a new computer and visual display as well as inclusion of autoland and HUD simulations.

c. DFRF Digital FBW F-8

This aircraft may be reasonably available but is not strictly an inflight simulator. If certain modifications of FCS parameters are possible it could be used to study some issues.

d. NASA ARC Simulators (VMS, FSAA)

These facilities would be especially useful if simulations could be combined with ongoing Shuttle development studies, e.g., the Sperry HUD studies noted in Ref. 21.

e. Calspan TIFS

This inflight simulator has been used for several previous Shuttle experiments.

f. Shuttle Training Simulators (STA, SMS, FSL)

Any use of these would probably have to be on a non-interference and therefore limited basis. However, contact with the STA group at NASA JSC has indicated that it may be possible to obtain flight data. This could be a useful adjunct to flight data extraction efforts.

## REFERENCES

1. Myers, T. T., D. E. Johnston, and D. T. McRuer, Space Shuttle Flying Qualities and Flight Control System Assessment Study, NASA CR-170391, June 1982.
2. McRuer, Duane and Thomas T. Myers, Handling Qualities of Aircraft with Relaxed Static Stability and Advanced Flight Control Systems. Vol. II: Ramifications of Flight-Critical Heavily-Augmented Relaxed Static Stability Airplane Characteristics on Flying Qualities, DOT/FAA/CT-82/130, Sept. 1982.
3. Mooij, H. A., W. P. de Boer, and M. F. C. van Gool, Determination of Low-Speed Longitudinal Maneuvering Criteria for Transport Aircraft with Advanced Flight Control Systems, National Aerospace Lab., NLR TR 79127 U, Dec. 1979.
4. Mooij, H. A. and M. F. C. Van Gool, "Handling Qualities of Transports with Advanced Flight Control Systems," presented at AGARD Flight Control Panel Symposium on Criteria for Handling Qualities of Military Aircraft, Ft. Worth, TX, Apr. 1982.
5. Weingarten, N. C. and C. R. Chalk, In-Flight Investigation of Large Airplane Flying Qualities for Approach and Landing, AFWAL-TR-81-3118, Sept. 1981.
6. Weingarten, N. C. and C. R. Chalk, "In-Flight Investigation of Large Airplane Flying Qualities for Approach and Landing," AIAA Paper 82-1296, Aug. 1982.
7. Stapleford, Robert L., Samuel J. Craig, and Jean A. Tennant, Measurement of Pilot Describing Functions in Single-Controller Multiloop Tasks, NASA CR-1238, Jan. 1969.
8. Weir, David H. and Duane T. McRuer, Pilot Dynamics for Instrument Approach Tasks: Full Panel Multiloop and Flight Director Operations, NASA CR-2019, May 1972.
9. McRuer, Duane, "Progress and Pitfalls in Advanced Flight Control Systems," AGARD CP-321, 1982.
10. Federal Aviation Regulations, Part 25, Airworthiness Standards: Transport Category Airplanes, Federal Aviation Administration, June 1974.
11. "Flying Qualities of Piloted Airplanes," MIL-F-8785B, Aug. 1969.
12. "Flying Qualities of Piloted Airplanes," MIL-F-8785C, Nov. 1980.

13. Klinar, W. J., D. W. Gilbert, et al., Flying Qualities Requirements for the Orbiter Utilizing Closed-Loop, Fly-by-Wire Control of Vehicle Response Parameters, NASA JSC-07151, Rev. 1, Dec. 1973.
14. Stapleford, Robert L., Richard H. Klein, and Roger H. Hoh, Handling Qualities Criteria for the Space Shuttle Orbiter During the Terminal Phase of Flight, NASA CR-2017, Apr. 1972.
15. Franklin, J. A., R. C. Innis, G. H. Hardy, and J. D. Stephenson, Design Criteria for Flightpath and Airspeed Control for the Approach and Landing of STOL Aircraft, NASA TP 1911, Mar. 1982.
16. Mooij, H. A. and M. F. C. van Gool, The Need for Stick Force Stability in Attitude-Stabilized Aircraft, NLR TR 77027U (Part II), 1976.
17. Mooij, H. A. and M. F. C. van Gool, "Flight Test of Stick Force Stability in Attitude-Stabilized Aircraft," J. Aircraft, Vol. 15, No. 9, Sept. 1978.
18. Tomlinson, L. R., "Control System Design Considerations for a Longitudinally Unstable Supersonic Transport," J. Aircraft, Vol. 10, No. 10, Oct. 1973, pp. 594-601.
19. Shomber, H. A., "Application of Integrated Active Controls to Future Transports," AIAA Paper 79-1654, 1979.
20. Integrated Application of Active Controls (IAAC) Technology to an Advanced Subsonic Transport -- Project Plan, NASA CR-3305, Dec. 1980.
21. Tsikalas, Gust M., "Space Shuttle Autoland Design," AIAA Paper 82-1604-CP, Aug. 1982.
22. Preliminary Analysis of STS-1 Entry Flight Data, NASA TM 81363, Aug. 1981.
23. Preliminary Analysis of STS-2 Entry Flight Data, NASA TM 81371, Apr. 1982.
24. Preliminary Analysis of STS-3 Entry Flight Data, NASA TM 81373, Aug. 1982.
25. Preliminary Analysis of STS-4 Entry Flight Data, NASA TM 81375, Sept. 1982.
26. Mattingly, T. K. and Henry W. Hartsfield, Jr., STS-4 Crew Report, NASA, Johnson Space Center, Memorandum, Aug. 1982.

27. Jex, Henry R. and Richard A. Peters, Excess Control Capacity System Description and Specification for the DEFT Application in the Calspan NT-33A, System Technology, Inc., TR-1167-1, Mar. 1981.
28. McRuer, D. T. and E. S. Krendel, Mathematical Models of Human Pilot Behavior, AGARDograph No. 188, Jan. 1974.
29. Newell, Fred D. and Paul E. Pietrzak, "In-Flight Measurement of Human Response Characteristics," J. Aircraft Vol. 5, No. 3, May-June 1968, pp. 277-284.
30. Allen, R. Wade and Henry R. Jex, "A Simple Fourier Analysis Technique for Measuring the Dynamic Response of Manual Control Systems," IEEE Trans., Vol. SMC-2, No. 5, Nov. 1972, pp. 638-643.
31. Heffley, Robert K. and Wayne F. Jewell, Development of a CTOL Piloting Technique Measurement Scheme for a Real-Time Simulator Environment NASA CR-152294, July 1979.
32. Jewell, Wayne F. and Ted M. Schulman, A Pilot Control Strategy Identification Technique for Use in Multiloop Control Tasks, NASA CR-152374, Aug. 1980.
33. Hanson, Gregory D. and Wayne F. Jewell, Non-Intrusive Parameter Identification Procedure User's Guide, Systems Technology, Inc., TR-1188-1, June 1982. (Same as Ref. 27).
34. Heffley, Robert K., Gregory D. Hanson, Wayne F. Jewell, and Warren F. Clement, Analysis of Pilot Control Strategy, Systems Technology, Inc., TR-1188-2, Sept. 1982.
35. Heffley, Robert K., Ted M. Schulman, Robert J. Randle, Jr., and Warren F. Clement, An Analysis of Airline Landing Flare Data Based on Flight and Training Simulator Measurement, Systems Technology, Inc., TR-1172-1R, Rev. Aug. 1982.
36. Heffley, Robert K., "Pilot Models for Discrete Maneuvers," AIAA Paper 82-1519-CP, Aug. 1982.
37. McRuer, Duane, "Human Dynamics in Man-Machine Systems," Automatica, Vol. 16, No. 3, May 1980, pp. 237-253.
38. Clement, Warren F., Classical Solutions of Time-Varying Linear Differential Equations Describing Manually Controlled Landing Approaches with Visually Derived Guidance, Systems Technology, Inc., WP-510-49, Oct. 1981.
39. Looney, B. J., Post-Detac HUD Monitor Description, Sperry Flight Systems, Autoland Memo 57, Nov. 1980.

40. van Gool, M. F. C. and H. A. Mooij, A Comparison of In-Flight and Ground-Based Pitch Attitude Tracking Experiments, National Aerospace Laboratory NLR, The Netherlands, NLR MP 76011 U, 1976.
41. Hoey, Robert G., et al., AFFTC Evaluation of the Space Shuttle Orbiter and Carrier Aircraft — NASA Approach and Landing Test, AFFTC-TR-78-14, May 1978.
42. Rutherford, J. F., R. C. Blanchard, and J. D. Harris, Data Processing Requirements for the High Resolution Accelerometer Package (HIRAP), Sept. 1982.
43. Bendat, Julius S. and Allen G. Piersol, Random Data: Analysis and Measurement Procedures, Wiley-Interscience, New York, 1971.
44. Lowery, H. J., D. B. Howes, and P. D. Gerke, Data Processing Requirements for the Aerodynamic Coefficient Identification Package (ACIP), NASA Johnson Space Ctr., 1982.
45. Nichols, M. E., STS-4 Aerodynamic Reference Data - Initial Issue, Rockwell International Internal Letter No. SAS/AERO/82-311, June 1982.
46. Entry/Landing/GRTLS Stability and Response Analytic Verification Plan, E-V-TP-1-200, Appendix A, Honeywell Inc., St. Petersburg, Feb. 1981.
47. Berry, D. T., B. G. Powers, K. J. Szalai, and R. J. Wilson, "A Summary of an In-Flight Evaluation of Control System Pure Time Delays During Landing Using the F-8 DFBW Airplane," A Collection of Technical Papers' Proceedings of AIAA Atmospheric Flight Mechanics Conference, Aug. 11-13, 1980, Danvers, MA, pp. 561-571.
48. Teper, Gary L., Richard J. DiMarco, and Irving L. Ashkenas, Analyses of Shuttle Orbiter Approach and Landing Conditions, NASA CR-163108, July 1981.
49. Manipulator Subsystem/Controller/Control Task Interactions, Systems Technology, Inc., TP-501, May 1982.
50. Jex, H. R., J. D. McDonnell, and A. V. Phatak, A "Critical" Tracking Task for Man-Machine Research Related to the Operator's Effective Delay Time. Part I: Theory and Experiments with a First-Order Divergent Controlled Element, NASA CR-616, Nov. 1966.

## APPENDIX A

### SPACE SHUTTLE FLIGHT MECHANICS IN APPROACH AND LANDING

#### A. TRANSLATIONAL EQUATIONS OF MOTION

Considerations of manual control approach and landing will be limited to symmetric motion for initial analysis. Thus to analyze the trajectory of the Shuttle, the longitudinal force (i.e., lift and drag) equations are adequate. The velocity vector may be defined in a tangent-normal coordinate system (Fig. A-1) as

$$\underline{V} = V\hat{e}_T \quad (A-1)$$

The vector acceleration is found by differentiating Eq. A-1

$$\begin{aligned} \underline{a} &= \dot{V}\hat{e}_T + V\dot{\hat{e}}_T \\ &= \dot{V}\hat{e}_T + V\dot{\gamma}\hat{e}_N \end{aligned} \quad (A-2)$$

The vector symmetric force equation is then given by Eq. A-3

$$\begin{aligned} \underline{a} &= \underline{mg} + \underline{F}_{AERO} \\ &= mg(-\sin\gamma\hat{e}_T - \cos\gamma\hat{e}_N) + L\hat{e}_N - D\hat{e}_T \end{aligned} \quad (A-3)$$

This vector force equation is equivalent to two scalar equations -- the familiar lift and drag force equations

$$mV\dot{\gamma} = -mg \cos\gamma + L \quad (A-4)$$

$$m\dot{V} = -mg \sin\gamma - D \quad (A-5)$$

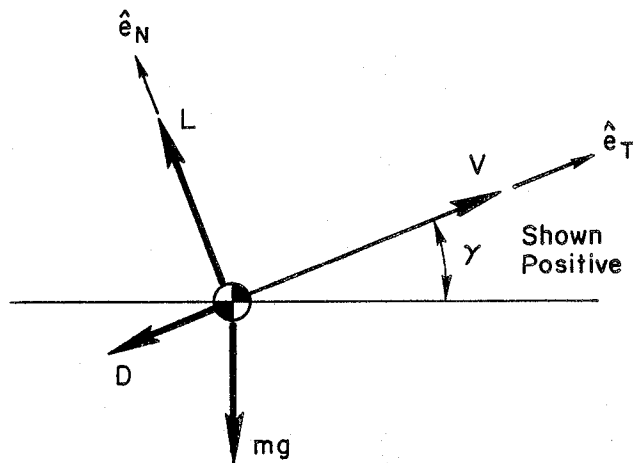


Figure A-1. Tangent Normal Coordinate System

where lift and drag are defined in terms of their respective nondimensional coefficients

$$L = \bar{q} S C_L \quad (\text{A-6})$$

$$D = \bar{q} S C_D \quad (\text{A-7})$$

and the dynamic pressure is defined in terms of the true velocity by Eq. A-8

$$\bar{q} = \frac{1}{2} \rho V^2 \quad (\text{A-8})$$

## B. LIFT COEFFICIENT

The lift coefficient for the Shuttle may be obtained from the Shuttle Aerodynamic Design Data book, Ref. A-1, and the low speed flight test data from the Approach and Landing Test (ALT) flights presented in Ref. A-2. For approach and landing, the Mach number is 0.5 or lower and thus the aerodynamics may be simplified by assumption of incompressible flow. The  $C_L$  equation may be further simplified by neglecting a number

of small terms (such as those due to body flap and speed brake) resulting in the simple and classical lift coefficient of Eq. A-9.

$$C_L \doteq C_{L_0} + C_{L_\alpha} \alpha + C_{L_{\delta_e}} \delta_e \quad (\text{A-9})$$

where

$$C_{L_0} = -0.05$$

$$C_{L_\alpha} = 0.045 \text{ deg}^{-1}$$

$$C_{L_{\delta_e}} = 0.018 \text{ deg}^{-1}$$

The definition of  $C_{L_0}$  and  $C_{L_\alpha}$  are shown in Fig. A-2. While the effect of lift due to elevator deflection,  $C_{L_{\delta_e}}$ , is important in consideration of path dynamics at the pilot station, for much of what follows  $C_{L_{\delta_e}}$  can be neglected. Ground effects, according to Ref. A-1 are negligible when the Shuttle is at least one wing span above ground level, but do become significant when the ground vehicle is within 1/2 wing span of the ground. However, for the approximate analysis here, ground effects will be ignored.

### C. DRAG COEFFICIENT

Similar approximations may be made for drag coefficient except that the effect of the speed brake is significant as is the effect of landing gear. Thus the drag coefficient may be given by Eq. A-10,

$$\begin{aligned} C_D &\doteq C_{D_0} + C_{D_L} C_L^2 + C_{D_{\delta_{SB}}} (\delta_{SB} - 25^\circ) + \Delta C_D (\delta_{e_{trim}}) + \Delta C_{D_{LG}} \\ &\doteq C_{D_0} + C_{D_L} C_L^2 + C_{D_{\delta_{SB}}} \delta_{SB} + \Delta C_{D_{LG}} \end{aligned} \quad (\text{A-10})$$

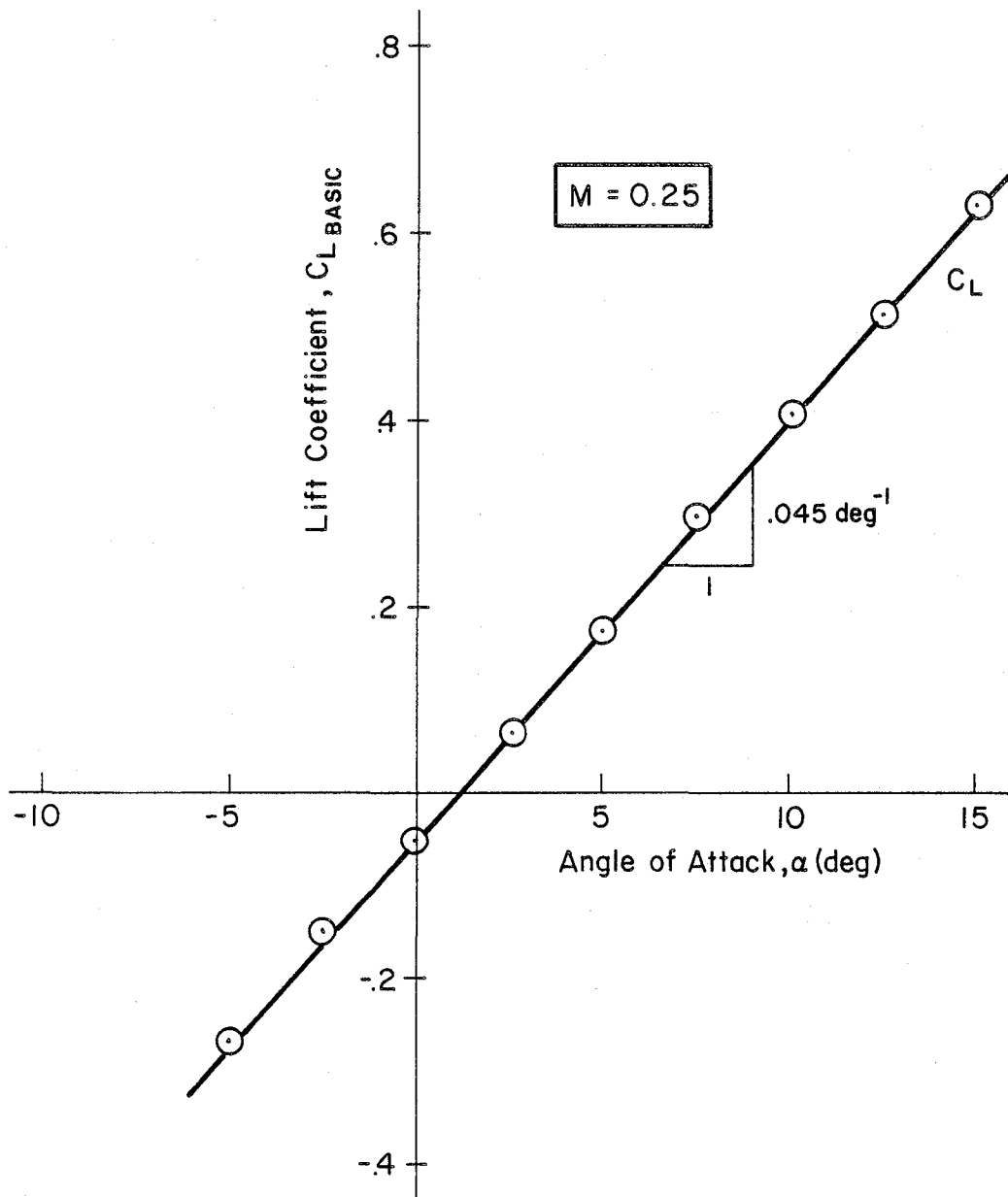


Figure A-2. Low Speed  $C_L$  vs.  $\alpha$ ,  $\delta_e = 0$

where

$$0 < \delta_{SB} < 87.5 \text{ deg}$$

$$C_{D_0} = 0.067$$

$$C_{D_L} = 0.173 \quad \text{Fig. A-3}$$

$$C_{D\delta_{SB}} = 0.00068 \text{ deg}^{-1} \quad \text{Fig. A-4}$$

$$\Delta C_{D_{LG}} = \begin{cases} 0 & \text{gear up} \\ 0.02 & \text{gear down} \end{cases}$$

The speed brake derivative was obtained from Fig. A-4 by linearizing around the 25 deg deflection point. It may be noted from Fig. A-4 that the speed brake is nonlinear for small deflections, i.e., less than 20 deg. However, as may be seen from flight data, the speed brakes are generally deployed in deflections greater than 25 deg or fully retracted. The landing gear increment is represented by two discrete values corresponding to zero for gear up and 0.02 for gear down. The basic drag of the Shuttle consists of a parabolic drag polar defined from the data in Fig. A-3. As for the lift coefficient, increments on drag coefficient due to ground effect are significant only very near the ground and will be neglected here.

#### D. EQUILIBRIUM GLIDE ON THE STEEP GLIDESLOPE

While the equivalent airspeed remains constant during the equilibrium glide, the true airspeed decreases due to the variation of atmospheric density with altitude. Thus, defining the equilibrium glide by  $\gamma = \text{constant}$  and  $\bar{q} = \text{constant}$ , the lift and drag equations (Eqs. A-4 and A-5) become

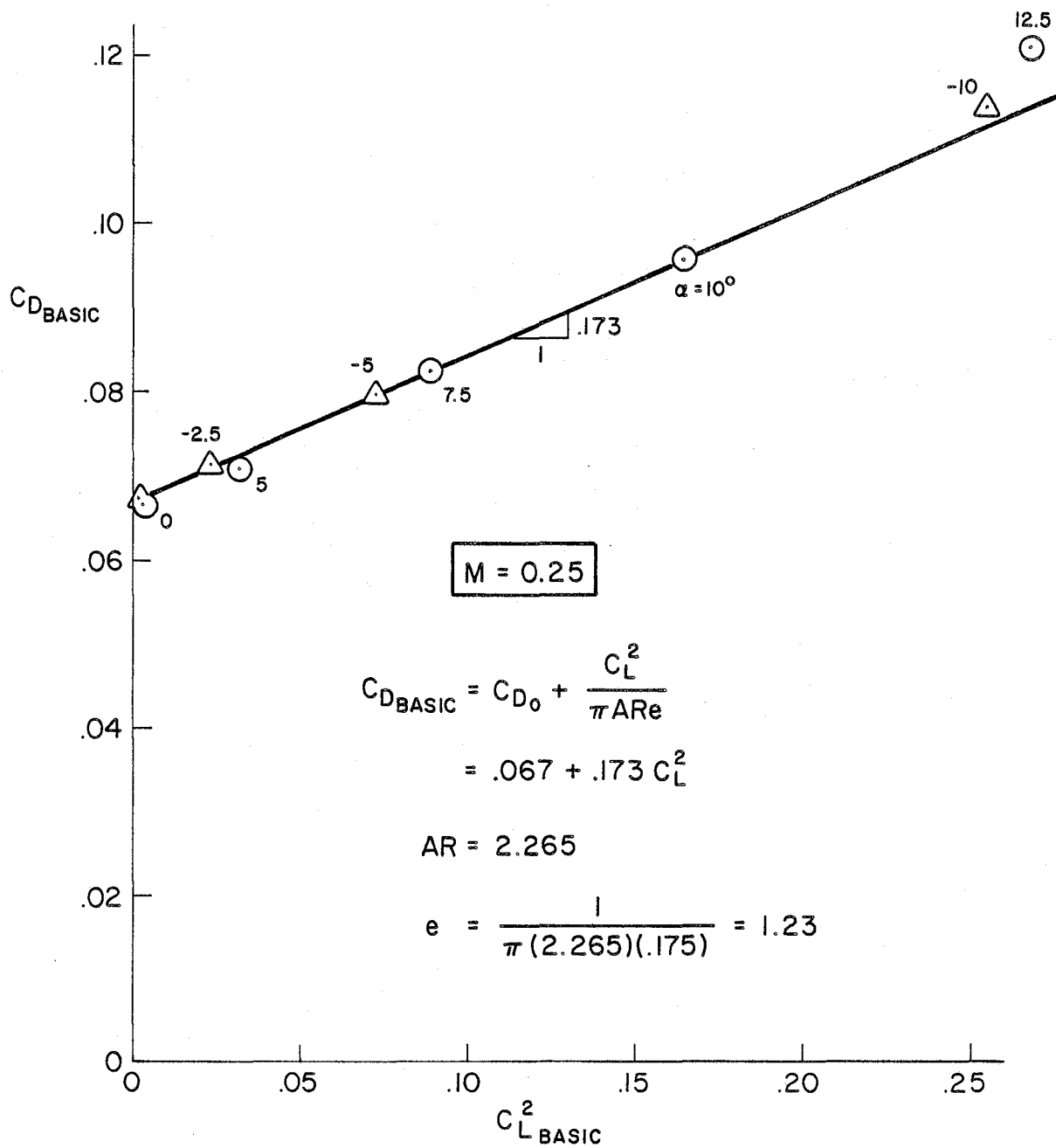


Figure A-3. Extraction of Drag Polar Constants,  $\delta_{SB} = 0$ , Gear Up

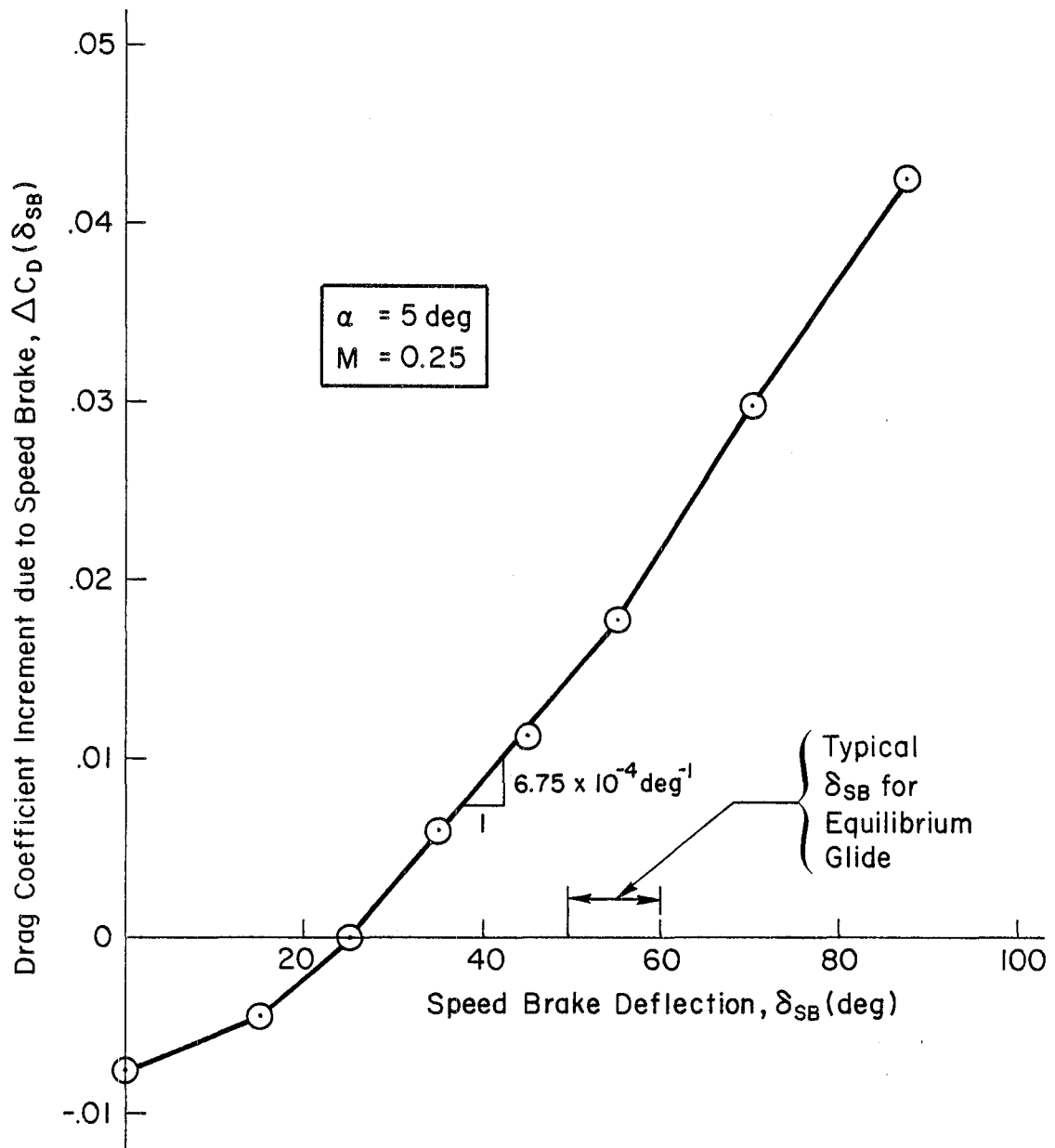


Figure A-4.. Speed Brake Effectiveness

$$m\dot{V}\dot{\gamma} = -mg \cos \gamma + \bar{q} SC_L = 0 \quad (\text{A-11})$$

$$m\dot{V} = -mg \sin \gamma - \bar{q} SC_D \quad (\text{A-12})$$

Ratioing Eqs. A-11 and A-12 gives an expression for the equilibrium glideslope

$$\begin{aligned} \frac{-mg \sin \gamma}{-mg \cos \gamma} &= \tan \gamma = \frac{\bar{q} SC_D + \dot{V}m}{-\bar{q} SC_L} \\ &= -\frac{C_D}{C_L} - \frac{\dot{V}m}{\bar{q} SC_L} \end{aligned} \quad (\text{A-13})$$

where  $\gamma < 0$  for a dive.

Over the altitude range of interest, the density ratio is given by (see Ref. A-3, pg. 478)

$$\begin{aligned} \sigma &= \frac{\rho}{\rho_0} = \left(\frac{T}{T_0}\right)^{(1/\alpha R)} - 1 \\ &= \left(1 - \frac{\alpha h}{T_0}\right)^{(1/\alpha R)} - 1 \end{aligned} \quad (\text{A-14})$$

where

$$\begin{aligned} T_0 &= 518.4 \text{ deg R} \\ \alpha &= 0.003566 \text{ } ^\circ\text{F/ft lapse rate} \\ R &= 53.35 \text{ ft/}^\circ\text{F} \end{aligned}$$

Thus, for altitude in feet, the density ratio is

$$\sigma = (1 - 6.88 * 10^{-6}h)^{4.26} \quad (\text{A-15})$$

For comparison at 10,000 ft

$$\sigma = 0.738 \quad \text{Eq. A-15}$$

$$\sigma = 0.7385 \quad \text{ICAO standard atmosphere table}$$

Because the altitude term in Eq. A-15 is small relative to unity

$$\sigma \doteq 1 - \left(\frac{\alpha h}{T_0}\right) \left(\frac{1}{\alpha R} - 1\right) = 1 - K_h h$$

where

(A-16)

$$\begin{aligned} K_h &= \frac{1 - \alpha R}{T_0 R} \\ &= 2.93 * 10^{-5} \text{ ft}^{-1} \end{aligned}$$

For comparison at 10,000 ft

$$\sigma = 0.707 \quad \text{Eq. A-16 (4 percent error)}$$

$$\sigma = 0.7385 \quad \text{ICAO standard atmospheric table}$$

The relation between the constant equivalent airspeed and the true airspeed is thus given by

$$v^2 = \frac{v_E^2}{\sigma} \doteq \frac{v_E^2}{1 - K_h h} \doteq (1 + K_h h) v_E^2 \quad (\text{A-17})$$

Differentiating Eq. A-17,

$$\frac{d}{dt} v^2 = 2v\dot{v} \doteq K_h h \dot{v}_E^2 \quad (\text{A-18})$$

Relating sinkrate to speed and flight path angle through

$$\dot{h} = V \sin \gamma \quad (A-19)$$

the rate of change of true airspeed is given by Eq. A-20

$$\dot{V} = \frac{1}{2} K_h \sin \gamma V_E^2 \quad (A-20)$$

For the nominal Shuttle approach

$$\gamma = -19 \text{ deg} \quad , \quad V_E = 481 \text{ fps}$$

Therefore

$$\begin{aligned} \dot{V} &= -1.16 \text{ ft/sec}^2 \\ &= -0.0343 \text{ g} \end{aligned}$$

Thus the second term in Eq. A-13 is given by

$$\frac{m\dot{V}}{qSC_L} = \frac{(1/2)K_h \sin \gamma V_E^2}{(1/2)\rho_0 V_E^2 SC_L} \quad (A-21)$$

From Eq. A-11

$$SC_L = \frac{mg \cos \gamma}{(1/2)\rho_0 V_E^2} \quad (A-22)$$

and Eq. A-21 becomes

$$\frac{m\dot{V}}{qSC_L} = \frac{K_h V_E^2}{2g} \tan \gamma \quad (A-23)$$

Thus Eq. A-13 may be written as

$$\tan \gamma \left( 1 + \frac{K_h V_E^2}{2g} \right) = - \frac{C_D}{C_L} \quad (\text{A-24})$$

The density variation term in Eq. A-24 is equivalent to an apparent 10 percent increase in L/D for the nominal Shuttle glide condition, e.g.,:

$$\frac{K_h V_E^2}{2g} = \frac{2.93 * 10^{-5} * 481^2}{2 * 32.2} = 0.105$$

Neglecting the density altitude effect gives the classical glide equation

$$\tan \gamma = - \frac{C_D}{C_L} \quad (\text{A-25})$$

The  $\gamma$ - $V_E$  curves with the density variation may be developed from Eq. A-10 (gear up) and Eq. A-25

$$\begin{aligned} \tan \gamma \left( 1 + \frac{K_h V_E^2}{2g} \right) &= - \frac{(C_{D_o} + C_{D_L} C_L^2 + C_D \delta_{SB} \delta_{SB})}{C_L} \\ &= - \frac{(C_{D_o} + C_D \delta_{SB} \delta_{SB}) \bar{q}}{(W/S) \cos \gamma} - C_{D_L} \frac{(W/S) \cos \gamma}{\bar{q}} \end{aligned} \quad (\text{A-26})$$

Multiplying Eq. A-26 by  $\bar{q} \cos \gamma$  and rearranging gives

$$\bar{q}^2 + B\bar{q} + C = 0 \quad (\text{A-27})$$

where

$$B = \frac{\sin \gamma}{\left[ \frac{K_h}{g\rho_0} \sin \gamma + \frac{(C_{D_0} + C_{D_{\delta_{SB}} \delta_{SB}})}{(W/S)} \right]}$$

$$C = \frac{C_{D_L}(W/S) \cos^2 \gamma}{\left[ (K_h/g\rho_0) \sin \gamma + (C_{D_0} + C_{D_{\delta_{SB}} \delta_{SB}})/(W/S) \right]}$$

Solution of Eq. A-27 gives the  $\gamma$ -V curve shown in Fig. 21. The positive (i.e., high speed) root of Eq. A-27 corresponds to the stable "front side" of the  $\gamma$ -V curve. The curves in Fig. 21 are shown for the nominal STS-4 landing weight.

#### E. PREFLARE PULLUP

The preflare begins at around 1700 ft AGL. At this low altitude it is reasonable to assume that the density is constant, i.e.,

$$\rho \doteq \rho_0$$

$$V \doteq V_E$$

The flight path angle is not quite "small" for the Shuttle on the steep glide slope, however, once preflare begins  $\gamma$  is rapidly reduced and it is reasonable to use small angle approximations. Thus the lift equation becomes

$$mV\dot{\gamma} \doteq -mg + \bar{q}SC_L \quad (A-28)$$

which divided by  $mg$  gives

$$\frac{V}{g} \dot{\gamma} = -1 + n \quad (\text{A-29})$$

The drag equation is

$$m\dot{V} = -mg\gamma - \bar{q}SC_D \quad (\text{A-30})$$

which divided by  $mg$  gives

$$\frac{\dot{V}}{g} = -\gamma - n \frac{C_D}{C_L} \quad (\text{A-31})$$

Definition of the drag coefficient in the preflare is complicated (especially for manual flight) by speed brake retraction and gear extension decisions, but an effective  $C_{D_0}$  may be used to account for gear and speed brake for a given status. Thus, the drag equation becomes

$$\frac{\dot{V}}{g} = -\gamma - \left( \frac{C_{D_0}}{W/S} \bar{q} + C_{D_L} \frac{W/S}{\bar{q}} n^2 \right) \quad (\text{A-32})$$

However, speed change during the preflare pullup is very slow until the flight path angle departs significantly from the equilibrium value and therefore, the pullup may be considered a constant speed maneuver to a first approximation.

## F. SHALLOW GLIDE AND FINAL FLARE

### 1. Deceleration Rate

From theoretical considerations and flight data, it may be seen that the incremental load factor in the final glide and flare is very small, unlike the preflare pullup. Thus it is reasonable to neglect the incremental load factor in the drag equation (although not in the lift

equation) and set  $\gamma$  equal to a constant, i.e.,  $\gamma_0$ . Thus the drag equation becomes

$$\begin{aligned} \dot{V} &= -\gamma_0 g - g \left( \frac{C_{D_0}}{W/S} \bar{q} + C_{D_L} \frac{W/S}{\bar{q}} \right) \\ &= -\gamma_0 g - g \frac{C_D}{C_L} \\ &= a + bV^2 + cV^{-2} \end{aligned} \tag{A-34}$$

where

$$\begin{aligned} a &= -\gamma_0 g \\ b &= -\frac{g C_{D_0} \rho}{2W/S} \\ c &= \frac{-2g C_{D_L} W/S}{\rho} \end{aligned}$$

The differential equation represented by Eq. A-34 is difficult to solve in closed form without additional approximations. Noting that the nominal wing loading is

$$\frac{W}{S} = \frac{188,000 \text{ lbs}}{2690 \text{ ft}^2} = 69.9 \text{ psf}$$

The effective  $C_{D_0}$ , with the speed brake retracted and the gear down is

$$C_{D_0} = 0.067 + 0.02 = 0.087$$

The drag to lift ratio is thus

$$\frac{C_D}{C_L} = 0.00124 \bar{q} + 12.09/\bar{q} \tag{A-35}$$

Figure A-5 shows a buildup of Eq. A-35 based on the nominal 32,000 lb landing payload case and it may be seen that the parasite and induced drag terms have opposite trends but roughly cancel over the dynamic pressure range of interest. This makes the drag-to-lift ratio approximately constant, which in turn implies, through Eq. A-34, that the deceleration rate,  $\dot{V}$ , is approximately constant. For the nominal value of  $\gamma_0 = -1.5$  deg, the deceleration rate can be expected to be between 0.23 and 0.33 g. Examination of flight traces indicates that this is a reasonable approximation and provides a numerical check, e.g., from STS-4

$$\frac{\Delta V}{\Delta t} \doteq -6.8 \text{ fps/sec} = -0.21 \text{ g}$$

## 2. Solution for Velocity and Kinetic Energy

Given a constant deceleration rate

$$\dot{V} \doteq -K\dot{\gamma} = \text{constant} \quad (\text{A-36})$$

The velocity may be determined by integrating with respect to time

$$\begin{aligned} V(t) &= K\dot{\gamma} \int_0^t dt + V_0 \\ &= -K\dot{\gamma}t + V_0 \end{aligned} \quad (\text{A-37})$$

$$\frac{C_D}{C_L} = \left( \frac{C_{D_0}}{W/s} \right) \bar{q} + \left( C_{D_L} \frac{W}{s} \right) \frac{1}{\bar{q}}$$

$$= .00124 \bar{q} + 12.09/\bar{q}$$

$$W = 188,000 \text{ lb}$$

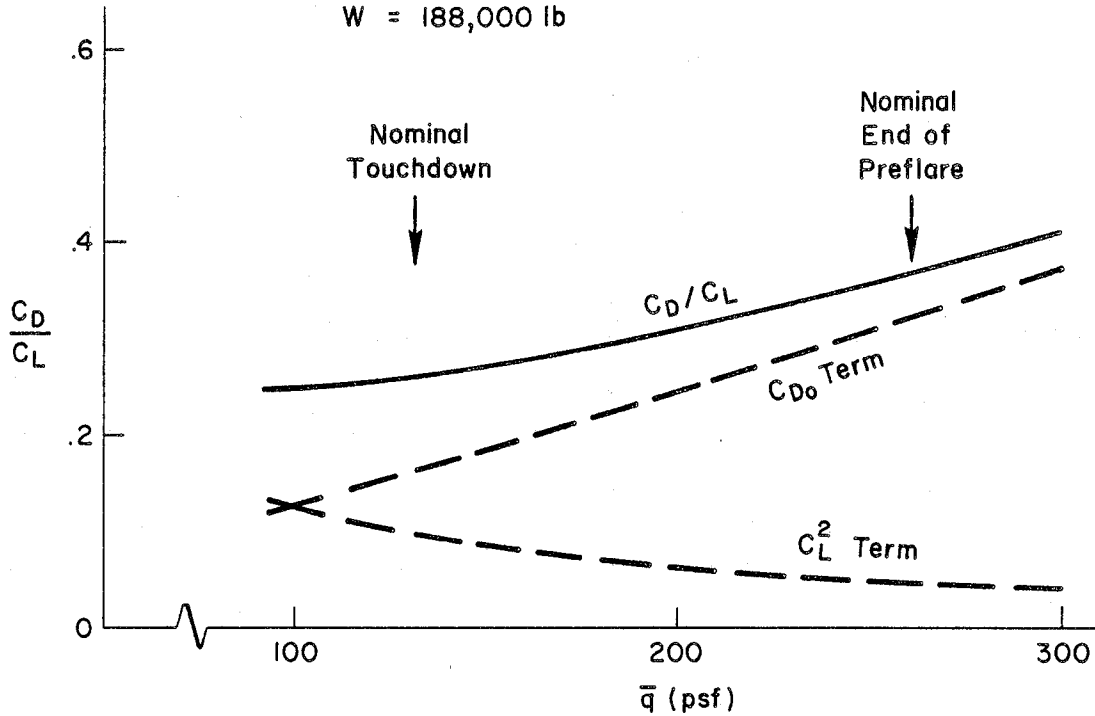


Figure A-5. Relative Contribution of Parasite and Induced Drag Terms to Deceleration

Alternatively, it is useful to parameterize the velocity on the distance traveled which leads to consideration of the specific kinetic energy, i.e.,

$$\begin{aligned} \dot{V} &= \frac{dV}{dt} = \frac{dV}{ds} \frac{ds}{dt} = V \frac{dV}{ds} \\ &= \frac{d}{ds} \left( \frac{1}{2} V^2 \right) = \frac{dE_K}{ds} = -K\dot{V} \end{aligned} \quad (A-38)$$

where

$$E_K = \frac{1}{2} V^2 = \text{specific kinetic energy}$$

For  $\gamma$  small,  $ds \doteq dx$  and

$$\begin{aligned} E_K(x) &= \int_0^x \frac{dE_K}{dx} dx + E_{K0} \\ &= -K_v X + \frac{1}{2} V_0^2 \end{aligned} \quad (A-39)$$

$$V(x) = (-2K_v X + V_0^2)^{1/2} \quad (A-40)$$

### 3. Manual Control

As discussed in Subsection IV-E, the pilot's control problem for the shallow glide and final flare is to control the trajectory using  $\gamma_0$  and  $T_f$  as control variables to achieve a touchdown with  $h_{TD}$ ,  $V_{TD}$ , and  $X_{TD}$  within specified limits. Treating  $\gamma_0$  and  $T_f$  as the pilot's control variables and flare height,  $h_f$ , as a predetermined constant, the flare distance,  $X_f$  is

$$X_f = -(h_0 - h_f)/\gamma_0 \quad (A-41)$$

The kinetic energy at the start of final flare is

$$E_{K_f} = -K_v X_f + \frac{1}{2} V_0^2 \quad (A-42)$$

and the velocity at the start of final flare is

$$V(X_f) = \sqrt{2E_{K_f}} \quad (A-43)$$

#### 4. Altitude Response in the Final Flare

The idealized flare law given by Eq. A-33 is

$$\dot{h} = -\frac{1}{T_f} (h + h_B)$$

The ordinary first order differential equation in Eq. A-33 forms an initial value problem to define the flare trajectory when combined with two initial conditions

$$h(0) = h_f \quad (A-44)$$

$$\dot{h}(0) = V_f \gamma_0 \quad (A-45)$$

where now time,  $t'$ , is measured from the start of flare. These two initial conditions require the continuity of altitude and flight path angle at flare initiation. Laplace transforming Eq. A-33

$$(sh(s) - h(0)) + \frac{1}{T_f} h(s) = -\frac{1}{T_f} \frac{h_B}{s} \quad (46a)$$

which may be solved for altitude using the Eq. A-44 initial condition.

$$h(s) = \frac{h_f}{(s + 1/T_f)} - \frac{h_B/T_f}{s(s + 1/T_f)} \quad (46b)$$

Inverse Laplace transforming gives the altitude as function of time

$$\begin{aligned} h(t') &= h_f e^{-t/T_f} - h_B (1 - e^{-t/T_f}) \\ &= (h_f + h_B) e^{-t/T_f} - h_B \end{aligned} \quad (A-47)$$

Differentiating Eq. A-45 gives the sinkrate as

$$\dot{h}(t') = - \left( \frac{h_f + h_B}{T_f} \right) e^{-t/T_f} \quad (\text{A-48})$$

Applying the  $\dot{h}$  initial condition, Eq. A-43

$$\dot{h}(0) = V_f \gamma_0 = - \left( \frac{h_f + h_B}{T_f} \right) \quad (\text{A-49})$$

Thus  $h_B$  is given by

$$h_B = -T_f V_f \gamma_0 - h_f \quad (\text{A-50})$$

The altitude bias,  $h_B$ , is the distance below the runway for the zero sinkrate asymptote, (see Fig. 22). Positive  $h_B$  occurs with positive sinkrate at touchdown ( $\dot{h}_{TD} < 0$ .)

a. Time for Touchdown  $t'_{TD}$

The elapsed time to touchdown measured from the start of flare,  $t'_{TD}$ , is derived as follows.

$$h(t'_{TD}) = (h_0 + h_B) e^{-t'_{TD}/T_f} - h_B = 0$$

$$e^{-t'_{TD}/T_f} = \frac{h_B}{h_0 + h_B} \quad (\text{A-51})$$

$$t'_{TD} = -T_f \ln \left( \frac{h_B}{h_0 + h_B} \right) \quad (A-52)$$

b. Touchdown Sinkrate

From of Eq. A-48 and A-52 the sinkrate at touchdown is

$$\begin{aligned} \dot{h}(t_{TD}) &= - \left( \frac{h_f + h_B}{T_f} \right) \left( \frac{h_B}{h_f + h_B} \right) \\ &= - \frac{h_B}{T_f} \\ &= V_f \gamma_0 + h_f / T_f \end{aligned} \quad (A-53)$$

c. Touchdown Speed

The velocity at touchdown is

$$V_{TD} = V_f - K_v t'_{TD} \quad (A-54)$$

d. Touchdown Distance

With an additional integration, the touchdown point measured from  $X_0 = 0$  is

$$\begin{aligned} X_{TD} &= \int_0^{t'_{TD}} V_f dt - K_v \int_0^{t'_{TD}} t dt + X_f \\ &= V_f t'_{TD} - \frac{K_v}{2} t'^2_{TD} + X_f \end{aligned} \quad (A-55)$$

The three controlled variables,  $\dot{h}_{TD}$ ,  $V_{TD}$  and  $X_{TD}$  are plotted in Figs. A-6 through A-8 based on Eqs. A-53, A-54, and A-55, respectively. A more revealing view of the control situation can be achieved by plotting contours of constant touchdown sinkrate, touchdown speed, and touchdown position in the  $\tau - \gamma_0$  control variable plane as shown in Fig. 23 constructed by crossplotting from Figs. A-6 through A-8.

#### REFERENCES

- A-1. Aerodynamic Design Data Book, Orbiter Vehicle, Rockwell International, Report SD72-SH-0060, Vol. 1, Nov. 1980.
- A-2. Freeman, Delma C. Jr. and Bernard Spencer, Jr., Comparison of Space Shuttle Orbiter Low-Speed Static Stability and Control Derivatives Obtained From Wind-Tunnel and Approach and Landing Flight Tests, NASA TP-1779, Dec. 1980.
- A-3. Perkins, C. D. and R. E. Hage, Airplane Performance Stability and Control, John Wiley & Sons, New York, 1956.

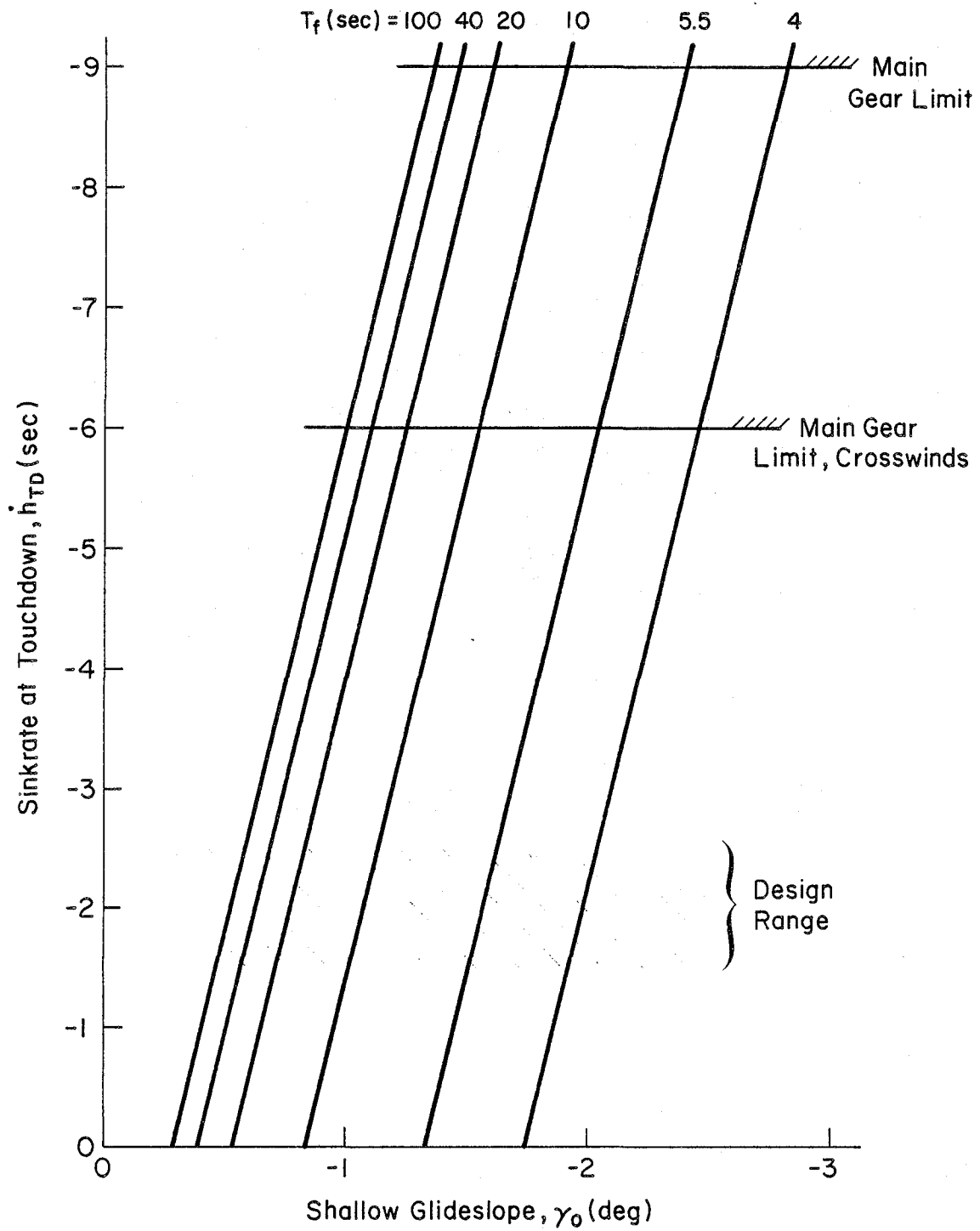


Figure A-6. Variation of Touchdown Sinkrate with Shallow Glideslope

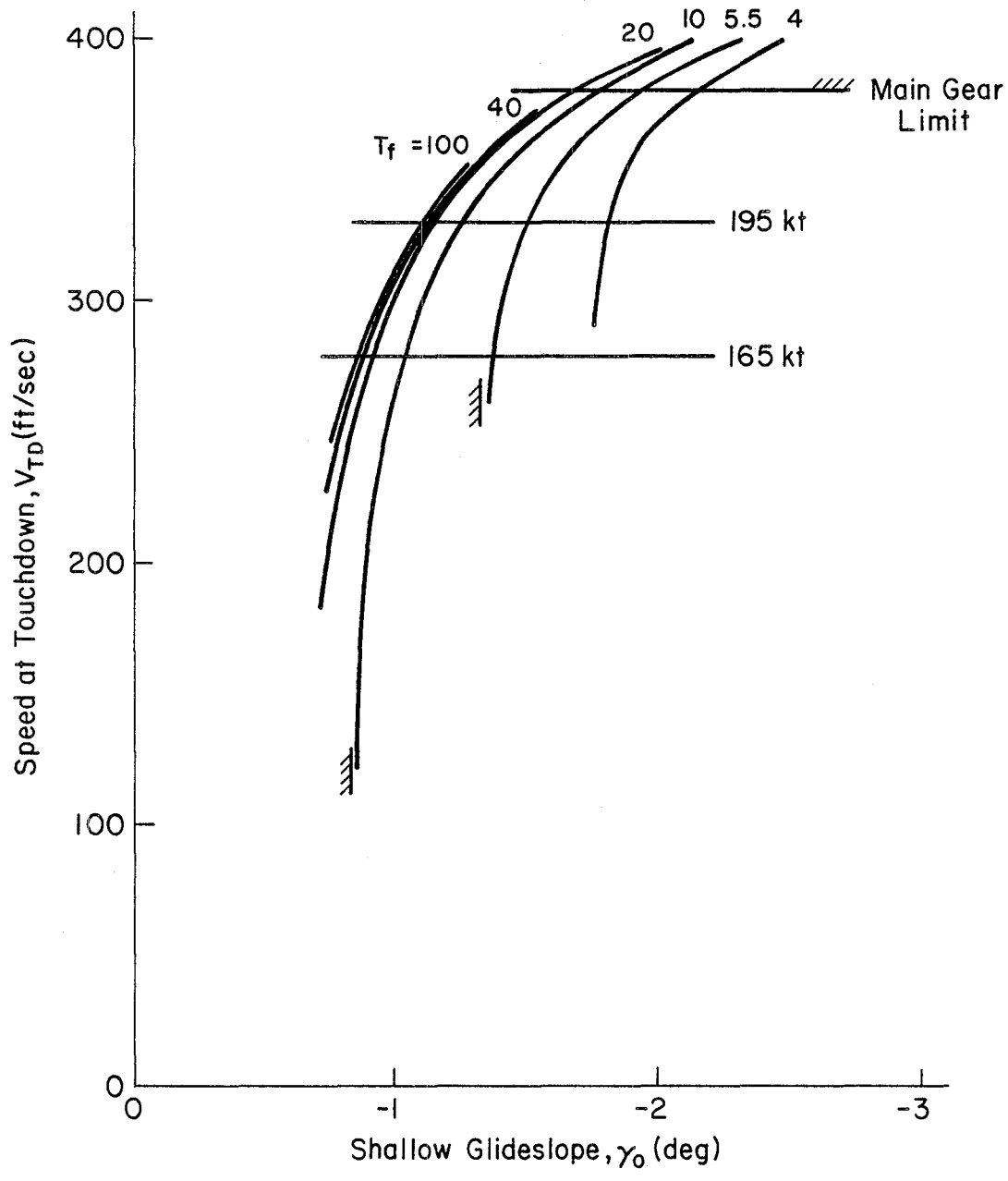


Figure A-7. Variation of Touchdown Speed with Shallow Sinkrate

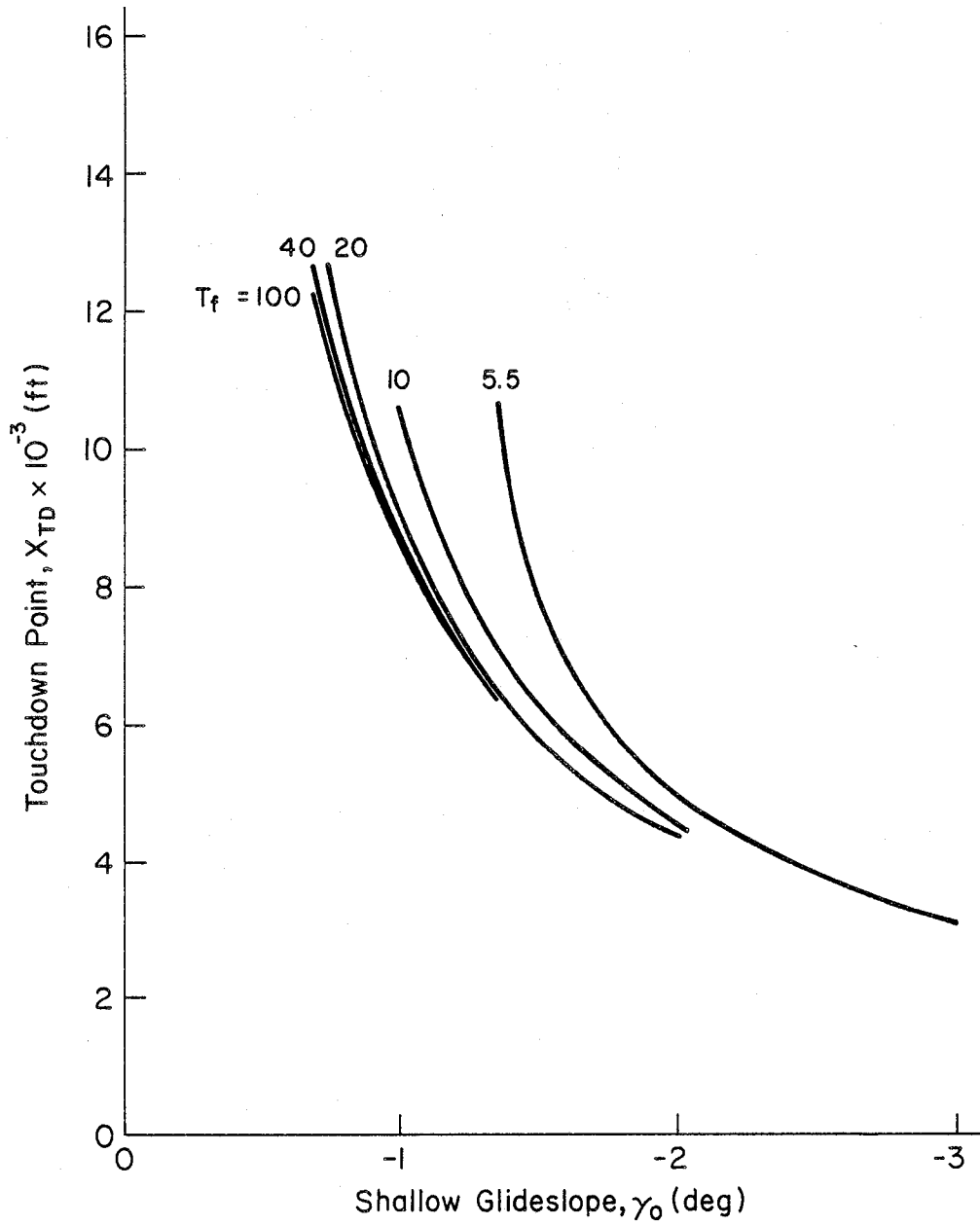


Figure A-8. Variation of Touchdown Point with Shallow Glideslope

## APPENDIX B

### PRELIMINARY QUESTIONS REGARDING STS-4 MANUAL FLYING QUALITIES

The Shuttle Orbiter, as a large, superaugmented, fly-by-wire, delta glider has some flying characteristics which are considerably different from more conventional aircraft. The current flying qualities criteria data base is drawn from experience with the latter and may not be applicable (appropriate) for Shuttle-like vehicles.

This is a solicitation of pilot comment on or assessment of STS-4 vehicle flying quality related characteristics which may lead to experiments to improve future Shuttle-like aircraft flying quality requirements and/or design criteria. The STS-4 flight segments of concern are those which were primarily under manual control: the HAC and the pre-flare, flare, and landing.

#### A. SPECIFIC QUESTIONS

1. In landing, are there any unusual characteristics of the Shuttle pitch attitude response to the rotational hand controller?
2. Are there any unusual characteristics of the Shuttle path (altitude, flight path angle) response to pitch attitude changes?
3. What differences in pitch trim and airspeed control, as compared to conventional aircraft, are required because of the zero stick force/speed gradient of the Shuttle's pitch rate command system?
4. To what extent is the manual control of speed brakes similar to conventional control of throttles? Is speed brake operation basically open loop or closed loop in approach?
5. What are the principal attitude and path references in approach and landing? Is the relative use of out the window versus panel displayed information conventional? When is the transition made from head down to head up?
6. Do you foresee any operational (as opposed to flight test) conditions (turbulence, crosswinds, night landing, etc.) which might approach flying qualities limits? What response characteristics of the Shuttle might be limiting in these situations?

7. To what extent did the actual Shuttle Orbiter flying characteristics in approach and landing differ from ground simulations and trainer aircraft flights?
8. For each of the manual control segments (HAC, pre-flare, flare, and landing) -- what do you feel were your primary cues for control?

**B. ADDITIONAL COMMENTS/ASSESSMENTS**

The following is a list of flying quality related characteristics which may or may not have adversely impacted manual control workload, task difficulty, attitude or path control precision, etc. These have not been integrated into a question format in order to avoid restricting the nature of your response. Comments are therefore solicited on any aspect in which a particular factor may stand out in your memory as adversely impacting the above during HAC, flare, or landing control. Please identify the flight segment being commented on.

**1. Longitudinal Control**

- a. Feel system inputs required to perform task
  - RHC displacements
  - RHC force gradient
  - Breakout sensitivity
- b. Pitch attitude response (to inputs required to perform task)
  - Effective time delay
  - Initial response onset
  - Overshoot
  - Settling time
  - Predictability
  - Sensitivity
  - PIO tendency
- c. Path response/control
  - Effective motion delay time
  - Predictability
  - PIO tendency
  - Any special control techniques employed? required?
- d. Airspeed control
  - Precision
  - Predictability

- e. Disturbances
  - Turbulence
  - Wind shear
  - Ground effect
- f. Workload
  - Control workload significant? dominant?
  - Other task workload detract from control task performance?
- g. Cooper-Harper rating (if possible)

## 2. Lateral-Directional Control

- a. Feel system
  - RHC displacements
  - RHC force gradient
  - Breakout sensitivity
  - Lateral-longitudinal harmony
- b. Roll attitude response
  - Effective time delay
  - Initial response time
  - Overshoot
  - Settling time
  - Predictability
  - Sensitivity
  - PIO tendency
  - Lateral acceleration at pilot
  - Roll ratcheting
- c. Heading response/precision
  - Roll into turns
  - Roll out of turns
- d. Workload
  - Control workload significant?
  - Other task workload detract from control task?
- e. Cooper-Harper rating (if possible)

## 3. Summary (Brief)

- a. Major problems
- b. Good features

**This Page Intentionally Left Blank**

**APPENDIX C**

**SPACE SHUTTLE FLYING QUALITIES QUESTIONNAIRE**

Respondant's name \_\_\_\_\_

Flight \_\_\_\_\_ on (date) \_\_\_\_\_

The Shuttle Orbiter, as a large, superaugmented, fly-by-wire, delta glider has some flying characteristics which are considerably different from more conventional aircraft. The current flying qualities criteria data base is drawn from experience with the latter and may not be appropriate for Shuttle-like vehicles. This questionnaire has been prepared to obtain the maximum information with minimum interference with crew schedules. No written replies are required but any comments will be of interest. The primary interest is in manual control from initiation of the HAC turn through touchdown.

1. Please check the control channels flown <u>manually</u> in each flight segment	HAC TURN	STEEP GLIDESLOPE CAPTURE	STEEP GLIDESLOPE GLIDE	PREFLARE	SHALLOW GLIDESLOPE CAPTURE AND GLIDE	FINAL FLARE AND LANDING	SLAPDOWN AND ROLLOUT
Pitch							
Roll/Yaw							
Speed Brakes							
Body Flap							
Comments:							

2. Please check the flight segments in which pitch RHC force/displacement characteristics could be improved with respect to	HAC TURN	STEEP GLIDESLOPE CAPTURE	STEEP GLIDESLOPE GLIDE	PREFLARE	SHALLOW GLIDESLOPE CAPTURE AND GLIDE	FINAL FLARE AND LANDING	SLAPDOWN AND ROLLOUT
a. Maximum force							
b. Maximum deflection							
c. Overall force/deflection gradient							
d. Shaping							
Comments:							

3. Please check the flight segments for which pitch attitude response to RHC inputs	HAC TURN	STEEP GLIDESLOPE CAPTURE	STEEP GLIDESLOPE GLIDE	PREFLARE	SHALLOW GLIDESLOPE CAPTURE AND GLIDE	FINAL FLARE AND LANDING	SLAPDOWN AND ROLLOUT
a. Appears to be "rate command"							
b. Appears to be "attitude command"							
c. Appears to be neither a or b							
d. Differs significantly from conventional aircraft of similar size							
Comments:							

4. Please check the flight segments in which pitch attitude response to RHC inputs could be improved with respect to	HAC TURN	STEEP GLIDESLOPE CAPTURE	STEEP GLIDESLOPE GLIDE	PREFLARE	SHALLOW GLIDESLOPE CAPTURE AND GLIDE	FINAL FLARE AND LANDING	SLAPDOWN AND ROLLOUT
a. Excessive time delay							
b. Excessive overshoot or oscillation							
c. Excessive rise time							
d. Excessive settling time							
e. Predictability							
f. Low sensitivity							
g. High sensitivity							
Comments:							

5. Please check the flight segments for which path (altitude, sinkrate, flight path angle or normal acceleration) response due to attitude change	HAC TURN	STEEP GLIDESLOPE CAPTURE	STEEP GLIDESLOPE GLIDE	PREFLARE	SHALLOW GLIDESLOPE CAPTURE AND GLIDE	FINAL FLARE AND LANDING	SLAPDOWN AND ROLLOUT
a. Differs from conventional aircraft of similar size							
b. Appears to have excessive time delay							
c. Creates problems for path control							
Comments:							

6. What percentage of the time is the pitch trim (RHC or panel) used in each flight segment	HAC TURN	STEEP GLIDESLOPE CAPTURE	STEEP GLIDESLOPE GLIDE	PREFLARE	SHALLOW GLIDESLOPE CAPTURE AND GLIDE	FINAL FLARE AND LANDING	SLAPDOWN AND ROLLOUT
100%		///	///	///		///	
Used Continuously							
50%							
Never Used							
0%		///	///	///	///	///	
Comments:							

7. What percentage of the time does the commander fly "headup" looking outside in each flight segment	HAC TURN	STEEP GLIDESLOPE CAPTURE	STEEP GLIDESLOPE GLIDE	PREFLARE	SHALLOW GLIDESLOPE CAPTURE AND GLIDE	FINAL FLARE AND LANDING	SLAPDOWN AND ROLLOUT
100%		///	///		///	///	
Continuously headup							
50%							
Never headup							
0%		///	///		///		///
Comments:							

8. For each flight segment, which of the following information sources are important to the commander	HAC TURN	STEEP GLIDESLOPE CAPTURE	STEEP GLIDESLOPE GLIDE	PREFLARE	SHALLOW GLIDESLOPE CAPTURE AND GLIDE	FINAL FLARE AND LANDING	SLAPDOWN AND ROLLOUT
a. Commander's view of landing site							
b. Commander's view of landing aids on ground							
c. Pilot's verbal instructions							
d. Pilot's altitude callouts							
e. Pilot's airspeed callouts							
f. Flight Director on ADI							
g. Pitch attitude display, ADI							
h. Beam deviation on HSI							
i. AMI							
j. AVVI							
k. Others							

9. During equilibrium glide on the outer glideslope, manual control of speed with the speed brakes is (check one or more)

a. Difficult \_\_\_\_\_

b. Difficult to do precisely \_\_\_\_\_

c. Not difficult \_\_\_\_\_

d. Subject to interference from manual path control efforts \_\_\_\_\_

e. Speed brakes were in AUTO \_\_\_\_\_

10. Speed brakes retraction is performed based on (check one or more)

a. Mentally averaged speed brake use on the outer glideslope \_\_\_\_\_

b. Predetermined altitude \_\_\_\_\_

c. Predetermined airspeed \_\_\_\_\_

d. Other cues \_\_\_\_\_

e. Speed brakes were in AUTO \_\_\_\_\_

11. Rate-command-attitude-hold pitch control systems such as used on the Shuttle are unconventional in that they produce "neutral speed stability" (zero stick force/speed gradient in the steady state). Check any of the flight segments in which you consider this characteristic undesirable.

- a. HAC turn \_\_\_\_\_
- b. Steep glideslope capture \_\_\_\_\_
- c. Steep glideslope glide \_\_\_\_\_
- d. Preflare \_\_\_\_\_
- e. Shallow glideslope capture and glide \_\_\_\_\_
- f. Final flare and landing \_\_\_\_\_

12. Once the preflare is completed and the final shallow glide is begun, is the shallow glide (check one or more):

- a. A region of approximately constant glideslope angle \_\_\_\_\_
- b. A region of approximately constant sink rate \_\_\_\_\_
- c. Neither of the above \_\_\_\_\_
- d. Really part of a continuous flare to touchdown \_\_\_\_\_
- e. Adjusted as required to set touchdown speed and sink rate \_\_\_\_\_

13. For each flight segment which of the following conditions have potential for significantly increasing workload in manual flight	HAC TURN	STEEP GLIDESLOPE CAPTURE	STEEP GLIDESLOPE GLIDE	PREFLARE	SHALLOW GLIDESLOPE CAPTURE AND GLIDE	FINAL FLARE AND LANDING	SLAPDOWN AND ROLLOUT
a. Steady winds							
b. Wind shears							
c. Turbulence							
d. Crosswinds							
e. Night landings							
f. Unavailability of information from pilot							
g. Other							

14. For each flight segment, what portion (rough percentage) of the total crew workload capacity was used	HAC TURN	STEEP GLIDESLOPE CAPTURE	STEEP GLIDESLOPE GLIDE	PREFLARE	SHALLOW GLIDESLOPE CAPTURE AND GLIDE	FINAL FLARE AND LANDING	SLAPDOWN AND ROLLOUT
100%		///	///	///		///	
Maximum Workload							
50%							
No Workload							
0%		///	///		///		///
Comments:							

TR-1187-1R

15. For which, if any, flight segments did you notice differences between the Orbiter and the STA with respect to	HAC TURN	STEEP GLIDESLOPE CAPTURE	STEEP GLIDESLOPE GLIDE	PREFLARE	SHALLOW GLIDESLOPE CAPTURE AND GLIDE	FINAL FLARE AND LANDING	SLAPDOWN AND ROLLOUT
a. Pitch response to RHC inputs							
b. Path (altitude, sinkrate, etc.) response to <u>attitude</u> changes							
c. Airspeed response to <u>attitude</u> changes							
Comments:							

C-14

16. Do you feel that the questions in this questionnaire are (check one or more)

a. Relevant \_\_\_\_\_

b. Irrelevant \_\_\_\_\_

c. Clear \_\_\_\_\_

d. Unclear \_\_\_\_\_

e. Other (Please comment)

17. Do you feel the format of this questionnaire is (check one or more)

a. Convenient \_\_\_\_\_

b. Needs improvement \_\_\_\_\_

c. Inconvenient \_\_\_\_\_

d. Not appropriate for obtaining accurate information \_\_\_\_\_

e. Other (Please comment)

1. Report No. NASA CR-170406	2. Government Accession No.	3. Recipient's Catalog No.	
4. Title and Subtitle SPACE SHUTTLE FLYING QUALITIES AND FLIGHT CONTROL SYSTEM ASSESSMENT STUDY - PHASE II		5. Report Date December 1983	
		6. Performing Organization Code	
7. Author(s) T. T. Myers, D. E. Johnston, and D. T. McRuer		8. Performing Organization Report No. 1187-1R	
		10. Work Unit No.	
9. Performing Organization Name and Address Systems Technology, Inc. 13766 South Hawthorne Blvd. Hawthorne, California 90250		11. Contract or Grant No. NAS4-2940	
		13. Type of Report and Period Covered Contractor Report - Final	
12. Sponsoring Agency Name and Address National Aeronautics and Space Administration Washington D.C. 20546		14. Sponsoring Agency Code RTOP 506-63-40	
		15. Supplementary Notes NASA Technical Monitor: Donald T. Berry, Ames Research Center, Dryden Flight Research Facility, Edwards, CA 93523. Phase I of this study is published as CR-170391 and Phase III is published as CR-170407.	
16. Abstract  This study defines a program of flying qualities experiments as part of the Orbiter Experiments Program (OEX). Phase I, published as CR-170391, reviewed flying qualities criteria and shuttle data. This report continues the review of applicable experimental and shuttle data to further define the OEX plan. An indirect approach to program implementation is proposed to circumvent operational constraints inherent in shuttle flights. This consists of limited inflight experiments correlated with extensive research simulation programs. An unconventional feature of this approach is the use of pilot strategy model identification to relate flight and simulator results. Instrumentation, software, and data analysis techniques for pilot model measurements are examined. The relationship between shuttle characteristics and superaugmented aircraft is established. STS flights 1 through 4 are reviewed from the point of view of flying qualities. A preliminary plan for a coordinated program of inflight and simulator research is presented.			
17. Key Words (Suggested by Author(s))  Space shuttle Flying qualities Flight control		18. Distribution Statement  Unclassified-Unlimited  STAR category 08	
19. Security Classif. (of this report) Unclassified	20. Security Classif. (of this page) Unclassified	21. No. of Pages 189	22. Price* A09

\*For sale by the National Technical Information Service, Springfield, Virginia 22161.

**End of Document**